INVESTIGATION AND DEVELOPMENT OF STEEL FIBER REINFORCED CONCRETE FOR DEPARTMENT OF TRANSPORTATION APPLICATIONS

by

ALEXANDER BLANKENSHIP

(Under the Direction of Stephan Durham)

ABSTRACT

This study involves a three-phase experimental and analytical investigation of the mechanical performance enhancement potentials of steel fiber reinforced concrete (SFRC). In phase I, thirteen mixtures were batched to study the fresh and hardened properties of SFRC containing varying fiber geometries and concentrations. Based on results of investigative mixtures' fresh properties, compressive strength, and modulus of rupture, mixtures were selected for Phase II large-scale static and impact beam testing. Phase II involved testing of large-scale SFRC beams containing differing levels of shear and flexural reinforcement to quantify the additional shear and flexural capacity provided by steel fibers. Within phase III, machine learning methods were used to construct SFRC compressive and flexural strength prediction models. From this study, SFRC was analyzed for potential use in GDOT applications with an understanding of the influence fiber reinforcement has on concrete fresh and hardened properties.

INDEX WORDS: Steel Fibers, High Performance Concrete, Steel Fiber Reinforced Concrete (SFRC), Flexural Strength, Modulus of Rupture, Toughness, Shear Strength, Residual Strength, Machine Learning

INVESTIGATION AND DEVELOPMENT OF STEEL FIBER REINFORCED CONCRETE FOR DEPARTMENT OF TRANSPORTATION APPLICATIONS

by

ALEXANDER BLANKENSHIP

B.S., The University of Georgia, 2019

A Thesis Submitted to the Graduate Faculty of The University of Georgia in Partial Fulfillment of the Requirements for the Degree

MASTER OF SCIENCE

ATHENS, GEORGIA

2020

INVESTIGATION AND DEVELOPMENT OF STEEL FIBER REINFORCED CONCRETE FOR DEPARTMENT OF TRANSPORTATION APPLICATIONS

by

ALEXANDER BLANKENSHIP

Major Professor:	Stephan A. Durham
Committee:	Mi G. Chorzepa
	Sidney Thompson

Electronic Version Approved:

Ron Walcott
Interim Dean of the Graduate School
The University of Georgia
August 2020

DEDICATION

This thesis is dedicated to my family, my fiancé, my friends, and everyone who has supported me along the way.

ACKNOWLEDGEMENTS

I would like to acknowledge all those that helped with the completion of this study. First and foremost, I would like to thank Dr. Stephan Durham. I would also like to thank my committee members Dr. Mi Geum Chorzepa and Dr. Sidney Thompson. On behalf of the University of Georgia, I would like to acknowledge the Georgia Department of Transportation for their financial support and involvement over the past year. Finally, I would like to thank Dr. Jidong Yang, Noah Chapman, Chandler Banks, and Mitch Perry for assisting me throughout this research.

TABLE OF CONTENTS

LIST OF TABLES

Page

LIST OF FIGURES

Page

1.0 INTRODUCTION

1.1 Fiber Reinforced Concrete

Concrete is a brittle material by nature, a composite material composed of rock, sand, water, cement, and air. While concrete is strong in compression, it possesses little tensile strength, leading to sudden catastrophic failures if not reinforced properly. It is for this reason that reinforcing steel is placed in the tensile zone of a concrete member to carry the tensile load. Often, the dimensions of the concrete element must be changed to accommodate the required amount of reinforcing steel while meeting the spacing requirements required by the codes. A possible design alternative is the use of fiber reinforced concrete (FRC). Fiber reinforced concrete utilizes randomly dispersed fibers within the concrete matrix to enhance the performance of the concrete mixture; most notably the flexural strength, crack resistance, shear strength, and energy absorption capabilities from impact loading. The additional strength developed from the introduction of fibers into the concrete matrix allows for reinforcing steel to be diminished.

The addition of fibers increases the first cracking load, stiffness, flexural strength and ductility of concrete. As the concrete member undergoes loading and micro cracks begin to form, fibers bridge these cracks preventing them from opening or propagating further, while carrying a portion of the tensile load. The ability of the concrete to carry load after initial cracking occurs is referred to as post crack behavior, or toughness. Toughness is the ability of a material to absorb energy during deformation before rupturing. For a material to possess high toughness, the material must be strong yet ductile to withstand high stresses and strains imposed from loading.

The impact resistance of FRC has been utilized in several industries, primarily military and nuclear applications, to help protect against projectile impacts. One other potential application of FRC is concrete median barrier (CMB) walls. CMB walls are often placed along bridges or highways where required by codes and are subjected to intense impacts from vehicles. Using current design procedure these barriers have a high rigidity which during a collision can be catastrophic with debris launched from the barrier wall, or the energy of impact being redirected back into the vehicle.

1.2 Study Objective

An objective of this study is to build off research conducted by Lopez (2018) and Tate (2019), who both studied the viability of incorporating recycled tire rubber as aggregate replacements and steel fibers into concrete for use in concrete median barrier (CMB) walls. Both Lopez and Tate reported performance improvements of concrete mixtures from the incorporation of steel fibers, despite the negative impacts that the rubber aggregate replacements had on the overall strength. The purpose of this study is to provide additional information on the use of steel fiber reinforced concrete (SFRC) for Georgia Department of Transportation (GDOT) applications. Within this study, the influence of steel fiber concentration and geometry on fresh and hardened concrete properties is observed. This research aims to investigate the shear and flexural strength of SFRC. The strength enhancements provided by SFRC can potentially provide enough capacity to eliminate a portion of the steel reinforcing bars, and even reduce the concrete thickness. While several studies have studied the response of unreinforced SFRC beams to static loading (Choi et al. (2007), Y.-K. Kwak et al. (2002), Yakoub (2011)), limited research has been conducted on SFRC beams containing conventional shear reinforcement at different ratios. Furthermore, the

potential of reducing concrete thickness design requirements in suitable applications, such as median barrier walls, are considered.

This study was conducted in three phases to assess the viability of reducing the amount of traditional steel reinforcing in concrete members that are subjected to intense loading. Within Phase I of the study, thirteen investigative mixtures were batched to measure concrete fresh properties, compressive strength, and modulus of rupture. Investigative mixtures comprised of SFRC utilizing different steel fiber geometries at fiber concentrations of 0.50%, 0.75%, and 1.00% by total volume of the mixture were tested. The information learned from Phase I testing was used for scaled beam testing in Phase II. Phase II focused on optimization of the steel reinforcement design of SFRC beams. During this phase, beam tensile and shear reinforcement designs were optimized based on properties of the selected SFRC mixture. Laboratory-scale SFRC beams were created for three-point static testing. The results of this study are used to make recommendations for optimized reinforcement design using steel fibers. In phase III machine learning methods are deployed to develop a highly accurate SFRC strength prediction model.

This study leads to a better understanding of the material saving potential presented by SFRC. The capability of SFRC to mitigate the need of flexural or shear reinforcing steel in concrete members is possible given the strength enhancements obtained with the use of SFRC. The decreased amount of required steel reinforcing bars in a concrete member provides an opportunity to reduced the section size of the concrete member. Ultimately, the use of steel fibers could lead to material savings, decreased labor time, and size reduction of concrete members when considering the improved mechanical performance of SFRC mixtures. Lastly, the knowledge gained from this study is used to make recommendations for the use of SFRC in Georgia Department of Transportation (GDOT) applications.

2.0 BACKGROUND

This study aims to build upon the work conducted by Lopez (2018) and Tate (2019), by further investigating the incorporation of industrial steel fibers into concrete mixtures for Georgia Department of Transportation (GDOT) applications. The work completed by Lopez and Tate provided methodology for testing and developing impact resistant SFRC. The research conducted by Lopez and Tate focused on fiber reinforced concrete mixtures containing rubber particulate aggregate replacements. This study focuses solely on the use of steel fibers within concrete mixtures, and thus this review focuses on the results obtained from the incorporation of fibers obtained by Lopez and Tate.

Lopez (2018) investigated rubberized concrete reinforced with various fiber types. Lopez began the study by designing and testing twelve preliminary mixtures to examine the mechanical properties of rubberized concrete mixtures incorporating polypropylene (PP), polyvinyl (PVA), and/or steel fibers. The water-to-cement (w/c) ratio was kept constant at 0.42 for all trial mixtures, along with a constant cement content of 611 lbs/yd^3 (360 kg/m^3). To determine the amount of fibers used per mixture, Lopez used the absolute volume method calculating the fiber concentration as a percentage of the total volume of the mixture. Mixtures were batched with steel fibers at concentrations of 0.50%, 0.75%, and 1.00%, PP fibers at a 1.00% by volume, and a hybrid of PP and PVA fibers totaling 1.00% fiber by total volume. Lopez studied the concrete mixtures' fresh properties such as slump, temperature, unit weight, and air content, as well as the hardened properties including compressive strength, modulus of rupture (MOR), and drop-weight impact.

Chemical admixtures such as high-range water reducing admixture (HRWRA), viscosity modifying admixture (VMA), and air entraining agent (AEA) were utilized to combat the negative impacts that the addition of fibers and the tire chips have on the fresh concrete properties. As noted by the ACI *Guide for Design with FRC* (ACI 544.4R-18), the traditional slump test is often not an accurate measure of the workability of FRC. For this reasoning, Lopez tested the slump of the concrete mixture prior to the addition of fibers. When comparing the workability of PP, PVA, and steel fibers, it was determined that steel fibers provided improved workability in comparison to PP and PVA. Based on these results, Lopez performed his later research using only steel fibers.

The goal of Lopez's research was to develop fiber reinforced rubber concrete mixtures which meet GDOT Class A requirements for compressive strength, 3,000 psi (20.7 MPa). It was determined that the addition of steel fibers alone had the greatest influence on the compressive strength of concrete mixtures. Lopez reported that steel fibers enhanced the MOR strength by 58.9% in comparison to the control mixture, while the addition of PP and the hybrid of PP and PVA fibers decreased the MOR strength by 35.4% and 20.1%, respectively. The impact resistance of the mixtures were tested utilizing a drop-hammer resilience test in accordance with ACI 544.2R. Three points were recorded during this test: initial crack, control failure, and ultimate failure. It was observed that the control specimens were broken into completely separate pieces at ultimate failure, while the SFRC specimens were held together by the fibers at ultimate failure. For the SFRC specimen a total of 135 drops were required to reach ultimate failure versus only 8 drops for the control specimen.

In addition, Lopez also tested eight large-scale beams measuring 90.0 in L x 6.0 in W x 10.0 in D (2286.0 mm x 152.4 mm x 254.0 mm) in static loading conditions. Each beam contained a reinforcement cage comprised of 2 - #3 longitudinal bars for compressive reinforcement, 2 - #4

longitudinal bars for tensile reinforcement, and #2 stirrups spaced 4.0 in (101.6 mm) on center. The steel reinforcement had a Youngs' Modulus of 29,000 ksi (200,000 MPa). The FRC beams were made with tensile reinforcement ratios ($\frac{A_s}{bd}$), of 0.20%, 0.78%, and 1.17% to better understand the effects of the fibers. Lopez found that a steel fiber volume ratio of 1.0% resulted in the highest toughness, or energy dissipation capacity.

Lopez also conducted scaled impact beam tests. The geometry and reinforcement of the impact beams were the same as those tested during static loading. Steel fiber volume fractions of 0.75% and 1.00% were utilized based on the results of the drop-hammer resilience tests. In total, Lopez constructed six impact beams, one control, one with only tire chip, two with only steel fiber, and two with steel fiber and tire chip concentrations. The impact beams were supported on steel I-beams, and the uplift force was restricted by tying the beam down using 2.0 in x 6.0 in (60.0 mm x 152.4 mm) pieces of lumber bolted down into the strong floor of the testing facility with 1.0 in. (25.4 mm) threaded rods. To simulate the impact of a projectile, a 400 lb (1 kN) steel drop-weight was dropped from a height of 20 ft (6.1 m) guided by a 1 ft x 1 ft (0.3 m x 0.3 m) steel sleeve. Displacement during testing was recorded using a motion capture camera system, along with motion capturing sensors located at the midspan of the beams. It was found that impact beams containing 1.0% steel fiber by volume had the greatest performance, showing no sign of failure after impact and redistributing the load to the supports effectively.

Tate (2019) built upon the work conducted by Lopez, investigating the addition of crumb rubber, industrial steel fibers (ISF), and recycled steel fibers (RSF) into concrete mixtures for impact performance capabilities. The goal of Tate's study was to determine the viability of repurposing tire waste material for use in concrete mixtures. Since the study conducted by Lopez was completed, GDOT adopted new concrete standards for CMBs, specifying Class AA concrete

(3,500 psi (24.1 MPa)) as the strength requirement. Following the methodology used by Lopez, Tate began the study by designing and testing a total of twelve mixtures to determine fresh and hardened concrete properties. Among the mixtures batched, two mixtures were batched with RSF content of 0.10% and 0.25%, with two mixtures batched incorporating ISF of 0.10% and 0.25% for comparison. Cement content was maintained at 635 lb/yd^3 (375 kg/m^3) and w/c was maintained at 0.42. Mixtures were designed with a target slump of 3.0 in (76 mm) and target air content of 5.00%.

Interestingly, Tate reported an increase in slump with the addition of steel fibers. This was determined to be due to the increased mixing time required for the fiber addition. Unit weight results showed a slight increase with the addition of steel fibers, as expected since steel fibers possess a higher density than other materials commonly used within concrete mixtures. Tate reported a decrease in the air content with addition of steel fibers, except for the 0.10% recycled steel fiber mixture which had a 9.00% air content in comparison with the 5.20% of the control mixture.

The SFRC mixtures exhibited promising compressive strength results, producing higher compressive strengths than the control and meeting the GDOT Class AA compressive strength requirement within seven days of age. At twenty-eight days of age, the 0.10% RSF, 0.25% RSF, 0.10% ISF, and 0.25% ISF mixtures exhibited a compressive strength increase of 12.3%, 67.7%, 55.7%, and 50.9%, respectively, in comparison to the control mixture. Despite GDOT not specifying a requirement for the MOR strength of concrete mixtures, Tate observed the MOR results, reporting that 0.10% RSF, 0.25% RSF, 0.10% ISF, and 0.25% ISF mixtures experienced an increase of 17.5%, 37.9%, 14.8%, and 26.2%, respectively, in comparison to the control mixture. Lastly, Tate investigated the impact resilience using a drop-weight hammer test of RSF

and ISF reinforced concrete beams. It was found that the RSF resulted in higher impact resistance compared to the ISF, which was a result of the variety of geometries present within the RSF, mostly due to the longer length of the fibers being able to mitigate the formation of cracks more effectively that ISF.

It was ultimately observed that the RSF concrete mixtures developed similar results for compressive and flexural strengths in comparison to ISF, with greater impact resistance. Despite this, the RSF mixtures had poor workability and required additional time to separate fibers to ensure that clumping did not occur and were well distributed throughout the mix. Additionally, there is concern that the random, and relatively long lengths of the RSF would cause compaction issues in tight spaces between steel reinforcing bars. While the ISF concrete mixtures did not perform as well as the RSF concrete mixtures in terms of impact resistance, the ISFs used within this study were short, being only 1.4 in (35 mm) long. For this reason, further investigation of longer ISFs is warranted before making recommendations in regards of type and quantity of steel fibers in concrete mixtures.

3.0 LITERATURE REVIEW

3.1 Overview

This literature review explores past research on the types of steel fibers available, effects on fresh and hardened concrete properties due to the inclusion of steel reinforcing fibers, and typical uses for fiber reinforced concrete mixtures in transportation applications.

3.2 Fiber Reinforced Concrete

Concrete is a brittle material by nature, possessing a small tensile strength in comparison to the compressive strength. Mankind has been experimenting with the implementation of fibers into mortar mixes since the beginning of composite materials. One of the earliest uses of fiber reinforcement is the addition of straw fibers or horse hair into sun-dried mud bricks. During these early experiments with fiber reinforced composites, the main benefit observed was the limitation of fragmentation post-cracking. These primitive fiber composites exhibited prolonged life from the decrease in degradation caused by temperature fluctuations and humidity. Research on fiber reinforced concrete (FRC) really began in the late 1800's, with the first patent being issued to A. Berard in 1874 for the use of granular waste iron in concrete. Many additional patents for fiber reinforcements were developed in the following years. In the 1960's, the development of fiber reinforcement began to accelerate with multiple types of fibers and fiber materials being introduced into the market (Naaman, 2018). Since the beginning of the modern development of fiber reinforcement there have been thousands of technical papers published and multiple guidelines and standards developed for fiber reinforced cements and composites.

The inclusion of fiber reinforcement within concrete has been shown to increase compressive and splitting tensile strengths, modulus of rupture, and toughness of the composite material (Song & Hwang, 2004). The fiber material type, geometry, orientation, and concentration within the concrete matrix has a direct impact on the shear strength and ductility of the concrete (Zollo, 1997). FRC design was developed based on the fracture mechanics concept, in which the fibers served to reinforce the matrix and bridge cracks. One role of the fibers within the concrete matrix is to mitigate crack propagation. Figure 1 illustrates how fibers effectively mitigate crack growth, and absorb energy while holding the composite together in the event of cracking.

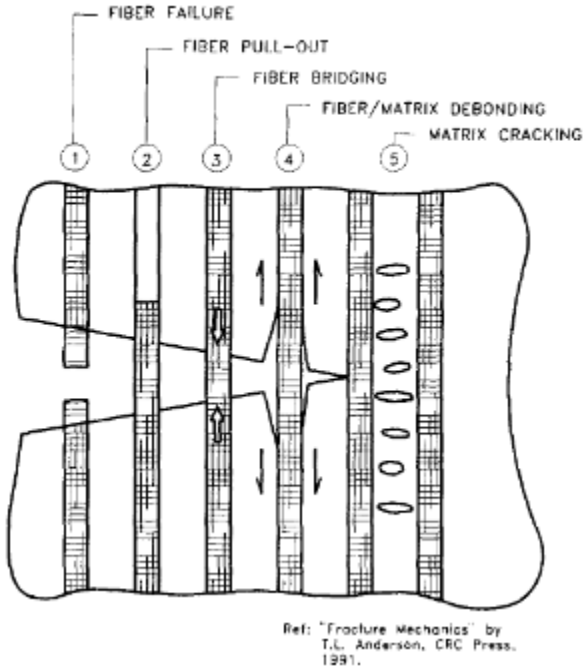

Figure 1: Energy-absorbing fiber/matrix mechanisms (Zollo, 1997)

3.2.1 Types of Fiber Reinforcement

There are many fiber types developed to reinforce concrete. Materials used for fibers include: steel, polypropylene, carbon, and glass among others. Fiber types may be organized into four main categories: metallic fibers, glass fibers, synthetic fibers, and natural fibers. Steel fibers are the most

widely used fiber type to reinforce concrete mixtures due to their high stiffness and malleability, which allows them to be manipulated and deformed into distinct shapes without effecting the high stiffness values (Dopko, 2018). There is a number of fiber deformation designs that have been incorporated into concrete and studied. Deformation of the fibers aid with mechanical anchorage into the composite and have a direct influence on fiber pull-out resistance. Types of fiber deformations include: hooked-end, twisted, bent, crimped and other anchorage methods. Steel fiber deformations commonly used in practice are illustrated in Figure 2. The effectiveness of the fiber is related to their bond strength, which is dependent on the strength of the concrete matrix. This is similar to the development length concept with traditional steel reinforcement bars in concrete beams.

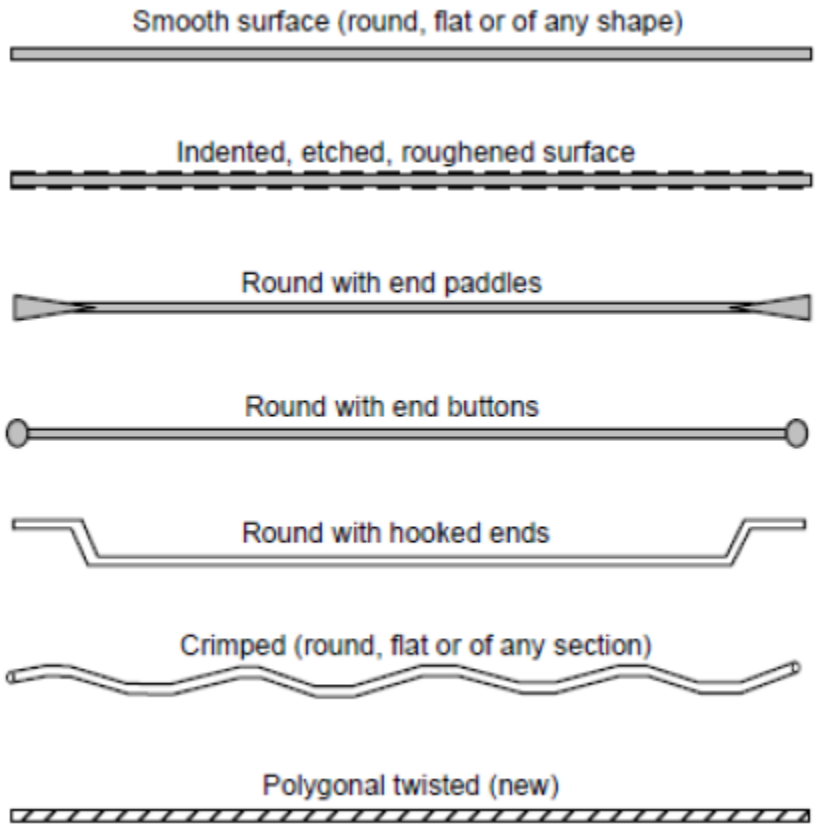

Figure 2: Types of Steel Fiber Deformations (Naaman, 2003)

The geometry of the fiber also influences the effectiveness of the fiber within the composite matrix. Several researchers have studied the geometries of the fibers, mainly the anchorage and aspect ratio, to determine the optimum fiber geometry. Yoo et al. (2017) studied fiber geometries and aspect ratios at different volume fractions, comparing straight, hooked-end, and twisted fibers of varying lengths. Within their study, it was concluded that while straight fibers produced higher strength results, a larger amount of fibers was required to achieve this strength in comparison to hooked-end fibers. Mixtures containing hooked-end fibers possessed higher MOR values and toughness indexes with low fiber volumes in comparison mixtures containing straight fibers at an equal fiber concentration. The hooked-end of the fibers provide additional anchorage within the composite material which helps to enhance the pull-out strength of the fibers, directly increasing the tensile strength of the composite.

In recent years, the end anchorage of these hooked-end fibers has been studied and improved upon. As shown in Figure 3, three-dimensional (3D), four-dimensional (4D), and five-dimensional (5D) configurations are being used in industry. Information regarding the benefits of these fibers is presented in the following section.

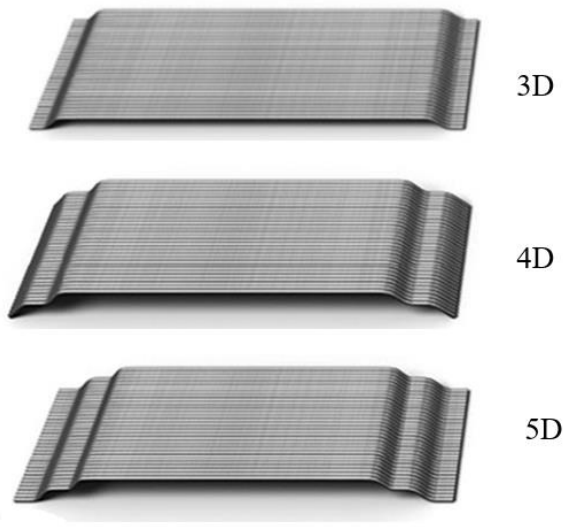

Figure 3: Examples of Steel Fiber End Anchorage (Bekaert Corp.)

The fiber pull-out strength, or the axial load required to pull the fiber out of the hardened concrete matrix, is dependent on the fiber geometry and its interaction with the concrete matrix. Abdallah (2017) compared the pull-out behavior of the 3D, 4D, and 5D end anchorages by measuring the force necessary to dislodge the fiber, concluding that the 5D possessed the greatest pull-out strength of the three. Water-to-binder (w/b) ratios of 0.11, 0.15, and 0.20 as well as varying embedment length including 0.4 in (10 mm), 0.8 in (20 mm), and 1.2 in (30 mm) were investigated by Abdallah. Abdallah found that for series with 3D, 4D, and 5D steel fibers with a w/b ratio of 0.20, the peak load was increased by 48.68%, 30.94%, and 43.95%, respectively, in comparison to straight fibers (Abdallah, 2017). Additionally, the longer the embedment length, the greater the pull-out resistance due to the greater surface area of fiber in contact with the binder matrix. By analyzing the pull-out results shown in Figure 4, a redistribution of the load occurs as the fiber begins to slip out of the matrix which is similar to load-deflection observations.

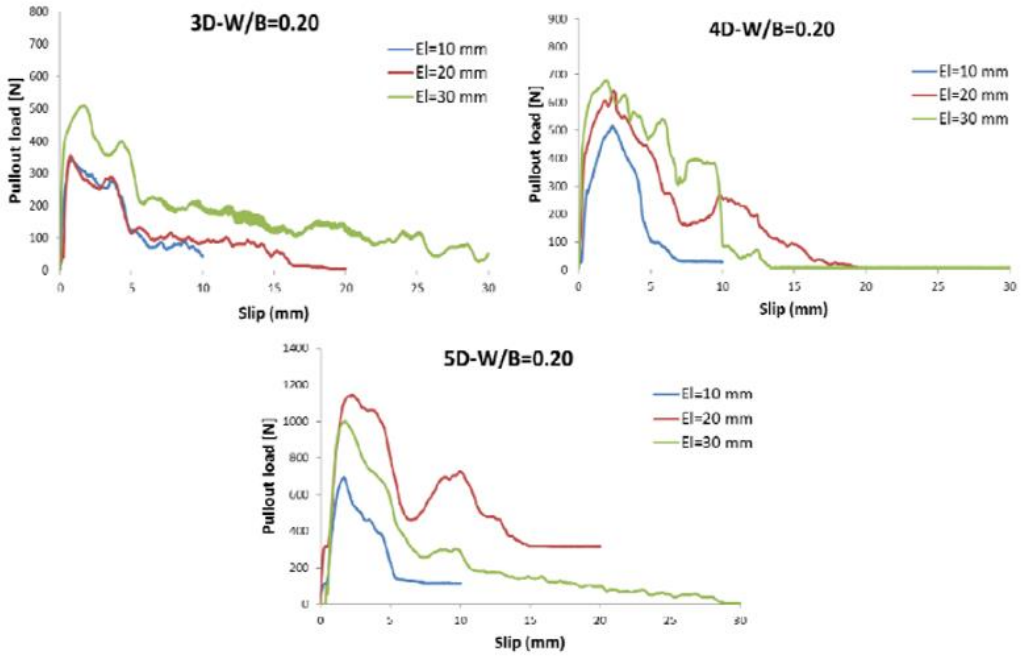

Figure 4: Steel Fiber Pullout Load Results (Abdallah, 2017)

3.2.2 FRC Applications

Fibers have been incorporated into bridge decks, bridge end piers and abutments, slab-on-ground projects, airport runways, and many other construction applications. The most typical application of SFRC being slabs-on-grade, bridge decks, and structural beams. This section reviews past and current use of SFRC within the concrete construction industry.

3.2.2.1 Slabs

Currently, slabs-on-grade are one of the main industrial applications of FRC. Fibers have been used to enhance the concrete performance for roadway pavements, residential and commercial slabs, airport runways, and other types of slabs. Fibers are integrated into the design to prevent crack propagation as a result of environmental exposure. This environmental exposure occurs in the form of thermal variations causing freezing and thawing, drying shrinkage after placement, and alkali silica reactions. These fibers are especially useful when the slab thickness requirements

create difficulties fitting reinforcing steel, given cover requirements. In some cases, steel fibers may be used as sole reinforcement for topping slabs for crack control and increasing post-crack moment capacity (ACI, 2018).

The reduction of concrete matrix cracking provided by the addition of fiber reinforcement has been utilized to increase joint spacing in slabs. While microcracks in the concrete may form, fibers bridge the cracks and prevent them from propogating further. Figure 5 shows a seamless 538,000 ft^2 (50,000 m^2) SFRC pavement placed at the Port of Brisbane, Australia. The concrete pavement contains a 42 lb/ft^3 (25 kg/m^3) fiber dosage, considered the largest joint-less concrete slab in Australia (ACI, 2018). This slab is able to withstand the harsh Australian environment without the formation of major cracks, despite the lack of joints.

Figure 5: Seamless SFRC Slab at Port of Brisbane, Australia (ACI, 2018)

An example of replacing traditional steel reinforcement with steel fibers is shown within Figure 6. In this project, the reinforcing steel within the elevated slabs was eliminated out of the design by taking advantage of the benefits obtained with steel fibers (ACI, 2018). The concrete

slab contains no additional reinforcement. The bars shown are anti-progressive collapse reinforcement (APC) spanning between the columns.

Figure 6: SFRC Elevated Slab in Highrise Construction (ACI, 2018)

3.2.2.2 Bridge Decks

Several states have incorporated fibers, both steel and synthetic, into their bridge deck projects. Some states have begun incorporating literature pertaining to the use of fibers into their bridge standards. Amirkhanian and Roesler (2019) developed a technical overview of FRC bridge decks, reporting all states that have adopted fiber criteria into their standards. Figure 7 shows states that have adopted literature into their standards pertaining to the use of FRC, color coded for the depth of specification. California, Oregon, and Delaware have required fibers to be used in all bridge decks. Missouri, Minnesota, and Idaho, among others, have required fibers to be used in specific bridge decks.

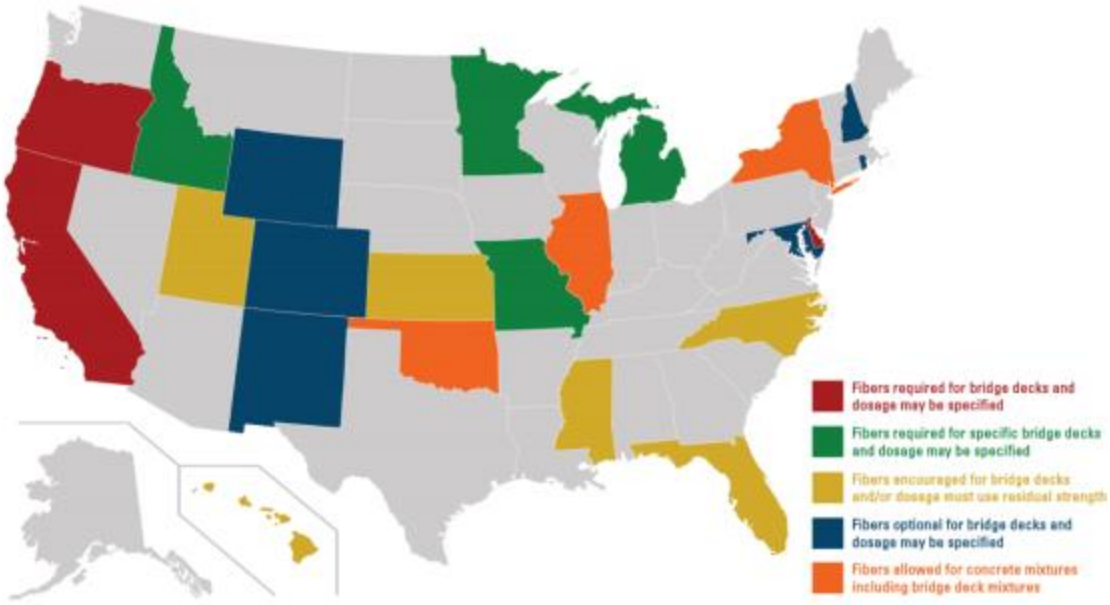

Figure 7: State DOTs with Fiber Specifications (A. R. Amirkhanian, Jeffery, 2019)

In 1992, the Ohio Department of Transportation (ODOT) conducted a large scale field investigation of steel fiber reinforced microsilica modified concrete (SFR-MSC) used in 14 bridge deck overlays (Baun, 1992). The study was conducted to develop a mixture that could combat common premature fatigue related distresses seen in bridge decks such as surface spalling, excessive delamination, and punching failures. From the study it was found that placement of the SFR-MSC mixture was similar to traditional concrete mixtures, with few difficulties during the finishing process (Baun, 1992). Ultimately, Baun concluded that SFRC provides excellent strength and promotes a longer design life for bridge decks.

3.2.2.3 Beams

Incorporation of fiber reinforcement into concrete beams has shown promising results in several studies (Banthia and Sappakittipakorn (2007), Deluce (2001), Lopez (2018), Soulioti et al. (2011)). Kopczynski and Whiteley (2016) incorporated steel fibers into shear wall coupling beams to

reduce the amount of steel reinforcement required in a congested concrete section. In traditional seismic design it can be assumed that the concrete has no contribution to the shear strength of coupling beams. Through testing, it was observed that addition of steel fibers contributed up to 60% of the shear strength of the beam, while also allowing for 40% of steel reinforcement to be eliminated from the design (Kopczynski & Whiteley, 2016).

In a study conducted in conjunction with the Florida Department of Transportation (FDOT), Yazdani (2002) studied the feasibility of reducing secondary reinforcement in the anchorage zone of prestressed post-tensioned bridge girders made with SFRC. From the study, it was indicated that 1.00% steel fibers by volume could be used to replace all secondary reinforcement for minimum concrete strength of 5900 psi (40.7 MPa), and replace 79.00% of secondary reinforcement for minimum concrete strength of 4710 (32.5 MPa) (Yazdani, 2002). These results indicated that fibers may be included into reinforced concrete beams to reduce the total amount of reinforcing steel in congested areas due to geometrical limitations of the design.

3.2.2.4 Shotcrete

Shotcrete is used for soil and rock stabilization in underground tunnel and mining projects. FRC shotcrete has been used to eliminate the extensive labor of erecting wire mesh or steel reinforcing bars which leads to savings of time and materials, while improving safety (ACI, 2018). The addition of fibers into shotcrete increases the post-crack performance and provides reduction of the number and width of cracks formed from temperature variations. Steel fibers and synthetic fibers have been used in shotcrete applications.

3.2.3 FRC Specifications

The governing specification for FRC in North America is ASTM C1116/C1116M-15 *Standard Specification for Fiber-Reinforced Concrete,* which covers all forms of FRC. For steel fibers specifically, specifications are further dictated by ASTM A820/A820M-16 *Standard Specification for Steel Fibers for Fiber-reinforced Concrete*. According to ASTM A820, there are five general types of steel fibers: cold-drawn wire (type I), cut sheet (type II), melt-extracted (type III), mill cut (type IV), and modified cold-drawn wire (type V).

3.2.4 Design of FRC Mixtures

American Concrete Institute (ACI) 544.4R-18 *Guide to Design with Fiber-Reinforced Concrete* provides design guidelines for FRC, which is discussed within this section. Within these guidelines concrete residual strength is considered as the main parameter, which is determined from standard three-point bending beam tests. The ultimate limit state (ULS) and serviceability limit state (SLS) are observed for strength requirements, crack width limits, and deflection limits. The SLS design level is considered for smaller deflections for which crack widths range from 0.016 in to 0.04 in (0.4 mm to 1.0 mm). ULS is considered for larger deflections in which crack widths range from 0.08 in to 0.14 in (2.0 mm to 3.5 mm).

3.2.4.1 Design of FRC for Flexure

The stress block concept used within traditional reinforced concrete design can also be used in the design of FRC. ACI provides expressions for calculating the flexural strength of SFRC. Three-point loading flexural tests performed following ASTM C1609/C1609M-19 is used to obtain design parameters. The needed design parameters are f_{600}^{D}, f_{150}^{D}, and $f_{e,3}$ which are FRC flexural residual strength at L/600, at L/150, and equivalent FRC flexural residual strength at L/150, respectively, reported in psi (MPa). The equivalent FRC flexural residual strength is a

measurement of the toughness of an FRC beam, and is used in place of f_{150}^{D} during design of continually supported beams, such as slabs-on-grade. The ultimate tensile strength of the cracked FRC section may be calculated using Equation 1. The nominal bending moment of the FRC section may be calculated using Equation 2.

$$f_{ut-FRC} = 0.37 f_{150}^{D} \tag{1}$$

$$M_{n-FRC} = f_{150}^{D}\, x\, \frac{bh^2}{6} \tag{2}$$

3.2.4.2 Design of FRC for Flexure-Hybrid Reinforcement

Hybrid reinforcement refers to the use of steel fibers as a reinforcing material in conjunction with traditional rebar reinforcement. Design of hybrid reinforced members is performed simply by summing the moment capacities obtained from the traditional reinforcement bars and fiber reinforcement, as shown in Equation 3. This type of design allows the tensile load to be carried by the hybrid action of the reinforcing rebar and fibers. The moment capacity then becomes a function of the rebar and fibers working together.

$$M_{n-HFRC} = M_{n-RC} + M_{n-FRC} \tag{3}$$

An expression developed by Campione and Letizia Mangiavillano (2008) takes into account the residual strength of SFRC and depth of the tensile zone, shown as Equation 5.

$$M_n = [\rho f_y (1 - 0.5\frac{0.80c}{d} + f_r(\frac{h-e}{d})(\frac{h}{d} - \frac{h-e}{2d} - 0.5\frac{0.80c}{d}]b_w d^2 \tag{5}$$

Where $e = \frac{\frac{f_{ctf}}{E_{ct}} + \varepsilon_{o85}}{\varepsilon_{o85}}$

3.2.4.3 Design of FRC for Shear

Many researchers have proposed expressions for predicting the ultimate shear capacity of SFRC beams without stirrups (D. H. Lee et al. (2017), Y.-K. Kwak et al. (2002), Yakoub (2011)). Recently Torres and Lantsoght (2019) performed a comparison of available proposed equations

for calculating the shear capacity of SFRC. From this comparison it was observed that the equations proposed by Y.-K. Kwak et al. (2002) predicts the ultimate shear capacity with the greatest accuracy with an average tested/predicted value of 1.209, standard deviation of 0.421, and coefficient of variation of 34.8 (Torres & Lantsoght, 2019). Equation 6 is the expression for predicting the ultimate shear capacity and the predicted inclined cracking load, f_{sp} , both proposed by Y.-K. Kwak et al. (2002).

$$V_u = [3.7ef_{sp}^{\frac{2}{3}}\left(\rho\frac{d}{a}\right)^{\frac{1}{3}} + 0.8v_b]b_w d \quad (6)$$

Where e = 1 when $\frac{a}{d} > 3.4$; e = $3.4\frac{a}{d}$ when $\frac{a}{d} \leq 3.4$; with $f_{sp} = \frac{f_{cuf}}{20-\sqrt{F}} + 0.7 + \sqrt{F}$

3.3 Mechanical Properties of FRC

The performance of a fiber reinforced composite material is governed by the fiber tensile strength, elastic modulus, ultimate strain, chemical compatibility with the mixture, fiber dimensions, and bond properties (Dopko, 2018). Since the development of FRC there have been numerous studies conducted on how these factors affect the performance of FRC. Within this literature review, various studies are referenced to develop an understanding of the effects of fiber reinforcement on the mechanical properties of concrete. Table 1 summarizes the referenced research papers, fiber types studied, and overall focus of each paper.

Table 1: Summary of Fiber Reinforced Concrete Studies Referenced

Author(s) (year)	Fiber Type(s)	Research Scope
Abdallah (2017)	Steel	Effects of hooked-end anchorages on bond-slip characteristics
Acikgenc et al. (2013)	Steel	Effects of fiber length and diameter on fresh and hardened properties
Al-Ameeri et al. (2013)	Steel	Mechanical properties of self compacting SFRC
Alavi Nia et al. (2012)	Steel, polypropylene	Impact resistance of FRC
Amirkhanian (2019)	Steel, synthetic	Overview of FRC bridge decks
Balaguru et al. (1988)	Steel	Properties of FRC: workability, behaviour under long-term loading, and air-void characteristics
Banthia et al. (2007)	Steel	Toughness enhancement through fiber hybridization
Baun (1992)	Steel	SFRC bridge deck overlays - ODOT
Bhutta et al. (2018)	Steel, polypropylene	Influence of inclination angle (0˚ and 45˚) on the interfacial bond-slip behavior of macro fibers
Bordelon (2007)	Steel, synthetic	Fracture behavior of concrete materials for rigid pavement systems
Choi et al (2007)	Steel	Shear strength of SFRC beams without stirrups
Deluce (2001)	Steel	Cracking behavior of SFRC containing conventional steel reinforcement
Dopko (2018)	Synthetic, carbon	Tailoring composite properties with discrete fibers
Guerini et al. (2018)	Steel, synthetic	Influence of fibers on slump, air content, and hardened properties
Guler et al. (2019)	Steel, synthetic, hybrid	Strength prediction models
Lee et al. (2017)	Steel	Shear capacity of SFRC beams
Lee et al. (2018)	Steel	Effect of steel fibers on fracture parameters
Lee et al. (2019)	Steel	Effect of hooked-end steel fiber geometry and volume fraction on flexural behaviour of bridge decks
Lopez (2018)	Steel, polypropylene, polyvinyl	Impact performance of recycled tire chip and fiber reinforced cementitious composites
Naaman (2003)	Steel	Presents technical background on development and design of steel fibers for use in composites
Natajara et al. (1999)	Steel	Statistical variations in impact resistance from drop weight tests of SFRC

Table 1: Sumary of Fiber Reinforced Concrete Studies Referenced

Author(s) (year)	Fiber Type(s)	Mechanical Properties
Song et al. (2004)	Steel	Mechanical properties of SFRC
Soulioti et al. (2011)	Steel	Effects of fiber geometry and volume fraction on flexural behaviour of SFRC
Tate (2019)	Steel	Use of rubber aggregates and recycled steel fiber for impact resistant concrete
Torres et al. (2019)	Steel	Infuence of fiber content on shear capacity of SFRC beams
Wafa et al (1992)	Steel	Influence of fiber contents on compressive strength, modolus of rupture, toughness, and splitting tensile strength
Yazici et al (2007)	Steel	Influence of aspect ratio and volume fraction on mechanical properties
Yoo et al. (2017)	Steel	Effects of fiber shape, aspect ratio, and volume fraction on flexural behabiour of UHPFRC

3.3.1 Effects of Fiber Reinforcement on Fresh Properties

Addition of fibers to the concrete matrix has been shown to have detrimental effects on fresh concrete properties. Decreased workability and increased unit weight are two negative effects that addition of fibers has on fresh properties of concrete mixtures.

The addition of steel fibers into concrete mixtures lowers the slump, and thus the workability of the mixture. The workability of the mixture is reduced due to surface area of fibers diminishing the cement paste available for the free movement of aggregates and fibers (Deluce, 2001). M. Acikgenc et al. (2013) found that the workability of FRC is linearly related to the fiber aspect ratio and volume. As the fiber aspect ratio or volume increased, the slump decreased (M. Acikgenc et al., 2013). Once the fiber volume content reached 1.50%, the slump was rendered zero and considered a poorly workable mixture. The slump test results by M. Acikgenc et al. (2013) is illustrated in Figure 8. Within the figure, the fiber types are denoted by the aspect ratio followed

by the fiber length (mm). For example, 80/60 is a fiber with an aspect ratio of 80 and a length of 2.4 in. (60 mm). The results show that the mixtures workability decreased with an increase in fiber length and aspect ratio.

Unit weight is increased with the inclusion of steel fibers, as the steel fibers possess a density that is much higher than any of the other materials commonly used within the concrete matrix (Dopko, 2018). Steel fibers are the heaviest of the fibers commonly used within concrete.

It is unclear within literature what effect the inclusion of steel fibers has on the air content of concrete due to limited studies reporting air content results. Balaguru (1988) found that the addition of steel fibers decreased the air content by a small fraction, with the specific surface area of air bubbles being smaller than that of normal concrete. However, in a recent study comparing steel and marco-synthetic fibers on concrete properties, Guerini et al. (2018) found that steel fibers cause a marginally small increase in air content without having any noticeable effect on the compressive strength. Lastly, Al-Ameeri (2013) noted an increase in entrapped air with the inclusion of steel fibers in self-consolidating concrete, stating that the increased air content may have lowered the compressive strength slightly, but was negligible.

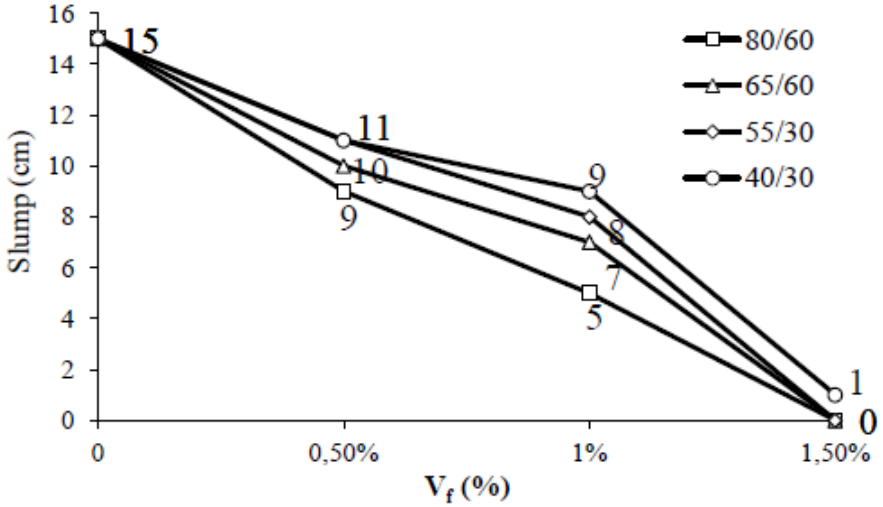

Figure 8: Influence of Fiber Volume on Slump (M. Acikgenc et al., 2013)

3.3.2 Effects of Fiber Reinforcement on Hardened Properties

It is widely known that the inclusion of fibers into the concrete matrix has positive effects on several of the hardened properties. Most notably, compressive strength, splitting tensile strength, and modulus of rupture are increased with the introduction of steel fibers. In a study conducted by Song and Hwang (2004) compressive strength, splitting tensile strength, and modulus of rupture were increased by 7.10%, 19.00%, and 28.10% respectively for mixtures with 0.50% steel fibers by total volume, and 11.80%, 50.00%, and 7.80% respectively in mixtures with 1.00% steel fibers by total volume.

3.3.2.1 Compressive Strength

The compressive strength of concrete is the most important property of concrete, being the basis for which concrete members are designed. Researchers have attempted to construct analytical models to predict the compressive strength behavior of SFRC (Song & Hwang, 2004, Dopko, 2018). These studies have concluded that the addition of steel fibers increase the compressive strength up to a certain percentage based on the fiber geometry. Song and Hwang (2004) found that the compressive strength of high strength concrete (HSC) was improved with the addition of steel fibers up to 1.50%, dropping slightly at 2.00%. Despite the drop in compressive strength, a 2.00% fiber volume yielded an increase in compressive strength of 12.90% in comparison to the control. These results are presented in Figure 9, along with the compressive strength prediction equation (Song & Hwang, 2004). The prediction equation, Equation 7, was able to accurately predict the compressive strength of the SFRC with an error less than 1.00%.

$$f'_{cf}\ (\text{MPA}) = 85\ (\text{MPa}) + 15.12V_f - 4.71V_f^2 \quad (7)$$

In another study observing the effect that steel fibers have on self-consolidating concrete (SCC), Al-Ameeri (2013) found that steel fibers increased the compressive strength by 10.55%

and 29.45% for 0.50% and 0.75% fiber content by total volume, respectively. The compressive strength lowered for fiber volumes greater than 0.75%, while still being 20.00% higher than the control mixture (Al-Ameeri, 2013). The increase in compressive strength was contributed to the steel fibers ability to enhance crack controlling by decreasing the amount of crack propagations. Ultimately a more ductile failure mode was experienced when compared to traditional concrete. As the concrete begins to crack and break apart during the compressive test, fibers bridge the crack formation and hold the specimen together resulting in a more ductile failure.

Lastly, Guler et al. (2019) analyzed many proposed strength prediction equations, showing that each one predicted that compressive strength increased with the addition of steel fibers, and increased with increasing fiber volume fraction or reinforcement index. Guler's study found that the expressions proposed by Abadel et al. (2016), Guler, and Padmarajaiah (1992) predicted the compressive strength of the SFRC mixtures within 4.00%, 1.00%, and 2.00% of the observed value, respectively.

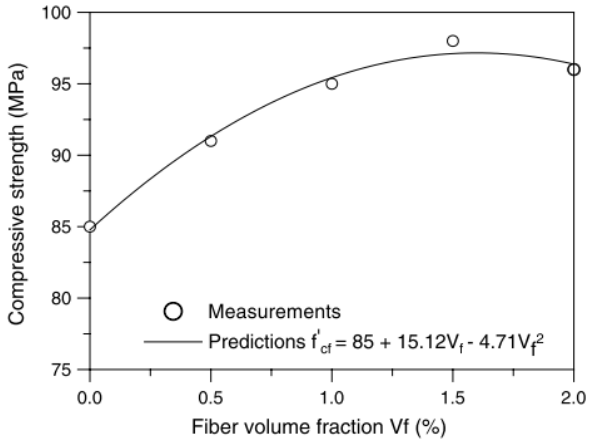

Figure 9: Compressive Strength Test Results (Song & Hwang, 2004)

However, other researchers have found that the addition of hooked-end fibers does not have an effect on the concrete's compressive strength. S.-J. Lee et al. (2019) studied the effects of

the aforementioned 3D, 4D, and 5D fiber end anchorages and volume fractions on bridge deck concrete. Their study tested fiber volume fractions of 0.37%, 0.60%, and 1.00% with each anchorage geometry. Results indicated a negligible effect on the compressive strength, as shown in Figure 10. S.-J. Lee et al. (2019) concluded that the fibers lead to both positive and negative effects on the compressive strength, resulting in no significant influence.

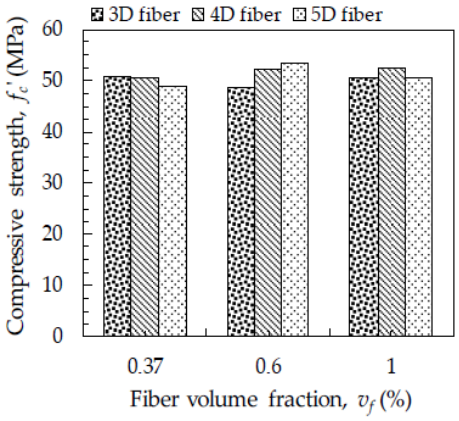

Figure 10: 3D, 4D, and 5D Compressive Strength Test Results (S.-J. Lee et al., 2019)

3.3.2.2 Flexural Strength

The Modulus of Rupture (MOR) is a measurement of the load at which a beam fails by flexure, or the ultimate bending strength at which rupture occurs. MOR is an incredibly important property for concrete as it indicates the bending capabilities of concrete before cracking. The MOR concept is based on the elastic beam theory, in which the maximum normal stress in the beam is calculated from the ultimate bending moment, M_u, with the assumption that the beam will behave elastically. This is calculated by Equation 8, in which f_r is the MOR, b is the beam width, and d is the beam depth.

$$f_r = \frac{6M_u}{bd^2} \tag{8}$$

Song and Hwang (2004) reported that for mixtures with 0.50%, 1.00%, 1.50%, and 2.00% steel fibers by volume, the MOR was increased by 28.10%, 57.80%, 92.20%, and 126.60%, respectively, compared to the control mixture. These results and prediction equation developed within the study are presented in Figure 11.

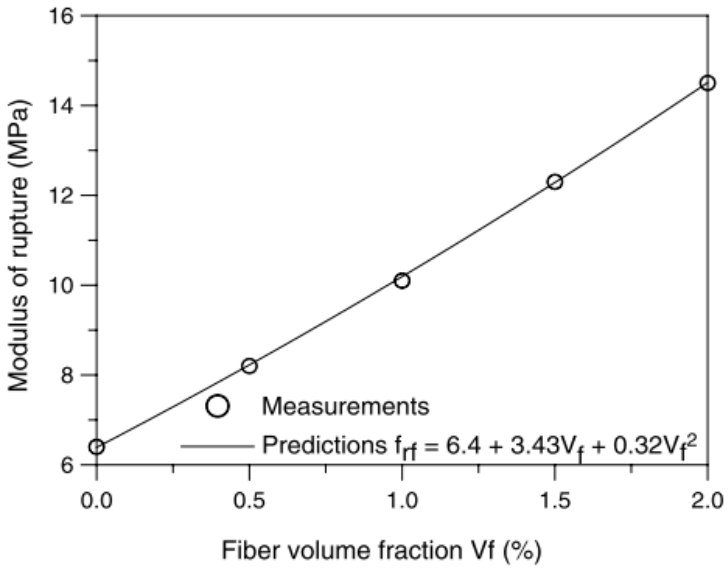

Figure 11: Modulus of Rupture Test Results (Song & Hwang, 2004)

From this prediction equation, Song and Hwang (2004) measured the MOR of their High Strength Concrete (HSC) mixture to be 928 psi (6.4 MPa), which equates to 0.69 $\sqrt{f'_c}$, in which f'_c is equal to 85 MPa. These measurements were compared to ACI 318-01 MOR equation of 0.63 $\sqrt{f'_c}$ for HSC in MPa which is slightly lower than the value measured by Song and Hwang. Yazıcı et al. (2007) examined the effect that aspect ratio and volume fractions of steel fibers have on mechanical properties, and reported that SFRC had a 3.00-80.00% increase in flexural strength when compared to the control mixture depending on the fiber geometry. In a study conducted by Guler et al. (2019), it was determined that the highest increase of flexural strength for SFRC was 53.70% in comparison to the control for a 0.75% fiber by volume mixture. From this information

it is concluded that the addition of steel fibers to the concrete matrix will increase the flexural capacity of the concrete.

In the study conducted by Guler et al. (2019), an increase in flexural strength with the addition of steel fibers were reported by a large variety of researchers. Guler's study compared a variety of proposed flexural strength prediction expressions, reporting that the expressions proposed by Abadel et al (2016), Guler, and Padmarajaiah (1992) accurately predicted the flexural strength of SFRC mixtures within 11.00%, 3.00%, and 19.00%, respectively, of the observed values.

3.3.2.3 Shear Strength

The addition of steel fibers to concrete increases the shear strength by transferring tensile stresses across crack surfaces, reducing the intensity of diagonal tensile cracking, and increasing the effective stiffness after cracking occurs (Choi et al., 2007). In a study conducted by Y.-K. Kwak et al. (2002), the influence of fiber volume fraction and *a/d* ratio (where *a* is the shear span and *d* is the effective depth) on strength and ductility of FRC beams without stirrups was studied. It was reported that the addition of fibers increased the ultimate shear strength by 122.00-180.00% in comparison to beams without fibers (Y.-K. Kwak et al., 2002). From the study, it was indicated that the failure mode of SFRC beams without stirrups shifted from a shear failure to a flexural failure with a 0.75% fiber volume percentage. Similar results were found by Marar et al. (2016) who investigated the influenced of fiber volume and aspect ratio on shear strength, reporting a 111.00-148.00% increase in shear strength with the addition of fibers.

Torres and Lantsoght (2019) investigated SFRC beams of various fiber volume percentages with no stirrups, reporting that a steel fiber volume percentage of 1.20% could be used to replace ACI 318-14 minimum stirrup requirements. Comparable results were reported by Choi et al.

(2007) suggesting that a 0.75% fiber volume percentage could be used to replace ACI 318-14 minimum stirrup requirements in SFRC beams.

3.3.2.4 Toughness

Toughness is considered the amount of energy absorbed during loading of a concrete member and is calculated by calculating the area under a load-deflection curve. Toughness is one of the most important characteristics of FRC. For a typical reinforced concrete beam the load-deflection curve has a steep increase until the initial cracking of the concrete occurs and the tensile steel begins to hold the load until rupture at which ultimate failure occurs. However, with FRC, loading continues past the failure of tensile steel as fibers work to bridge cracks and effectively redistribute the load as deflection continues to increase. Within the study conducted by Acikgenc et al. (2013) it was concluded that the aspect ratio has the greatest effect on the toughness enhancement of SFRC. Further, mixtures containing fibers with the largest aspect ratio resulted in the highest toughness. Figure 12 shows the increase in load and deflection of the SFRC mixture when compared to the control. Figure 13 shows the toughness enhancements found by the study.

Song and Hwang (2014) observed similar results by developing toughness indexes to compare the increase in toughness. The toughness indexes were calculated by dividing the measured flexural toughness at a specified deflection by the first crack deflection of the non-fiber reinforced concrete. Control mixtures possessed a toughness index of 1, while fiber volume fractions of 0.50%, 1.00%, 1.50%, and 2.00% possessed indexes of 3.0, 3.3, 4.2, and 6.5 respectively . Similar results were reported by Naaman et al (2003). Figure 14 compares the stress elongation behavior of conventional FRC to high-performance FRC (HPFRC) subjected to tensile loading (Naaman, 2003).

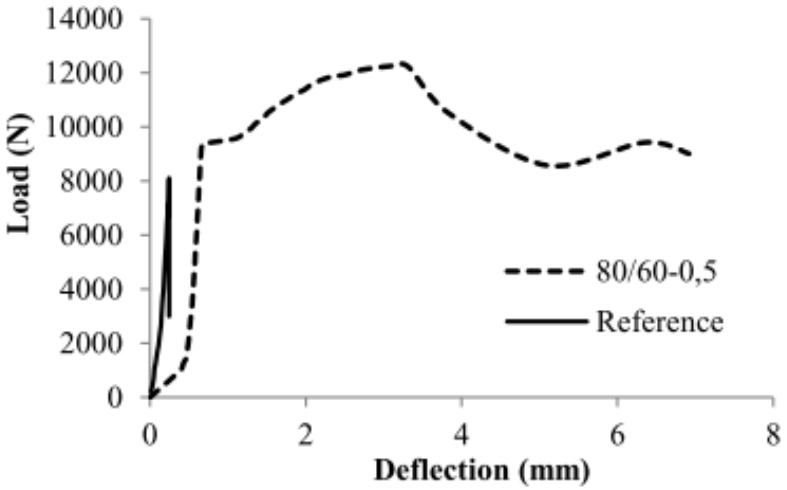

Figure 12: Load-Deflection Curve (M. Acikgenc et al., 2013)

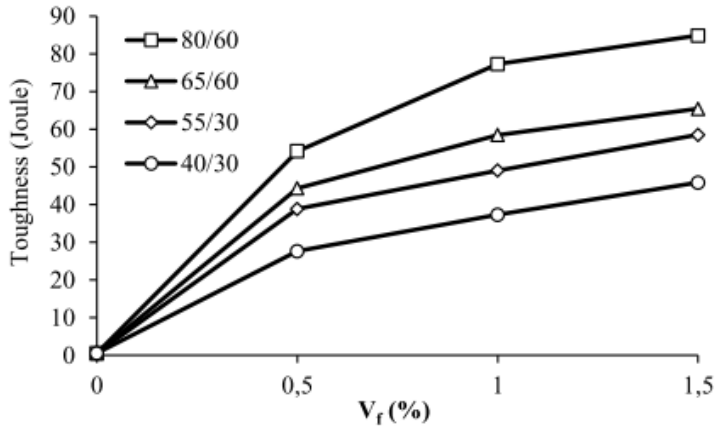

Figure 13: Toughness Enhancement of SFRC (M. Acikgenc et al., 2013)

Soulioti et al. (2011) examined the effects that hooked-end fibers and waved fibers have on flexural behavior of concrete, concluding that hooked-end fibers had a greater increase in the flexural capacity that waved fibers. Based on these findings, it is concluded that the addition of fiber reinforcement to concrete mixtures increases the member toughness, and prolongs member life during periods of high deflection.

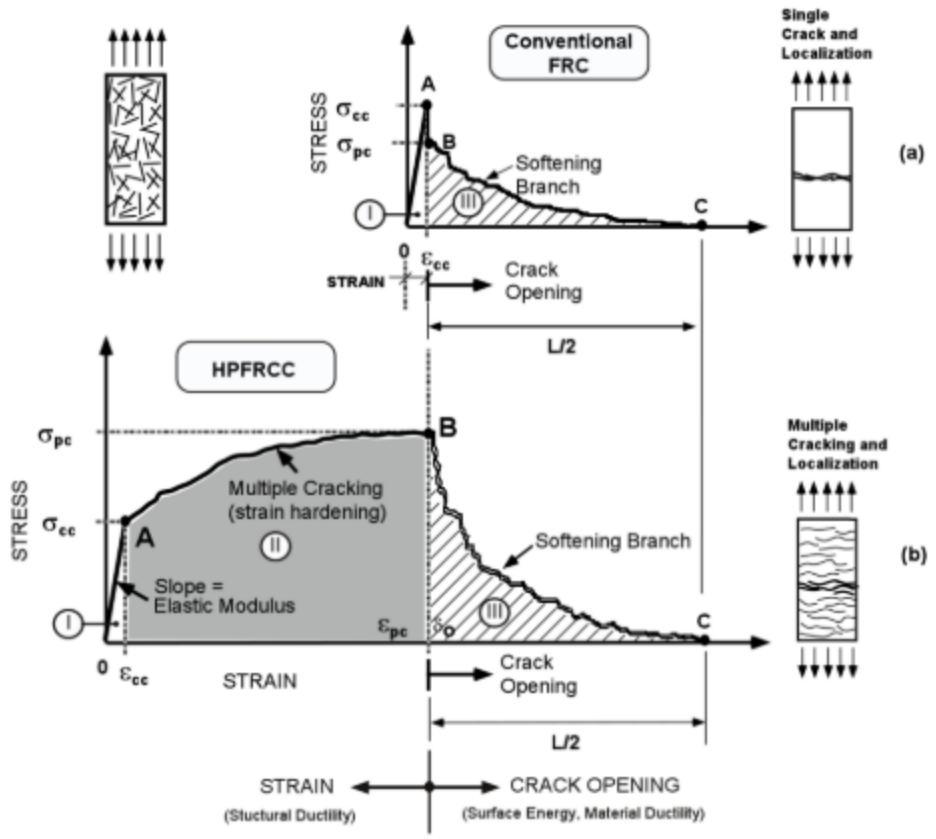

Figure 14: Typical Stress Elongation Response of Fiber Reinforced Concrete (Naaman, 2003)

3.3.2.5 Energy Absorption and Impact Resistance of FRC

Concrete brittleness is increased as compressive strength increases. The use of fibers in high-strength concrete mixtures for impact resistance has been performed by construction, nuclear, and military applications for several years to combat this increase in brittleness. The impact resistance of concrete is the ability of the material to withstand a high velocity projectile impact which may occur from wind gusts, earthquakes, vehicle impacts, and others. As concluded in the previous section, researchers have found that the addition of steel fibers greatly increases the energy absorption capabilities, or toughness, of concrete. However, there is little research published on the impact resistance of SFRC due to the complexity of quantitatively investigating dynamic

events and measuring the SFRC response. Energy wave propagation occurs throughout the composite material during a dynamic impact causing difficulty in measuring an accurate response.

One method of measuring impact resistance of concrete is by a drop-weight test proposed by ACI 544.4R-18 *Guide to Design with Fiber-Reinforced Concrete*. The concentrations and orientations of fibers within concrete, placement methods, flow of the fresh concrete, and the degree of compaction all influence the impact resistance of the composite (Nataraja, 1999). Nataraja (1999) studied the statistical variations of the drop weight impact test, concluding that the observed coefficients of variation for SFRC are 57.00% for first-crack resistance and 46.00% for ultimate resistance. Due to the high variance in the impact test results, a goodness-of-fit test indicated poor fitness of impact-resistance test results to a normal distribution at a 95.00% level of confidence for both SFRC and plain concrete (Nataraja, 1999). Despite the low statistical confidence, it was evident that the steel fibers contributed to the impact resistance of the concrete with more observed impacts before failure. Similar results were found in a study by Alavi Nia et al. (2012) in which concrete mixtures included steel and polypropylene fibers. Hooked end steel fibers with an aspect ratio of 80 were used at 0.50% and 1.00% volume fractions and produced better performance than polypropylene due to greater length, tensile strength, and advanced end anchorage (Alavi Nia et al., 2012).

Another method of measuring the impact resistance of concrete is through scaled beam impact tests. Tate (2019) tested scaled beams, measuring 90.0 in x 6.0 in x 10.0 in (2286.0 mm x 152.4 mm x 254.0 mm) for impact loading by investigating the viability of tire chips and recycled steel fibers into concrete mixtures for GDOT use, as discussed within the background section of this study. To conduct this test, impact beams were placed beneath a 20 ft high, 1 ft x 1 ft (6.0 m, 0.3m x 0.3m) vertical steel sleeve used to guide a 400 lb (181 kg) drop weight to impact the mid-

span of the beam. The impact force was measured using a load cell placed under the pinned support of the beam. Deflection was determined using an NDI Optotrak Certus HD motion capture camera and sensors placed at the mid-span of the beam. The load cell had a sampling rate of 10,000 Hz while the motion capture camera recorded at 400 Hz. The movement of the drop weight was captured by an accelerometer with a sampling rate of 20,000 Hz attached to the arm of the drop weight. Figure 15 illustrates the reinforced concrete beams used for the study. Figure 16 shows the placement of motion capture sensors at the beam mid-section. Figure 17 illustrates the drop weight schematic, showing the three steel weights attached together summing to 400 lbs. (181 kg). Figure 18 shows the drop weight at the top of the vertical sleeve held with the releasing clamp.

Lopez concluded that the addition of steel fibers into the concrete mixture greatly enhanced the impact resistance and energy absorption of the concrete. The SFRC beam resulted in a maximum deflection at initial impact of 2.6 in (66.0 mm), while the control beam deflected 4.0 in (101.6 mm) upon initial impact. Additionally, the failure mode of the SFRC beam was much preferable to the control. Upon impact the control beam developed large cracks and released shrapnel exposing reinforcing steel. The SFRC beam developed small cracks and released no shrapnel as shown in Figure 19. It was observed that the distance of crack propagations from the point of impact was less for the SFRC beam than the control beam.

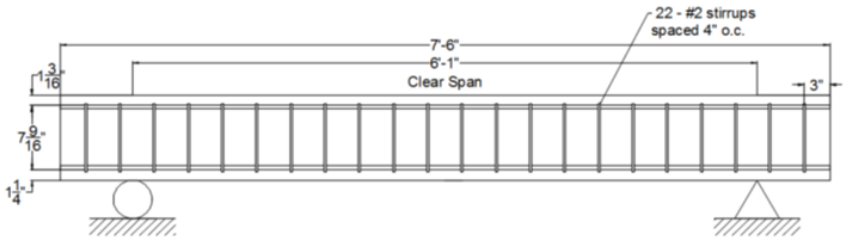

(a) Longitudinal Section of RC Test Specimen

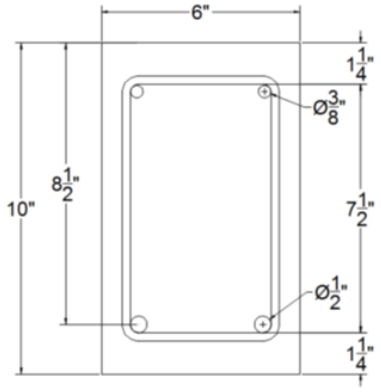

(b) Cross Section of RC Test Specimen

Figure 15: RC Beam Sections (Lopez, 2018)

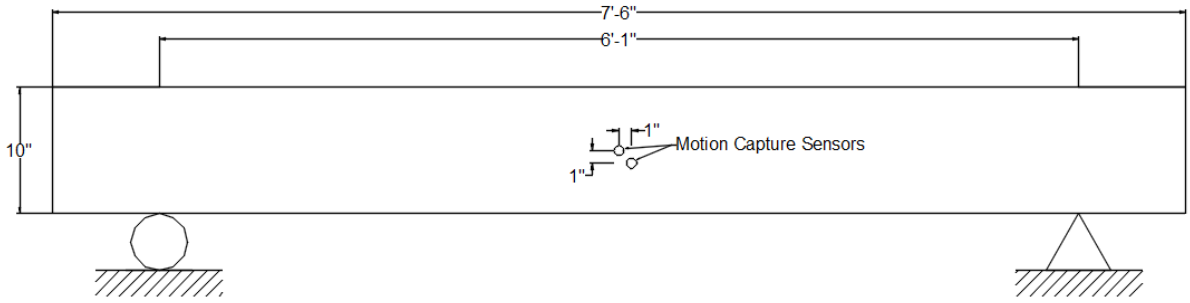

Figure 16: Location of Motion Capture Sensors (Lopez, 2018)

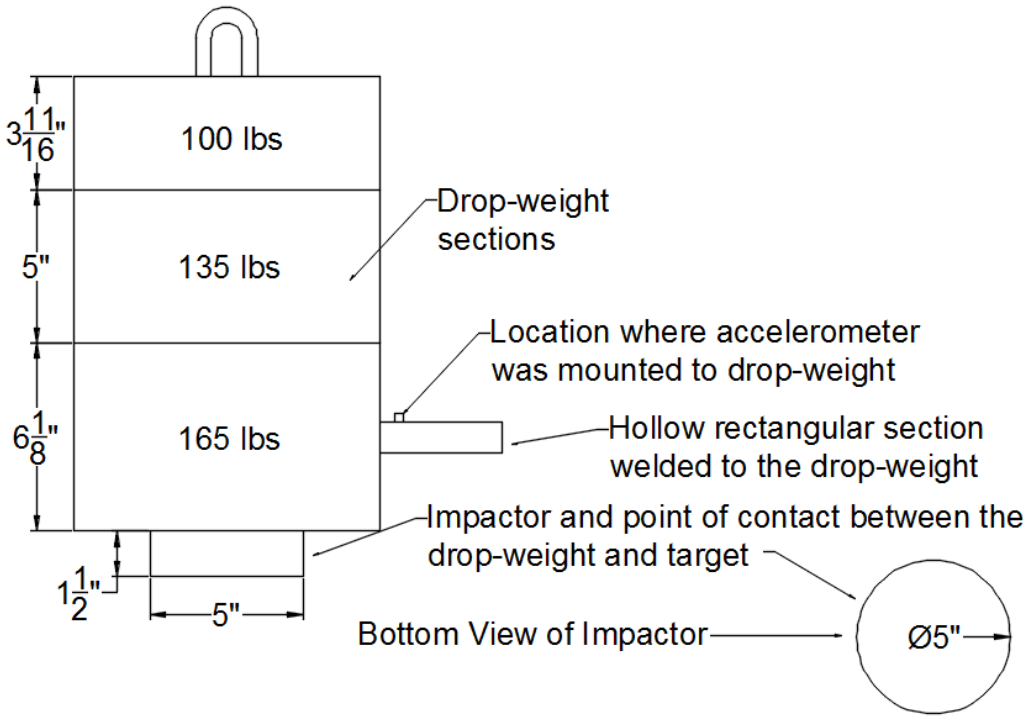

Figure 17: Drop Weight Schematic (Lopez, 2018)

Figure 18: Drop Weight at Top of Steel Sleeve (Lopez, 2018)

Figure 19: Anterior View of Fractured Impact Beam Specimens (Lopez, 2018)

3.4 Machine Learning Prediction Modeling

Machine learning is a highly disciplinary field in which computer algorithms build mathematical models based on a training data set to make predictions or decisions. Machine learning strategies have been used by researchers to predict the mechanical properties of concrete and other materials with great accuracy (Feng et al. (2020), Young et al. (2019), Ziolkowski and Niedostatkiewicz (2019)). There are many factors that can influence the mechanical properties of concrete, which often can not be accurately accounted for by design expressions. Machine learning algorithms are able to use training data sets to learn the correlations between all included parameters that influence an outcome to develop accurate outcome predictions.

3.4.1 Decision Trees

Decision trees is a machine learning method for classification and regression problems. Decision trees are “rule-based” models that identiy logical splits in the data based on parameters and sorts the data accordingly (Young et al., 2019).

The decision trees are made up of nodes and leaves. The nodes are the splits within the decision tree in which a question about the data must be answered, which comes in a form of a yes or no

question. The model splits the dataset based on various parameters in the dataset. For an analysis of SFRC, these parameters are the mixture proportions and fiber properties used with each SFRC mixture. As the model moves through the decision tree, it is directed by each node as it approaches a final outcome. The leaves represent the final point of a branch in which a value of a prediction, or a data class, is determined. One method of improving the accuracy of the classification tree models is by pruning the trees. Within the pruning process, the overall size of the decision tree is diminished by removing nodes that have little power in classifying the predictions. Over pruning is a possibility as a tree that is too small may not accurately depict the sample data, however too large of a tree could potentially overfit the data and generate inaccurate predictions.

Behnood et al. (2017) developed a M5P model tree algorithm using 1,912 distinctive data records acquired from literature to predict the compressive strength of normal concrete (NC) and high-performance concrete (HPC). Models trees are able to provide mathematical equations and are easier to develop and implement. These types of models are capable of estimating linear relationships between input and output variables (Behnood et al., 2017). Figure 20 illustrates the decision tree model developed from this study.

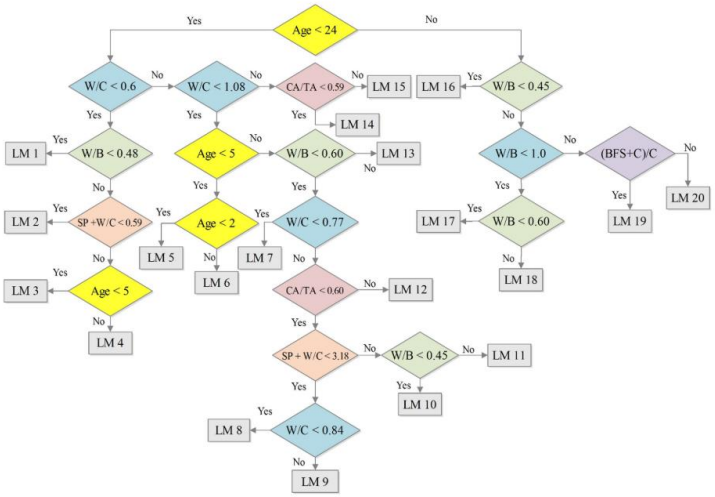

Figure 20: Generated Decision Tree using M5P Algorithm (Behnood et al., 2017)

Chou et al. (2014) provided a comprehensive study using advanced machine learning techniques and base learners to predict the compressive strength of HPC. Covering individual and ensemble learning classifiers constructed from four different base learners; multilayer perception (MLP), neural network, support vector machine (SVM), classification and regression tree (CART), and linear regression (LR). The conclusion drawn from this review was that ensemble learning techniques are better than individual learning techniques, and validated the applicability of ML, voting, bagging, and stacking techniques for simple and efficient simulations of concrete compressive strength.

Deepa et al. (2010) used classification algorithms such as multilayer perceptron, M5P tree models, and linear regression to predict the compressive strength of concrete. The data used was collected from other studies in India. M5P is a reconstruction of Quinlan's M5 algorithm for inducing trees of regression models. M5P combines a conventional decision tree with the possibility of linear regression functions at the nodes (Deepa et al., 2010).

Deepa et al. assessed the accuracy of these models by examining the root mean square error (RMSE), the mean absolute error (MAE), and the coefficient of determination (R^2). These were computed using Equations 9 - 11.

$$RMSE = \sqrt{1/n \sum_{i=1}^{n} (Pi - Ai)^2} \tag{9}$$

$$MAE = 1/n \sum_{i=1}^{n} |Pi - Ai| \tag{10}$$

$$R^2 = \frac{\sum_{i=1}^{n} (Pi - \bar{P})(Ai - \bar{A})}{\sqrt{\sum_{i=1}^{n} (Pi - \bar{P})^2 \sum_{i=1}^{n} (Ai - \bar{A})^2}} \tag{11}$$

This study conducted by Deepa showed that tree-based models perform remarkably well in predicting the compressive strength of concrete mixtures. Reporting the results shown by Table 2.

Table 2: Compressive Strength Prediction Models Accuracy Summary (Deepa et al., 2017)

Technique	R^2	RMSE	MAE	Time Taken (s)
Multilayer Perception	0.7908	9.9054	7.678	2.06
Linear Regression	0.7009	11.1066	8.8388	0.02
M5P Model Tree	0.8872	7.1874	5.008	0.41

3.5 Literature Review Summary

This literature review covered various aspects of FRC, such as commonly used fiber types, applications, specifications, and design of FRC, mechanical properties of SFRC, and use of machine learning methods for strength predictions. The key takeaways from the literature review are as follows:

- Various studies have shown that fiber reinforced concrete exhibits enhanced compressive and flexural strengths in comparison to conventional concrete mixtures. While hardened properties of FRC are enhanced, the use of chemical admixtures is recommended to correct the decreased workability of fresh FRC mixtures in comparison to conventional concrete.
- Fiber reinforcement is a promising alternative to conventional steel reinforcement in large-scale concrete beams. Reinforced FRC beams exhibit greater toughness, increased ductility, and greater ultimate loads compared to conventional reinforced concrete beams.
- Machine learning methods are a promising strength prediction option. The use of machine learning techniques allow for all aspects of concrete mixture proportioning to be taken into account when developing predictions. Additionally, there are few machine learning models deployed for SFRC strength predictions.

4.0 PROBLEM STATEMENT

Some state DOT's have updated their infrastructure standards and specifications to include language regarding fiber reinforcement within concrete mixtures for applications such as bridge decks and overlays (Roesler et al., 2019). Increased impact energy absorption, flexural strength, shear strength, and tensile strength are provided by fiber reinforcement. Implementations of fibers into the concrete matrix up to 1.50% volume fraction can increase the flexural strength by 150% and the direct tensile strength by up to 40% (PCA, 2015). As of now, GDOT has no provisions for steel fiber reinforcement within concrete. Inclusion of steel fibers could lead to reduction of steel reinforcing bars or concrete thickness in suitable applications, such as concrete median barriers (CMBs). Ultimately, the use of FRC leads to materials, time, and cost savings.

The purpose of this study was to investigate the potential use of steel fibers as a partial replacement for shear and longitudinal reinforcement in concrete members subjected to intense loading. The first phase of this project involves the development and batching of preliminary investigative mixtures to determine the influence of aspect ratios, end anchorages, and volume fractions on the properties of both fresh and hardened concrete. The following properties of fresh concrete were measured: slump, unit weight, air content, and temperature. The compressive strength and modulus of rupture (MOR) were measured for each SFRC mixture. Based on the results of this testing phase, fiber types and quantities were selected for large-scale beam testing in Phase II. Phase II focused on measuring the flexural and shear capacities of beams constructed with chosen SFRC mixtures. Within Phase II, steel reinforcement optimization is performed considering the added strength from the steel fibers. Tensile steel is balanced and the ability of the

fibers to act as shear reinforcement is studied. Lastly, Phase III explores employing machine learning methods to develop accurate prediction models for SFRC compressive strength and MOR. Using the data collected within this study and previous research documented within the Chapter 3, decision tree models were trained and used to estimate the mechanical properties of other GDOT mixtures using steel fiber reinforcement.

The ultimate goal of this work was to assess the potential to reduce the required materials needed for reinforced concrete members through the use of SFRC. One potentional application would be CMB walls, which are frequently subjected to vehicular impact loading. The impact force could cause concrete shrapnel to be hurtled out, raising safety concerns for those involved in the vehicular crash and bystanders nearby. GDOT constructed over 42,000 LF (12,802 m) of CMBs in 2013, (Darling, 2017). Reduction of reinforcing steel bars or concrete thickness of CMBs could lead to substantial economic savings for the GDOT. Another suitable application would be concrete roads or bridge decks. By enhancing the strength of the concrete and resistance to cracking, the design thickness of roads or bridge decks could be lowered.

5.0 CONCRETE MATERIALS

5.1 Materials

Type I/II portland cement, natural coarse and fine aggregates, industrial steel fibers, and admixtures were used in this research.

5.1.1 Cementitious Materials

Type I/II portland cement was used within this study as per ASTM C150/C150M-19 *Standard Specification for Portland Cement*. This was in accordance with Section 830 of the GDOT Supplemental Specification manual. Physical and chemical properties of the Type I/II portland cement used in this study are shown in Table 3.

Table 3: Chemical and Physical Properties of Type I/II Cement

Chemical and Physical Properties		Test Results	ASTM C150 Specifications
SiO_2	(%)	19.7	---
Al_2O_3	(%)	4.7	6.0 max
Fe_2O_3	(%)	3	6.0 max
CaO	(%)	63.3	---
MgO	(%)	3.1	6.0 max
SO_3	(%)	3.2	3.0 max
CO_2	(%)	1.7	---
Limestone	(%)	4	5.0 max
$CaCO_3$ in Limestone	(%)	98	70 min
C_3S	(%)	54	---
C_2S	(%)	15	---
C_3A	(%)	7	8 max
C_4AF	(%)	9	---
$C_3S + 4.75\ C_3A$	(%)	89	100 max
Loss of Ignition	(%)	2.7	3.0 max
Blaine Fineness	(cm^2/g)	387	260 - 430
Air Content of PC Mortar	(%)	8	12 max
Specfic Gravity		3.16	---

5.1.2 Natural Aggregates

Natural aggregates used within this research were locally sourced from Athens, Georgia, and meet ASTM C33/C33M-18 *Standard Specification for Concrete Aggregates.* Hansen Aggregates provided graded #57 coarse aggregate stone consisting of a nominal maximum aggregate size (NMAS) of 1 in (2.54 mm). Fine aggregate was sourced from Redland Sand, Inc. in Watkinsville, Georgia, for this study. As per ASTM C33, a sieve analysis was performed on both the coarse and fine aggregates. The results of these analyses are shown in Figures 21 and 22, respectively.

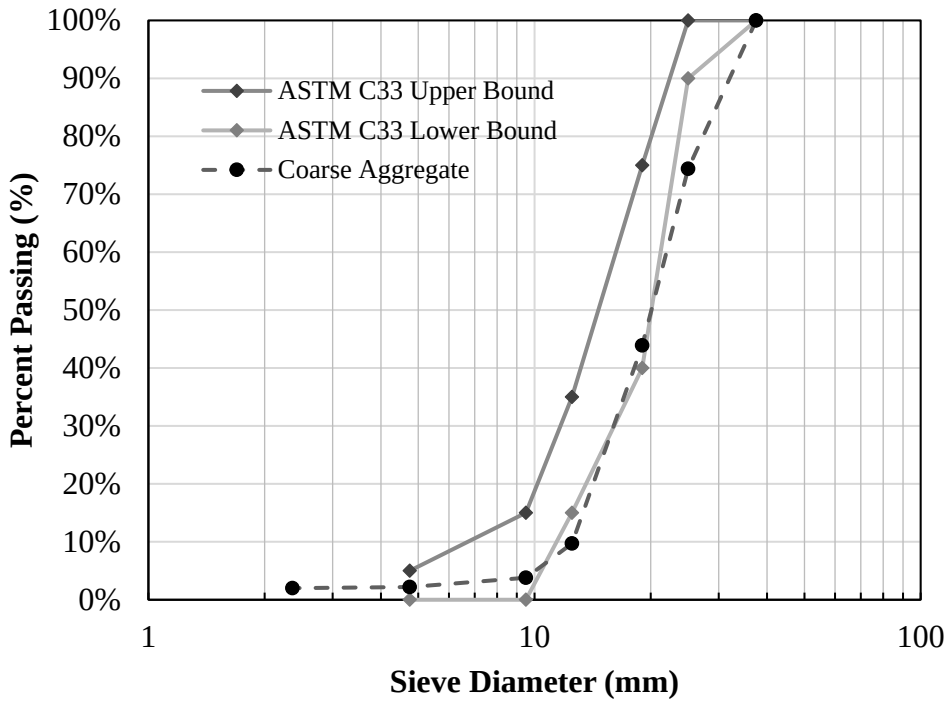

Figure 21: Sieve Analysis of Natural Coarse Aggregate per ASTM C33

The sieve analysis of the natural coarse aggregate shows that the provided coarse aggregate falls slightly below the ASTM C33 lower bound specification for two sieve sizes. This indicates that the coarse aggregate is slightly coarser than specifications call for. This has been deemed acceptable by the research team.

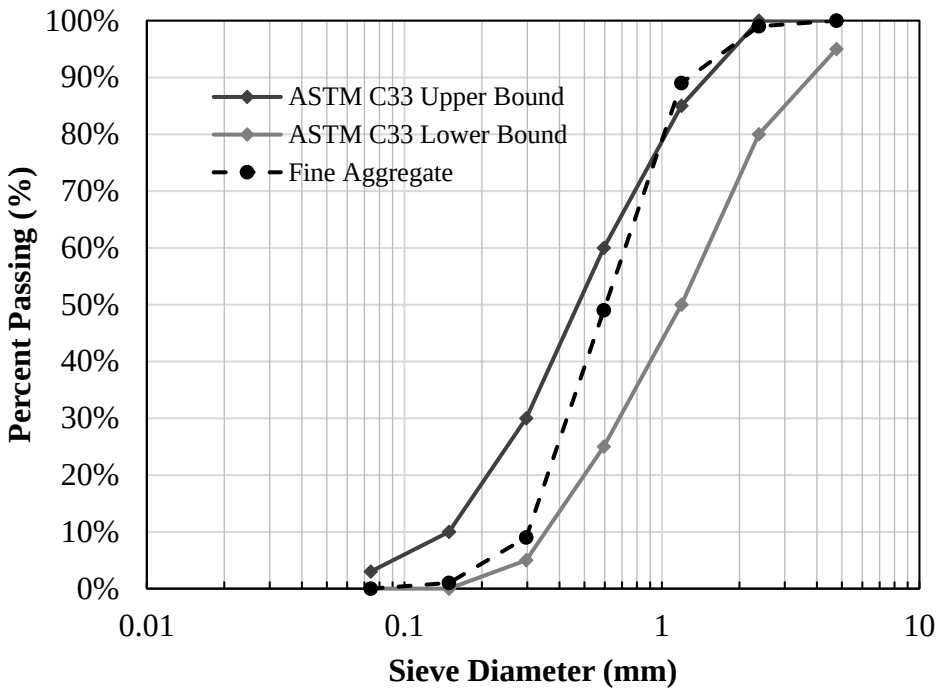

Figure 22: Sieve Analysis of Natural Fine Aggregate per ASTM C33

5.1.3 Fiber Reinforcement

Four types of Dramix® steel fibers supplied by the Bekaert Corporation were used in this study. Fibers varied in geometries, mainly in length and end anchorage. The fiber types and properties used within this study are listed in Table 4. The fiber name provides information on the fiber geometry. Within the description "3D/45", 3D refers to the end anchorage, and 45 refers to the aspect ratio, or the length of the fiber divided by the diameter. All fibers used within this research were galvanized for improved corrosion resistance. Fibers 3D/80, 4D/65, and 5D/65 are all glued bundles held together by water-soluble glue that breaks apart during the mixing process. The 3D/45 fibers are loose, non-glued fibers. These fibers possess a Youngs' modulus of 29,000 ksi (200,000 MPa) and 0.80% strain at ultimate strength. Figure 23 illustrates the different lengths and end anchorages, while Figure 24 shows the difference between the loose fibers (3D) and the glued fibers (4D and 5D).

Table 4: Physical Properties of Type I/II Cement

Fiber Types and Properties

Fiber Name	Length, in. (mm)	Diameter, in. (mm)	Aspect Ratio	Min Dosage, lb/yd^3 (kg/m^3)	Tensile Strength, ksi (MPa)
Dramix® 5D/65	2.4 (60)	0.04 (0.90)	65	25 (15)	334 (2,300)
Dramix® 4D/65	2.0 (50)	0.03 (0.75)	65	34 (20)	261 (1,800)
Dramix® 3D/80	2.4 (60)	0.03 (0.75)	80	17 (10)	178 (1,225)
Dramix® 3D/45	1.4 (35)	0.03 (0.75)	45	18 (10)	178 (1,225)

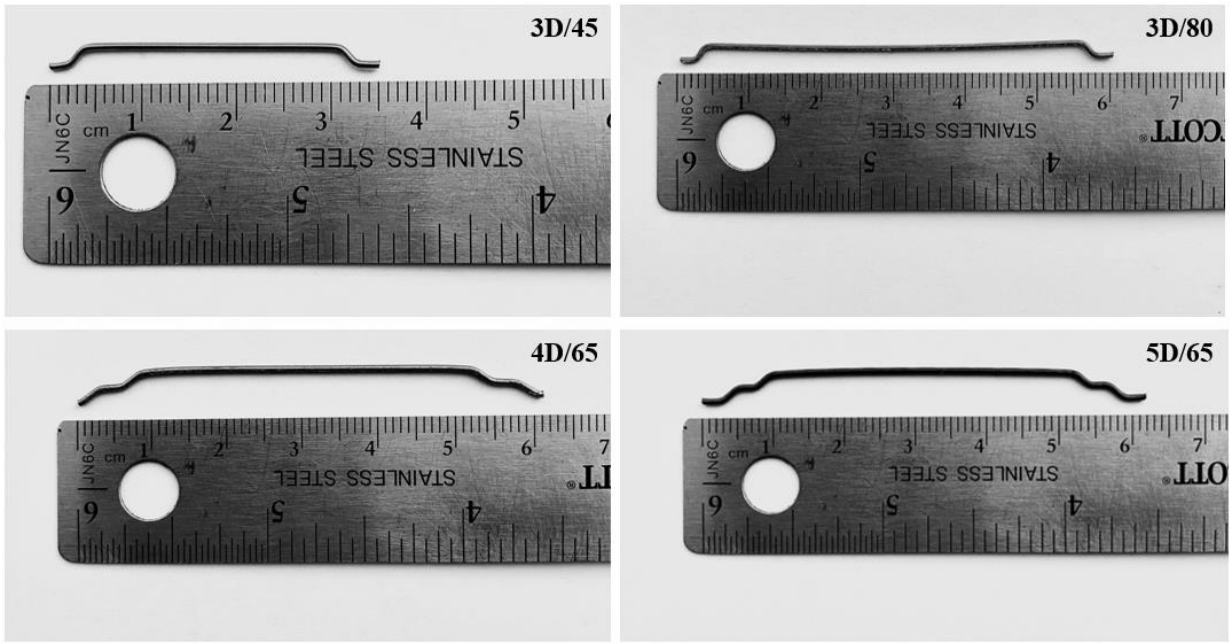

Figure 23: Dramix® Steel Fibers Used

(a) Loose Fibers (b) Glued Fibers

Figure 24: Comparison of Loose and Glued Fibers

5.1.4 Chemical Admixtures

Fibers greatly affect the workability of concrete as discussed in Chapter 3. In addition, the air content is typically lowered as a result of the extended mixing time necessary to adequately disperse the fibers throughout the concrete mixture. To combat these effects, High Range Water-Reducing Admixture (HRWRA), Viscosity Modifying Admixture (VMA), and Air Entraining Admixture (AEA) were used to enhance the homogeneity, fluidity, and air content of the mixtures. Admixtures were supplied by GCP Advanced Technologies. The admixtures used and the recommended dosages are summarized in Table 4.

Table 5: Admixtures Used and Recommended Dosages

Admixture	GCP Admixture Used	Recommended Dosage, fl oz / 100 lbs (mL / 100 kg)
HRWRA	ADVA® 198	3 to 6 (195 to 375)
VMA	V-MAR® F100	3 to 12 (195 to 780)
AEA	DAREX® AEA	1/2 to 3 (30 to 195)

ADVA® 198 is a HRWRA that is polycarboxlate-based and designated by ASTM C494 as a Type A and F admixture. This HRWRA was utilized to increase the slump of the concrete while maintaining a low water content. V-MAR® F100 was selected as the VMA to modify the concrete rheological properties, increasing the lubrication and improving surface texture. Finally, DAREX® AEA was used to impart workability into the mix by increasing the amount of semi-microscopic air bubbles in the mix. DAREX® AEA is formulated for job site mixers and highway pavers.

6.0 EXPERIMENTAL PLAN

6.1 Research Objective

The objective of this research is to analyze the potentials of SFRC for use in GDOT applications, such as CMB walls, bridge decks, slabs, or other applications. Research shows that SFRC mixtures provide many benefits, including enhanced flexural strength, ductility, shear strength, and energy absorption capabilities in comparison to conventional concrete. Many state DOTs, such as Florida DOT (FDOT), Minnesota DOT (MnDOT), Colorado DOT (CDOT), and others throughout the United States has approved specifications on the use of fibers within concrete applications, such as those discussed in Chapter 3. This research focuses on an experimental investigation into material reduction and improved peformance of structural concrete elements through the utilization of steel fibers in standard GDOT concrete mixtures. This is achieved in part through steel reinforcement optimization of SFRC beams. Four geometrically different steel fibers are considered for this investigation.

Phase I of this study investigated trial batches at varying fiber volume fractions to determine fresh and hardened properties of SFRC mixtures. The findings of phase I were used to determine a fiber geometry and concentration for use in Phase II. In Phase II, expressions for SFRC strength found in literature are applied for the optimization of tensile and shear steel reinforcement in reinforced concrete beams. Experimental load-deflection tests were performed on large scaled beam specimens and compared with published expressions. The SFRC beams examined in this phase consisted of different amounts of steel reinforcement. Phase III used the data collected from this study to train machine learning models to predict the compressive and flexural strengths of

GDOT standard mixtures containing steel fiber reinforcement. Using data collected from previous work and from this study, a database was constructed and used to develop classification and regression tree models to predict hardened properties of GDOT mixtures containing SFRC.

The ultimate goal of this study was to analyze the potential use of steel fiber reinforcement in GDOT standard concrete mixtures. Implementing steel fiber reinforcement into these standard concrete mixtures can lead to enhanced mechanical performance and potential material and cost savings.

6.2 Research Methodology

6.2.1 Overview

This research was conducted in three phases. In phase I, fresh and hardened properties of thirteen investigative SFRC mixtures were collected. The properties of these mixtures were analyzed and informed the selection of SFRC mixtures utilized in Phase II testing which involved scaled beam testing and design optimization. Phase II investigates the static loading responses of large-scale SFRC beams. Based on the results of Phase II the tensile and shear steel reinforcement is optimized for performance. This phase provides experimental data on the flexural and shear resistance provided by fibers. Phase III focuses on the development of machine learning models for estimating SFRC mechanical properties. These models are used to analyze the correlation between the SFRC mixture constituents and produce predictions of compressive strength and MOR based on the mixture parameters.

6.3 Phase I - Testing for Concrete Properties

The main objective of this phase is to determine the effects of aspect ratio and end anchorage on properties of SFRC. To accomplish this, thirteen mixtures were designed and tested which included a control mixture and SFRC mixtures with different fiber geometries at varying fiber

volumes percentages. Mixtures used Dramix® steel fibers and were batched with fiber volume fractions of 0.50%, 0.75%, and 1.00%. Fresh concrete properties, compressive strength, and MOR were measured and recorded for each mixture. Based on the observed properties, fiber geometries and quantity were selected for use in for large-scale SFRC beam testing. For investigative mixtures, the concrete mixture design constituents were held constant, whereby only the fiber amount and geometry changed to isolate the effect of fibers on concrete performance.

6.3.1 Mixture Design Proportioning

Concrete mixtures were designed based on GDOT Class AA concrete, for which the requirements are presented in Table 6. For all mixtures, cement content was maintained at 635 lb/yd^3 (375 kg/m^3) with a constant water to cement ratio (w/c) of 0.42. Mixtures were designed for a target slump of 3.0 in (76 mm) and an air content of 5%. The concentration of fibers was calculated as a percentage of the total volume of concrete. Dosages of chemical admixtures were determined based on recommendations made by manufacturers. Chemical admixtures HRWRA, VMA, and AEA were utilized to ensure workability of the concrete mixture.

Table 6: GDOT Concrete Class Specifications (2018)

English								
Class of Concrete	(2) Coarse Aggregate Size No.	(1 & 6) Minimum Cement Factor lbs/yd^3	Max Water/ Cement ratio lbs/lb	(5) Slump acceptance Limits (in) Lower-Upper		(3 & 7) Entrained Air Acceptance Limits (%) Lower-Upper		Minimum Compressive Strength at 28 days (psi)
"AAA"	67,68	675	.440	2	4	2.5	6.0	5000
"AA1"	67,68	675	.440	2	4	2.5	6.0	4500
"AA"	56,57,67	635	.445	2	4	3.5	7.0	3500
"A"	56,57,67	611	.490	2	4	2.5 (3)	6.0	3000
"B"	56,57,67	470	.660	2	4	0.0	6.0	2200
"CS"	56,57,67 Graded Agg.*	280	1.400	-	3½	3.0	7.0	1000 (4)

Table 6: GDOT Concrete Class Specifications (2018) Cont.

metric								
Class of Concrete	(2) Coarse Aggregate Size No.	(1 & 6) Mini mum Cement Factor kg/m^3	Max Water/ Cement ratio kg/kg	(5) Slump acceptance Limits (mm) Lower - Upper		(3 & 7) Entrained Air Acceptance Limits (%) Lower-Upper		Minimum Compressive Strength at 28 days (MPa)
"AAA"	67,68	400	.440	50	100	2.5	6.0	35
"AA1"	67,68	400	.440	50	100	2.5	6.0	30
"AA"	56,57,67	375	.445	50	100	3.5	7.0	25
"A"	56,57,67	360	.490	50	100	2.5 (3)	6.0	20
"B"	56,57,67	280	.660	50	100	0.0	6.0	15
"CS"	56,57,67 Graded Agg.	165	1.400		90	3.0	7.0	7 (4)

6.3.2 Mixture Design

6.3.2.1 Phase I mixtures and Identification

A mixture identification system was developed to display information of each mixture efficiently. An example of the mixture identification is 3D/45/0.5. First, the type of end anchorage (3D, 4D, or 5D) is shown, followed by the fiber's aspect ratio, then the total fiber volume percentage. As previously stated, the fiber volume content varied from 0.50% to 1.00% in 0.25% increments. These volume percentages were selected based on current published research reviewed within Chapter 3. It has been shown that the benefits of steel fibers peak at volume percentages of 1.50%. However, concrete mixtures in which the fiber volume surpasses 1.00% typically produce unworkable concrete. Table 7 lists the mixture design for the twelve SFRC mixtures tested during the Phase I investigation. Each mixture studied in Phase I are variations of the control mixture. This allows for the hardened property enhancements obtained by the use of fibers to be examined independently and not influenced by other variables of the concrete mixture.

Table 7: Phase I Mixture Design Matrix (SSD).

Mix Description	W/C	Cement, lb/yd^3 (kg/m^3)	Coarse Aggregate, lb/yd^3 (kg/m^3)	Fine Aggregate, lb/yd^3 (kg/m^3)	Steel Fiber, lb/yd^3 (kg/m^3)
Control	0.42	635 (375)	1800 (816.4)	1135 (514.8)	0
3D/45/0.50	0.42	635 (375)	1800 (816.4)	1135 (514.8)	65.70 (29.8)
3D/80/0.50	0.42	635 (375)	1800 (816.4)	1135 (514.8)	65.70 (29.8)
4D/65/0.50	0.42	635 (375)	1800 (816.4)	1135 (514.8)	65.70 (29.8)
5D/65/0.50	0.42	635 (375)	1800 (816.4)	1135 (514.8)	65.70 (29.8)
3D/45/0.75	0.42	635 (375)	1800 (816.4)	1135 (514.8)	98.60 (44.7)
3D/80/0.75	0.42	635 (375)	1800 (816.4)	1135 (514.8)	98.60 (44.7)
4D/65/0.75	0.42	635 (375)	1800 (816.4)	1135 (514.8)	98.60 (44.7)
5D/65/0.75	0.42	635 (375)	1800 (816.4)	1135 (514.8)	98.60 (44.7)
3D/45/1.00	0.42	635 (375)	1800 (816.4)	1135 (514.8)	131.4 (59.6)
3D/80/1.00	0.42	635 (375)	1800 (816.4)	1135 (514.8)	131.4 (59.6)
4D/65/1.00	0.42	635 (375)	1800 (816.4)	1135 (514.8)	131.4 (59.6)
5D/65/1.00	0.42	635 (375)	1800 (816.4)	1135 (514.8)	131.4 (59.6)

6.3.3 Concrete Mixture Production and Curing

6.3.3.1 Batching Preparations

Concrete batching was performed in a 12.5 ft^3 capacity Workman II Multimixer and procedures outlined by ASTM C192/C192M-18 *Standard Practice for Making and Curing Concrete Test Specimens in the Laboratory* were followed. Materials were first collected and weighed in color coded five-gallon plastic buckets. Buckets containing cementitious materials were sealed with a lid to prevent hydration as a result from moisture in the air. Moisture content of the coarse and fine aggregates was taken prior to batching to make any necessary water adjustments due to aggregate moisture. Admixtures were measured and added to the water prior to mixing.

6.3.3.2 Preparation of Molds

Preparation of molds followed the procedures outlined in ASTM C192/C192M-18 *Standard Practice for Making and Curing Concrete Test Specimens in the Laboratory.* Specimen molds were placed together and greased to ensure that the concrete does not stick to the mold during the

demolding process. After greasing, molds were kept inside with a plastic tarp near the area to be stored. Six compressive strength cylinders measuring 4.0 in x 8.0 in (101.6 mm x 203.2 mm), and three MOR beams measuring 3.0 in x 4.0 in x 16.0 in (76.2 mm x 101.6 mm x 406.4 mm) were made per batch.

6.3.3.3 Mixing Procedures

The multimixer was "buttered" by adding a small amount of cement and water to the mixer to help with sticking of concrete prior to batching each mixture. Once the water was drained from the mixer, coarse aggregate was added along with a small amount of water containing admixtures. Once the surface of the coarse aggregate was saturated, fine aggregate was added followed by incrementally adding cement and the rest of the allocated water. Once all materials, excluding the fibers, were added to the mixer the concrete was mixed for an additional three minutes. A slump test was performed on the mixed concrete prior to the addition of the steel fibers. As per the steel fiber manufacturers specifications, the fibers were then added incrementally to the concrete and mixed for an additional three minutes to allow for the fibers to become evenly distributed throughout the mixture. Three of the four fibers used in this study are initially held together by a water-soluble glue that dissolves when in contact with the mixtures water. For this reason, it is important to allow the concrete to continue mixing such that the fibers are properly distributed throughout the mixture. Once the mixing was deemed complete by visual inspection, the concrete was placed into a dampened wheelbarrow and transported to the testing and specimen fabrication location.

6.3.3.4 Placement of Testing Specimens

The fiberous concrete renders a slump less than 1.0 in (25.4 mm), therefore, a vibration table was used to help with concrete consolidation within the specimen molds. Cylinders were placed on the

vibration table and a tamping rod was used to internally consolidate the concrete per ASTM C192/C192M-18 *Standard Practice for Making and Curing Concrete Test Specimens in the Laboratory*. Cylinders were placed in two equal layers and a steel 0.4 in (10.0 mm) tamping rod was used to perform the internal consolidation. Each layer was tamped 25 times with the rod to ensure consolidation and blending of the two layers. Before placement in the designated curing location, the top surface of the cylinder was finished to obtain a smooth surface. MOR beams were placed in two layers of equal volume and internally consolidated with a steel 0.6 in (16.0 mm) tamping rod before surface finishing and movement to the curing location. Test specimens were demolded 24 $\pm$ 8 hours after placement and placed in a moist curing tank.

6.3.3.5 Curing of Concrete Specimens

Once the test specimens were demolded, they were labeled with the respected mixture identification and placement date then placed within a curing tank. The curing tank was filled with water, containing a calcium hydroxide concentration to promote lime saturation, maintained at a temperature between 69.8 ˚F and 77.0 ˚F (21 ˚C and 25 ˚C) using a heater and circulation pump in accordance with ASTM C511-13 *Standard Specification for Mixing Rooms, Moist Cabinets, Moist Rooms, and Water Storage Tanks Used in the Testing of Hydraulic Cements and Concretes.* For Phase II mixtures, concrete cylinders were cured underneath moist burlap sacks and thick plastic, along with their respective large-scale beams, for consistency.

6.3.4 Fresh Concrete Property Testing

Slump, unit weight, temperature, and air content was tested on the fresh concrete. The slump test was performed prior to the addition of fibers per fiber manufacturer's specifications. These tests were performed per outlined standards set by GDOT, American Society for Testing and Materials (ASTM), and American Association of State and Highway Transportation Officials (AASHTO)

specifications. Table 8 summarizes the respected specification for each of the fresh concrete property tests performed.

Table 8: Fresh Concrete Property Tests and Specifications

Fresh Concrete Tests	Standard Identification	Test Intervals
Slump	ASTM C143/C143M-15a, AASHTO T 119	Batching Day
Unit Weight	ASTM C138/C138M-17a, AASHTO T 121	Batching Day
Temperature	ASTM C1064/C1064M-17, AASHTO T 309	Batching Day
Air Content	ASTM C231/C231M-17a, AASHTO T 152	Batching Day

6.3.5 Hardened Concrete Property Testing

Compressive strength and modulus of rupture (MOR) were measured for the hardened concrete. The compressive strength was tested at 1, 7, and 28 days of age. MOR was measured at 28 days of age. The compressive strength and flexural strength tests were performed ultizing the procedures outlined by ASTM and AASHTO standards, summarized in Table 9. The basis of Phase II testing involving large-scale static and impact beam testing of SFRC beams was based on the data collected (fiber geometries and volume concentration) from the Phase I trial mixtures.

Table 9: Hardened Concrete Property Tests and Specifications

Hardened Concrete Tests	Standard Identification	Test Intervals
Compressive Strength	*ASTM C-39*, AASHTO T 22	1, 7, 28 Days
Flexural Strength	*ASTM C-78*, AASHTO T 97	28 Days

6.3.6 Data Analysis

This experimental design outlined in the Phase I investigation allowed for the influence of the industrial steel fiber geometries and volume concentrations on concrete mixtures to be examined. Fresh properties were analyzed to ensure that mixtures meet requirements set forth by GDOT and were suitable for both cast-in-place and precast applications. It was paramount to ensure that the designed mixtures were suitable for industry use. Compressive strength and MOR were measured

to determine which fiber geometry and concentration yields the largest enhancement of concrete hardened properties. Additionally, failure modes of the compressive test cylinders were considered when analyzing the results. A statistical analysis was performed on compressive and flexural strength results to better understand the level of influence variables such as fiber aspect ratio, end anchorage, and volume concentration had on concrete properties. Results from statistical analysis was considered when concluding which fiber geometry to use in Phase II testing.

6.3.7 Design Summary

Phase I provides insight into the influence of fiber aspect ratio, end anchorage, and volume concentration on concrete properties. From the investigative mixtures, parameters such as optimal fiber concentration and geometry were selected. Because each fiber within this study has a slightly different geometry, each fiber influences concrete properties differently than other fibers of equal volume concentration. Results were analyzed for the selection of SFRC mixtures with favorable properties for large-scale beam testing. Considerations such as overall concrete strength benefits, workability, failure modes, and cost were weighed when deciding on a mixture for further testing within Phase II.

6.4 Phase II – Testing of Laboratory-Scale Beam for Static Loading

Phase II involved subjecting laboratory-scale SFRC beams to static loading. Laboratory-scale beam testing provided experimental data necessary for the optimization of reinforced concrete member designs. Within this phase, SFRC beams with varying levels of shear reinforcement were made and subjected to static loading utilizing a 220-kip (978.6 kN) hydraulic actuator at the University of Georgia STRuctural ENGineering Testing Hub (STRENGTH) laboratory. A load-deflection curve was developed by performing a three-point bending test on laboratory-scale beams. Toughness, or the total energy required to deform a material, was calculated by summing

the area under the load-deflection curve. The flexural toughness parameters were obtained through the three-point static bending test. This information provides insight into the amount of energy that the SFRC material is able to dissipate during deformation.

6.4.1 Beam Configuration

A total of eight beams were used in this testing phase measuring 90.0 in L x 6.0 in W x 10.0 in D (2286.0 mm x 152.4 mm x 254.0 mm). All beams utilized steel reinforcement with a Young's modulus of 29,000 ksi (200,000 MPa) and a minimum yield strength of 60,000 psi (420 MPa). The reinforcement for the control beam included 2 – #3 longitudinal bars and 2 – #4 longitudinal bars for the compressive and tensile reinforcement, respectively, resulting in a reinforcement ratio of 0.80%. These bars were held in place with #2 stirrups spaced at 4.0 in (101.6 mm) on center. A preliminary set of laboratory-scale SFRC static beams were tested prior to reinforcement optimization to better understand the load vs. deflection results of the SFRC mixtures. Like Lopez and Tate, SFRC beams included a third steel reinforcing bar in the tensile region of the beam to balance the tensile strength with the increased compressive strength of the fibrous concrete. Results of the preliminary static beam tests were considered when determining reinforcement designs for additional SFRC beams. Table 10 summarizes the designs for all eight beams batched within this study phase. Each of the eight beams tested within this study phase varied in either mixture design or reinforcement ratio. Figure 25 illustrates the longitudinal cross-sections of the laboratory-scale beams with varying shear reinforcement ratios. Figure 26 illustrates cross-sections of laboratory-scale beams with varying tensile reinforcement ratios.

Table 10: Phase II Beam Design Summary

Beam ID	ρ	Concrete Mixture	Shear Reinforcement	Tests
C1	0.80%	Control	#2 Stirrups 4 in o.c.	Flexure
C2	0.80%	Control	#2 Stirrups 4 in o.c.	Flexure
B1	1.21%	3D/45/0.50	#2 Stirrups 4 in o.c.	Flexure
B2	1.21%	3D/80/0.50	#2 Stirrups 4 in o.c.	Flexure
B3	1.21%	4D/65/0.50	#2 Stirrups 4 in o.c.	Flexure
B4	1.21%	5D/65/0.50	#2 Stirrups 4 in o.c.	Flexure
B5	1.21%	4D/65/0.50	#2 Stirrups 8 in o.c.	Flexure
B6	1.03%	4D/65/0.75	#2 Stirrups 4 in o.c.	Flexure
B7	1.03%	4D/65/0.75	#2 Stirrups 8 in o.c.	Flexure

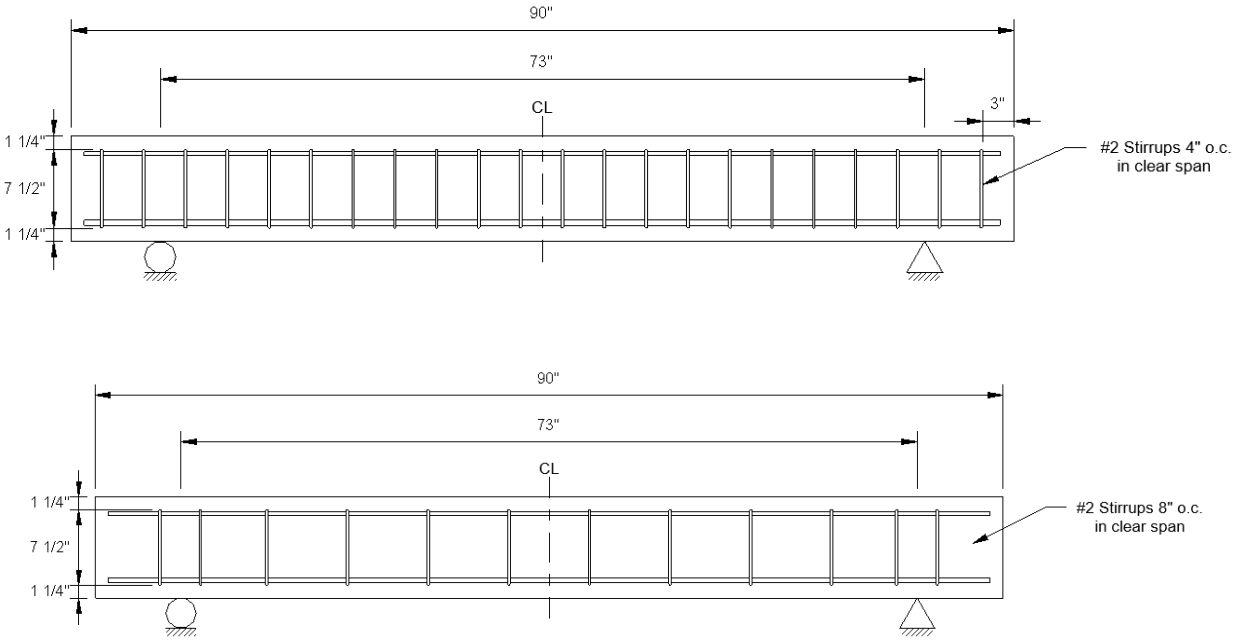

Figure 25: Longitudinal Cross Sections of Laboratory-Scale Beams

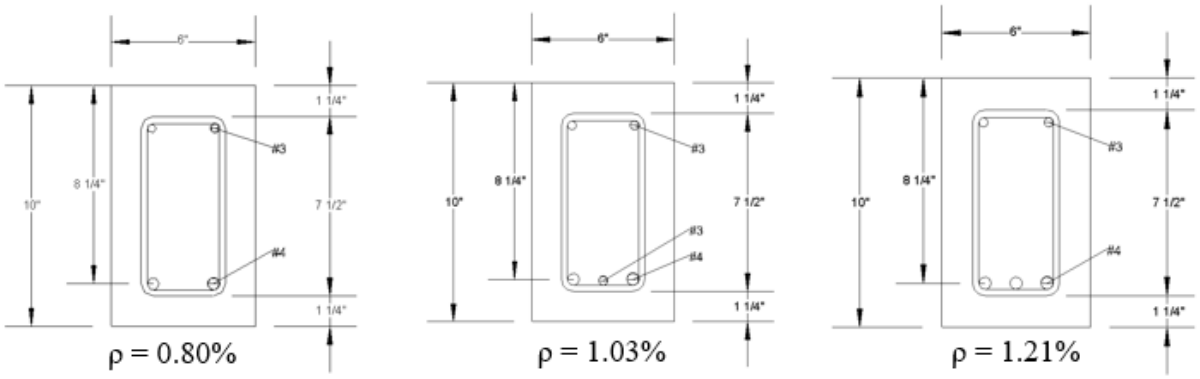

Figure 26: Cross Sections of Laboratory-Scale Beam Specimens

6.4.2 Laboratory-Scale Static Beam Testing

Laboratory-scale static beam testing was performed by applying a load at the midspan of the simply supported reinforced concrete beam. From the three-point bending test, the toughness of the FRC beams was measured by integrating the load-deflection curve. This testing allowed for the observation of crack formation over time as the deflection increased. To begin this phase of the study, five beams (one control, and one for each fiber type at a 0.50% fiber by volume concentration) were batched for static testing to determine the impact each steel fiber geometry had on SFRC beams flexural performance when subjected to three-point bending. Results collected from these initial tests were used in conjunction with results from Phase I testing for the selection of an SFRC mixture used in the remainder of the study phase. A SFRC mixture was selected, and additional SFRC beams were batched using the selected mixture for static testing. With the selection of a new mixture design for SFRC beams, the tensile reinforcement was balanced with the compressive strength provided by the selected mixture and shear reinforcement was varied as per the beam designs denoted in Table 10.

6.4.2.1 Static Beam Test Configuration

The static test configuration using the hydraulic actuator is shown by Figure 27. The scaled beams were supported by steel wide flange columns on pin and roller supports to prevent the development of axial forces that could lead to artificial strut action. A pin and roller supported beam system was chosen to allow for movement of the beam at the roller support as mid-span deflection increased. The total unsupported span length was 73.0 in (1854.2 mm). A 220-kip (978.6 kN) hydraulic actuator was used to apply a load a midspan, where a steel plate measuring 0.5 in x 14.8 in x 14.8 in (12.7 mm x 374.7 mm x 374.7 mm) was used to distribute the load to the beam. The steel plate was used to distribute the load such that a three-point bending test was performed. The hydraulic actuator was set to deflection controlled, which increased at a fixed rate of 0.005 in (0.127 mm) per second.

Figure 27: Static Beam Test Setup

6.4.2.2 Mixture Design

Concrete mixtures for large-scale static beams were designed to meet the requirements of GDOT Class AA concrete. Cementitious content was held constant at 635 lb/yd^3 (375 kg/m^3) with a w/c of 0.42 for all beams. Preliminary static beams were batched containing a 3D, 4D, and 5D fiber geometries and a fiber volume percentage of 0.50%. Subsequent beams were batched using the 4D/65/0.75 mixture.

6.4.2.3 Beam Preparation

Each beam required two batches of concrete to be mixed separately due to capacity limitations of the drum mixer. Batches of concrete were placed in two layers and internally vibrated to ensure proper consolidation of concrete between the reinforcing steel and blending of the layers. Six compressive cylinders were prepared from each batch for testing. Beams were released from wooden molds one to two days after placement and covered with moist burlap and plastic tarps for curing. Compressive strength cylinders made from these batches were placed under moist burlap and plastic for consistency. Both the compressive strength cylinders and static beams were tested at 28 days of age.

6.4.2.4 Data Analysis

Static three-point testing was performed to develop a load-deflection curve. This was analyzed by integrating the function between load and mid-span deflection to determine the toughness of the SFRC mixtures. To calculate the toughness, the change in deflection (Δx) at various points was multiplied by the corresponding load measurement and summarized. Data from preliminary laboratory-scale static beam testing was used for optimization of the steel reinforcement design. Steel reinforcement ratios in conjunction with steel fibers were analyzed for balancing of the design. These results were used to draw conclusions on the energy dissipation capacities of the

SFRC mixtures. In addition to static testing, fresh properties and compressive strengths of the optimized mixtures were measured and reported.

6.5 Phase III – Mechanical Property Prediction Models

This study phase involved the use of machine learning classification and regression tree methods for the prediction of SFRC compressive strength and MOR values based on concrete mixture parameters. These models were developed using a database constructed with data from this experiemental study and from previously published literature. The database was split, 80% for the training data set used for training the model, and the remaining 20% as the test data set for comparison of the mechanical property predictions. The types of decision tree methods used were random forests, bootstrap aggregation or "bagging", and gradient boosting.

6.5.1 Data Acquirement

The data was acquired from various research papers that were published on the mechanical properties of SFRC. By collecting experimental results from various published investigations, an an established database for training a prediction model was created. From this literature review, concrete mixture proportions, fiber properties, and measured concrete mechanical property data was collected and categorized.

In total, the database included experimental results from 13 published sources (M. Acikgenc, Alyamac, Kursat E., Ulucan, Zulfu C. (2013), Al-Ameeri (2013), Alavi Nia et al. (2012), Campione and Letizia Mangiavillano (2008), Guerini et al. (2018), Guler et al. (2019), Y.-K. Kwak, Eberhard, Marc O., Kim, Woo-Suk, Kim, Jubum (2002), S.-J. Lee et al. (2019), Marar et al. (2016), Song and Hwang (2004), Soulioti et al. (2011), and Torres and Lantsoght (2019)) and results collected totallying 103 observations. The database constructed in Table 11 includes SFRC mixture properties cement proportion (cp) [lb/ft^3], coarse aggregate proportion (cap) [lb/ft^3],

fine aggregate proportion (fap) [lb/ft^3],, water to cement ratio (wc), fiber length (fl) [in], fiber aspect ratio (ar), volume of fibers (Vf) [%], and reinforcement index ($ri = Vf \times l_f / d_f$).

The experimental data taken from literature varies with respect to the cementitious material chemical properties, aggregate types, and mixture / curing processes. Some of the research papers only listed the aggregate proportions, and not the aggregate type or properties. Additionally, some reported mechanical property results in graphical form only, and results had to be extrapolated from the graphs for the purpose of this analysis. Histograms of the input parameters illustrating the range of data may be found in the Appendix.

Table 11: SFRC Mixture Parameter Database

Reference	Mix ID	Input Parameters									
		cp	**cap**	**fap**	**wc**	**fl**	**ar**	**Vf**	**ri**	**fc**	**mor**
Acikengc et al. (2013)	80/60	20	54	54	0.65	2.36	80	0.5	40	3550	544
	80/60	20	54	54	0.65	2.36	80	1	80	3400	725
	80/60	20	54	54	0.65	2.36	80	1.5	120	3300	943
	65/60	20	54	54	0.65	2.36	65	0.5	32.5	3550	1189
	65/60	20	54	54	0.65	2.36	65	1	65	3500	696
	65/60	20	54	54	0.65	2.36	65	1.5	97.5	3500	870
	55/30	20	54	54	0.65	1.18	55	0.5	27.5	3550	943
	55/30	20	54	54	0.65	1.18	55	1	55	3500	624
	55/30	20	54	54	0.65	1.18	55	1.5	82.5	3200	696
	40/30	20	54	54	0.65	1.18	40	0.5	20	3550	798
	40/30	20	54	54	0.65	1.18	40	1	40	3300	609
	40/30	20	54	54	0.65	1.18	40	1.5	60	2800	667
Al-Ameeri (2013)	SF1	35	52	42	0.49	1.18	60	0	0	5133	682
	SF2	35	52	42	0.49	1.18	60	0.5	30	5452	798
	SF3	35	52	42	0.49	1.18	60	0.75	45	6554	1088
	SF4	35	52	42	0.49	1.18	60	1	60	6264	1233
	SF5	35	52	42	0.49	1.18	60	1.25	75	6163	1378
	SF6	35	52	42	0.49	1.18	60	1.5	90	6105	1523

Table 11: SFRC Mixture Parameter Database

Reference	Mix ID	Input Parameters									
		cp	**cap**	**fap**	**wc**	**fl**	**ar**	**Vf**	**ri**	**fc**	**mor**
A. Alavi Nia et al. (2012)	W/C 0.46 St 0.5	24	55	57	0.46	2.36	80	0.5	40	6525	1668
	W/C 0.46 St 1.0	24	54	57	0.46	2.36	80	1	80	6815	537
	W/C 0.36 St 0.5	28	54	57	0.36	2.36	80	0.5	40	8265	725
	W/C 0.36 St 1.0	28	54	56	0.36	2.36	80	1	80	8700	696
Campione, et al. (2008)	1	28	66	53	0.49	1.18	60	1	60	5248	798
	2	28	66	53	0.49	1.18	60	1	60	5049	480
	3	28	66	53	0.49	1.18	60	1	60	5018	783
Guerini (2018)	C45-PC	17	39	27	0.5	0	0	0	0	6212	780
	C45-s1-0.5%	27	62	43	0.5	1.38	65	0.5	33	6753	972
	C45-s1-1.0%	27	62	43	0.5	1.38	65	1	65	6792	811
	C45-s2-0.5%	27	62	43	0.5	2.36	65	0.5	33	6334	863
	C45-s2-1.0%	27	62	43	0.5	2.36	65	1	65	6740	885
	C50-s1-0.5%	27	62	46	0.45	1.38	65	0.5	33	7724	812
	C50-s1-1.0%	27	62	46	0.45	1.38	65	1	65	7050	795
	C50-s2-0.5%	27	62	46	0.45	2.36	65	0.5	33	7570	876
	C50-s2-1.0%	27	62	46	0.45	2.36	65	1	65	6840	929
Guler et al. (2019)	Guler_Control	25	78	44	0.4	0	0	0	0	5970	1335
	H30_0.25	25	78	44	0.4	1.18	40	0.25	10	5535	1575
	H30_0.5	25	78	44	0.4	1.18	40	0.5	20	5748	1724
	H30_0.75	25	78	44	0.4	1.18	40	0.75	30	5996	1847
	H60_0.25	25	78	44	0.4	2.36	67	0.25	17	5900	1614
	H60_0.5	25	78	44	0.4	2.36	67	0.5	34	6007	1876
	H60_0.75	25	78	44	0.4	2.36	67	0.75	50	6360	2053
Kwak et al. (2002)	FHB1-2	30	66	35	0.33	1.97	0	0	0	9077	1293
	FHB2-2	30	66	35	0.33	1.97	62.5	0.5	31	9251	1465
	FHB3-2	30	66	35	0.33	1.97	62.5	0.75	47	9947	1552
	FHB1-3	30	66	35	0.33	1.97	62.5	0	0	9077	--
	FHB2-3	30	66	35	0.33	1.97	62.5	0.5	31	9251	--
	FHB3-3	30	66	35	0.33	1.97	62.5	0.75	47	9947	--
	FHB1-4	30	66	35	0.33	1.97	62.5	0	0	9077	--
	FHB2-4	30	66	35	0.33	1.97	62.5	0.5	31	9251	--
	FHB3-4	30	66	35	0.33	1.97	62.5	0.75	47	9947	--
Kwak et al. (2002)	FNB2-2	19	69	44	0.62	1.97	62.5	0	0	4466	--
	FNB2-3	19	69	44	0.62	1.97	62.5	0.5	31	4466	1124
	FNB2-4	19	69	44	0.62	1.97	62.5	0.75	47	4466	--

Table 11: SFRC Mixture Parameter Database Cont.

Reference	Mixture ID	Input Parameters									
		cp	cap	fap	wc	fl	ar	vf	ri	fc	mor
Lee et al. (2019)	3D-0.37	18	54	50	0.35	2.36	67	0.37	25	7395	1003
	3D-0.6	18	54	50	0.35	2.36	67	0.6	40	7105	1015
	3D-1.0	18	54	50	0.35	2.36	67	1	67	7540	1266
	4D-0.37	18	54	50	0.35	2.36	67	0.37	25	7395	998
	4D-0.6	18	54	50	0.35	2.36	67	0.6	40	7685	1077
	4D-1.0	18	54	50	0.35	2.36	67	1	67	7685	1119
	5D-0.37	18	54	50	0.35	2.36	67	0.37	25	6960	983
	5D-0.6	18	54	50	0.35	2.36	67	0.6	40	7830	993
	5D-1.0	18	54	50	0.35	2.36	67	1	67	7250	1079
Marar et al. (2016)	C30-Control	28	50	50	0.5	0	0	0	0	5786	--
	C30-65-0.5	28	50	50	0.5	2.36	65	0.5	33	5539	--
	C30-65-1.0	28	50	50	0.5	2.36	65	1	65	6873	--
	C30-65-1.5	28	50	50	0.5	2.36	65	1.5	98	5583	--
	C30-80-0.5	28	50	50	0.5	2.36	80	0.5	40	5873	--
	C30-80-1.0	28	50	50	0.5	2.36	80	1	80	5960	--
	C30-80-1.5	28	50	50	0.5	2.36	80	1.5	120	6322	--
	C50-Control	36	44	46	0.43	0	0	0	0	8048	--
	C50-65-0.5	36	44	46	0.43	2.36	65	0.5	33	7671	--
	C50-65-1.0	36	44	46	0.43	2.36	65	1	65	8019	--
	C50-65-1.5	36	44	46	0.43	2.36	65	1.5	98	8439	--
	C50-80-0.5	36	44	46	0.43	2.36	80	0.5	40	7613	--
	C50-80-1.0	36	44	46	0.43	2.36	80	1	80	7540	--
	C50-80-1.5	36	44	46	0.43	2.36	80	1.5	120	7308	--
Song et al. (2004)	Control	30	66	46	0.28	0	0	0	0	12325	928
	0.5	30	66	46	0.28	2.36	64	0.5	32	13195	1189
	1	30	66	46	0.28	2.36	64	1	64	13775	1465
	1.5	30	66	46	0.28	2.36	64	1.5	96	14210	1784
	2	30	66	46	0.28	2.36	64	2	128	13920	2103
Soulioti et al. (2011)	Plain	27	23	76	0.5	0	0	0	0	6757	645
	H0.5	27	23	76	0.5	1.22	41	0.5	21	7308	551
	H1	27	22	75	0.5	1.22	41	1	41	6366	667
	H1.5	27	22	74	0.5	1.22	41	1.5	62	7279	841
Torres et al. (2019)	Control	36	37	55	0.4	0	0	0	0	2987	418
	M1-0.3	35	35	53	0.45	2.36	80	0.3	24	4785	418
	M2-0.6	35	35	53	0.45	2.36	80	0.6	48	4031	782
	M3-0.9	34	34	51	0.5	2.36	80	0.9	72	4220	870
	M4-1.2	32	32	49	0.55	2.36	80	1.2	96	4394	893

6.5.2 Decision Tree Models

Three types of decision tree machine learning methods were implemented within this study phase. The methods used were random forests, bootstrap aggregation or "bagging", and gradient boosting. Random forests are an ensemble of individually generated decision trees that each make their own prediction. All of the trees that were developed by this analysis were uncorrelated, meaning that the predictions made from one tree do not influence the predictions made by another tree. Random forests were uncorrelated because when developing decision trees, each node of a tree considers a random sample of m predictors of the total set of p predictors.

As decision trees often have high variance, bagging reduces the variance of the statistical learning method. Bagging is the process in which the random forest allows each tree to randomly pull from the same dataset to train the decision tree. As decision trees often have high variance, bagging reduces the variance of the statistical learning method by generating B different bootstrapped training data sets and then averaging all of the predictions together to obtain the final prediction. Random forests have higher variance, but less bias than bagging.

Gradient boosting was the last tree ensemble method explored within this study phase. With this method an initial tree was trained using all of the training dataset and all input variables. The subsequent tree was trained to fit the residuals, or the difference between the predicted and observed values, to improve the accuracy of the prediction. This method continually learns from each tree for a specified number of iterations. To obtain the estimation value, the predictions of all trees constructed within the boosting ensemble are added together and averaged.

6.5.3 Data Analysis and Model Validation

Machine learning is a powerful statistical method used to develop accurate estimations of SFRC mechanical properties and to measure the correlation between mixture parameters. From the

machine learning models a better understanding of the influence each parameter has on the compressive strength and MOR of SFRC mixtures was developed. These correlations and influences were measured by comparing the accumulated reduction in MSE each time a variable was selected as a node split for a tree within the forest. This provides important information on how steel fibers interact with the concrete mixture consituents and how mechanical properties may be enhanced.

Validation of the models was performed by examining the RMSE and coefficient of determination. Additionally, prediction values obtained by the model were compared with predictions obtained by the proposed design expressions discussed in literature. As discussed within the literature review, Guler et al. (2019) has reported the expressions shown in Table 12 to be accurate SFRC mechanical property prediction expressions. These equations were chosen to be compared against the machine learning models developed within this study for comparison. The mechanical property values measured within Phase I were used for to measure the accuracy of the models with GDOT specific concrete mixtures.

Table 12: SFRC Mechanical Property Strength Expressions

Researcher	Compressive Strength	Flexural Strength
Abedel et al.	$f'_c = f'_c + 5.222RI_v$	$f'_f = f'_f + 5.222RI_v$
Guler et al.	$f'_c = 0.92f'_c - 1.44v_f + 14.6RI_v$	$f'_c = 0.24f'_c + 1.12v_f + 7.1RI_v$
Padmarajaiah	$f'_c = f'_c + 1.998RI_v$	$f'_f = f'_f + 5.222RI_v$

6.5.4 Design Summary

The goal of this study phase was to develop an improved SFRC mechanical property prediction model superior to those published that can be utilized by GDOT for future SFRC applications. Though the development of the machine learning models, an understanding of the influence each mixture parameter has on the mechanical properties of SFRC was obtained and reported. Machine

learning models can be used to accurately estimate the compressive and flexural strengths of SFRC concrete mixtures without having to perform destructive and time consuming material testing. Within this study phase, a reliable SFRC strength prediction method was obtained and GDOT standard concrete mixtures were analyzed to determine the potential mechanical property strength enhancements obtainable with steel fiber reinforcement. This model can be used by GDOT professionals to determine where steel fibers could be beneficial for GDOT projects. Additionally, after successful model validation, the model was deployed to a webpage where other users may analyze and determine SFRC mixtures.

7.0 EXPERIMENTAL RESULTS

7.1 Phase I – Investigative Mixture Results

Twelve investigative mixtures were batched with varying industrial steel fibers and volume ratios. These steel fibers possessed different geometries, varying in length and end anchorages. Four mixtures were batched containing a concentration of 0.50% by volume steel fibers, each with a designated steel fiber type. Four mixtures were batched with 0.75% by volume steel fibers, and four with 1.00% by volume steel fibers. For all mixtures, the cement content was kept constant at 635 lb/yd^3 (375 kg/m^3), and the w/c ratio maintained at 0.42 to meet GDOT Class AA concrete specifications. The primary objective of the initial trial mixture phase was to determine the influence that steel fibers have on the fresh and hardened properties of the concrete mixtures. Results are considered and optimized mixtures are developed to move forward into Phase II large-scale static beam testing.

7.1.1 Fresh Properties of Investigative Mixtures

The fresh concrete properties slump, air content, temperature, and unit weight are important properties to consider for concrete production and usage. These properties give insight as to how viable the mixtures are for industry in terms of ease of placement, consolidation, and finishing of the concrete as well as the long-term durability of the concrete. Based on past research, it is known that the addition of steel fibers into concrete mixtures has a negative impact on the fresh properties of the concrete. These negative impacts include decreased slump, increased air content, and increased unit weight. Based on this information, it becomes incredibly important to build an understanding of how the fibers used within this study will affect these fresh properties.

Additionally, information collected from these fresh property tests help to further optimize the dosage of admixtures used within the Phase II investigation. Table 13 lists the results collected from fresh property testing of the Phase I mixtures.

Table 13: Fresh Concrete Property Test Results of Investigative Mixtures

Mix Description	Slump, in (mm)	Air Content (%)	Unit Weight, lb/ft^3 (kg/m^3)	Temperature, F˚ (C˚)
Control	4.5 (114.3)	5.0	148.0 (2370.7)	72.2 (22.3)
3D/45/0.50	4.0 (101.6)	3.0	150.9 (2417.2)	73.0 (22.8)
3D/80/0.50	3.5 (88.90)	3.0	151.2 (2422.0)	74.7 (23.7)
4D/65/0.50	3.0 (76.20)	2.0	150.1 (2404.4)	73.2 (22.9)
5D/65/0.50	3.5 (88.90)	2.5	149.6 (2396.4)	64.4 (18.0)
3D/45/0.75	3.5 (88.90)	2.5	150.0 (2402.8)	69.3 (20.7)
3D/80/0.75	4.0 (101.6)	3.0	151.6 (2428.4)	69.8 (21.0)
4D/65/0.75	4.0 (101.6)	2.5	149.8 (2399.6)	73.4 (23.0)
3D/45/1.00	4.5 (114.3)	3.0	151.0 (2418.8)	68.0 (20.0)
3D/80/1.00	5.0 (127.0)	3.5	152.0 (2434.8)	69.1 (20.6)
4D/65/1.00	5.0 (127.0)	3.2	150.6 (2412.4)	72.0 (22.2)
5D/65/1.00	4.0 (101.6)	3.2	151.2 (2422.0)	73.1 (22.8)

7.1.1.1 Slump

As the literature and ACI 544.4R-18 suggests, slump was tested prior to the addition of steel fibers, as the traditional slump test is not an accurate test method for SFRC mixtures. The workability of the mixtures after the addition of fibers was determined during the placement process, by which a visual inspection was performed observing the ease of placing and finishing the concrete within the specimen molds. The slump values obtained from the testing range from 3 to 5 in, most of which fall within the range of the GDOT Class AA standards of 2 to 4 in. As the higher volume ratio of fibers leads to a less workable concrete, more HRWRA and VMA was utilized to further the workability of the concrete before addition of the fibers. Results of the slump testing is illustrated in Figure 28.

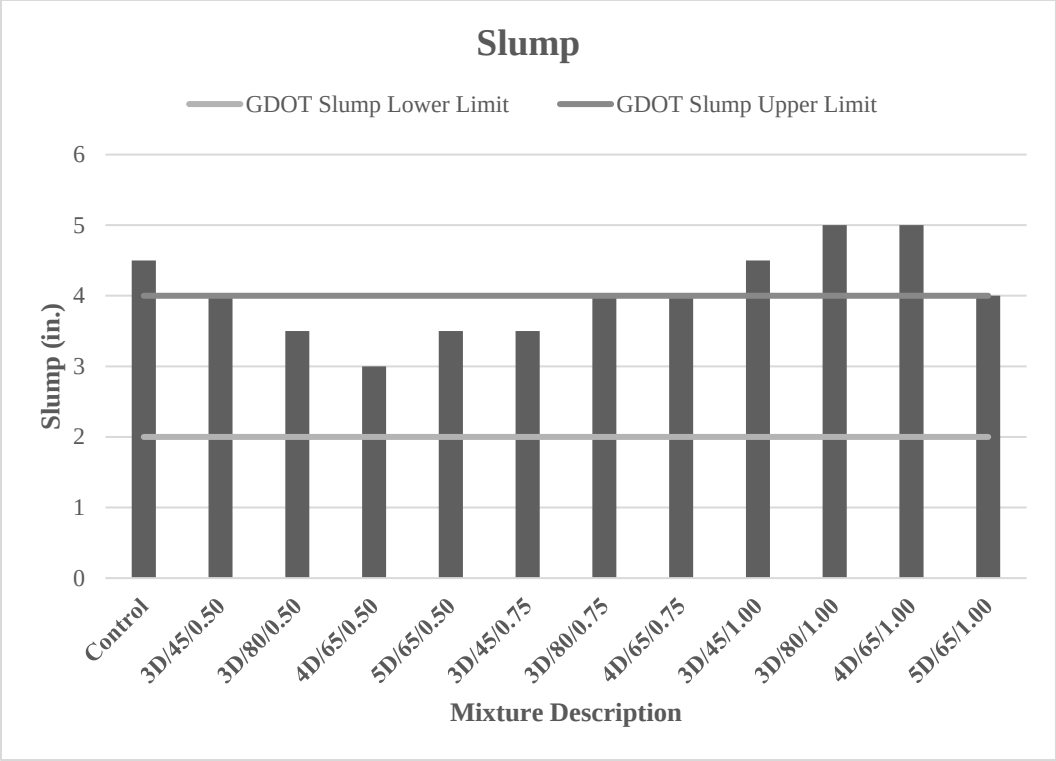

Figure 28: Phase I Slump Test Results Prior to Addition of Fibers

Overall, the addition of fibers had only a slight negative affect on the workability of the concrete. At higher volume ratios, fiber clumping was evident despite the increased mixing time. While the control mixture was able to be placed into molds without the use of a vibrating table, the SFRC mixtures required the use of a vibrating table to properly consolidate the concrete into the molds. This was due to the fibers pushing the larger aggregate out in some situations, especially with the longer fibers. At the 1.00% fiber volume ratio, it became difficult to finish the surface of the testing specimens as there were often fibers that stuck out in random directions being lodged within the aggregate and had to be pulled out of the mixture. In an effort to more closely observe the manner in which the fibers consolidate within the concrete, a cylinder was made holding back some of the cement paste such that the aggregate would be more visible. Figure 29 shows fiber clumping occurring within the cylinder, circled in white, creating a void in which the coarse

aggregate could not consolidate into. In addition, the condition could be a function of the gradation of the coarse aggregate. This can be avoided by using a smaller coarse aggregate that can fit between the clumping fibers.

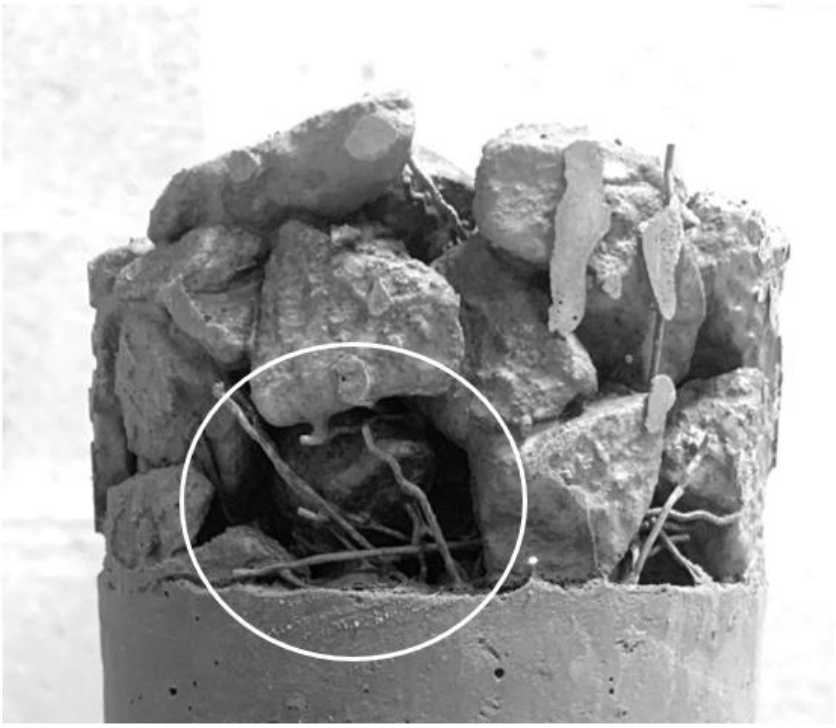

Figure 29: Fiber Clumping Within Compressive Cylinder

7.1.1.2 Air Content

The air content was fairly consistent for all SFRC mixtures, being slightly lower than the air content of the control mixture. This could be due to the addition of fibers decreasing the amount of entrapped air or the surface area of the air bubbles as was discussed in Chapter 3. The extended mixing time within the drum type mixer could have played a role in the decreased air content within the concrete. The SFRC mixtures possessed air contents that were 1.50% to 3.00% lower in comparison to the 5.00% air content of the control mixture. Its observed that the fiber type had negligible effects on the air content. Air content increased slightly with increasing fiber volume

concentration, but by a small margin. Despite this, all mixtures met the GDOT Class AA concrete standards for air content. Figure 30 illustrates the air content test results for Phase I mixtures.

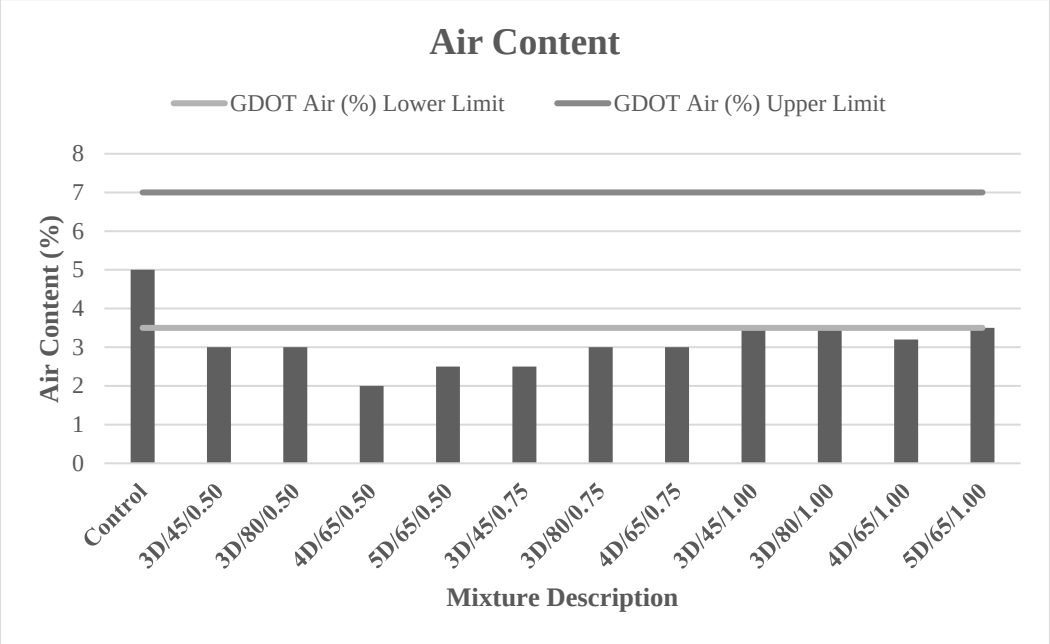

Figure 30: Phase I Air Content Test Results

7.1.1.3 Unit Weight

As expected, the unit weight of mixtures containing steel fibers was higher than the control. This is due to the fibers being made of a higher density material that other materials found within the concrete. Despite the increase in unit weight, the highest increase was only 2.7% higher than the control unit weight. The unit weights of the SFRC mixtures ranged from 149.6 to 152.0 lb/ft^3 (2396.4 to 2434.8 kg/m^3), a difference of 1.60%. Aside from the initial increase in unit weight, the change of unit weight due to the addition of steel fibers is considered negligible. The results of the unit weight tests are shown in Figure 31.

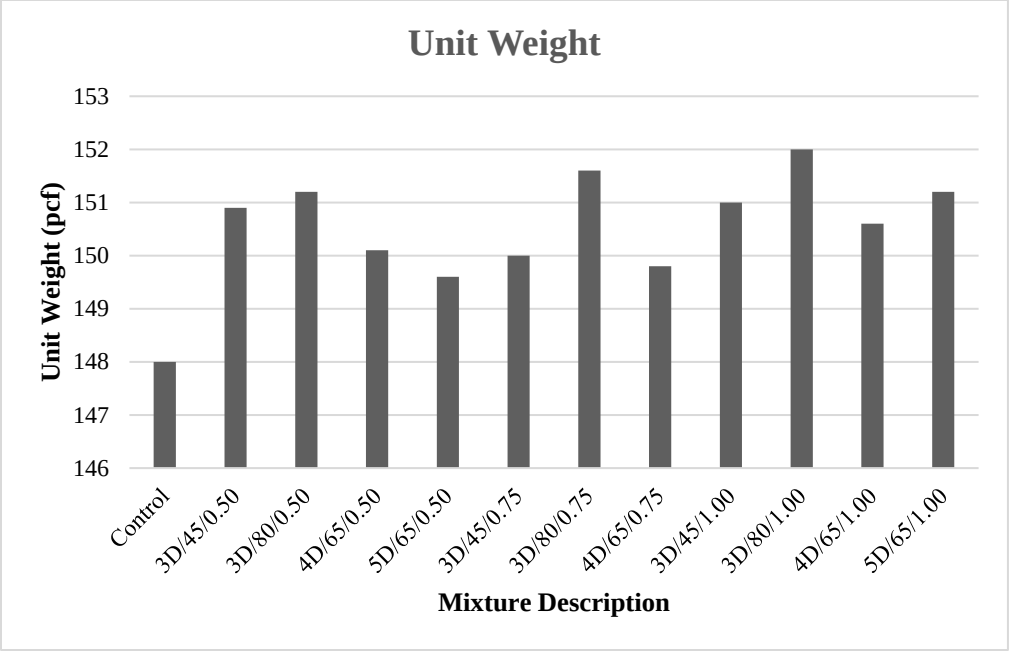

Figure 31: Phase I Unit Weight Test Results

7.1.1.4 Temperature

Overall the addition of steel fibers into the concrete mixture did not appear to have any effect on the temperature of the concrete. The ambient temperature of the air ranged from 60 to 75 F˚ (15.6 to 23.8 C˚) during the mixing and placement processes, which is reflected by the temperature results of the SFRC mixtures. The ambient temperature had a greater influence on the temperature of the fresh concrete than fibers. This temperature range is considered appropriate temperatures for the concrete and is illustrated in Figure 32.

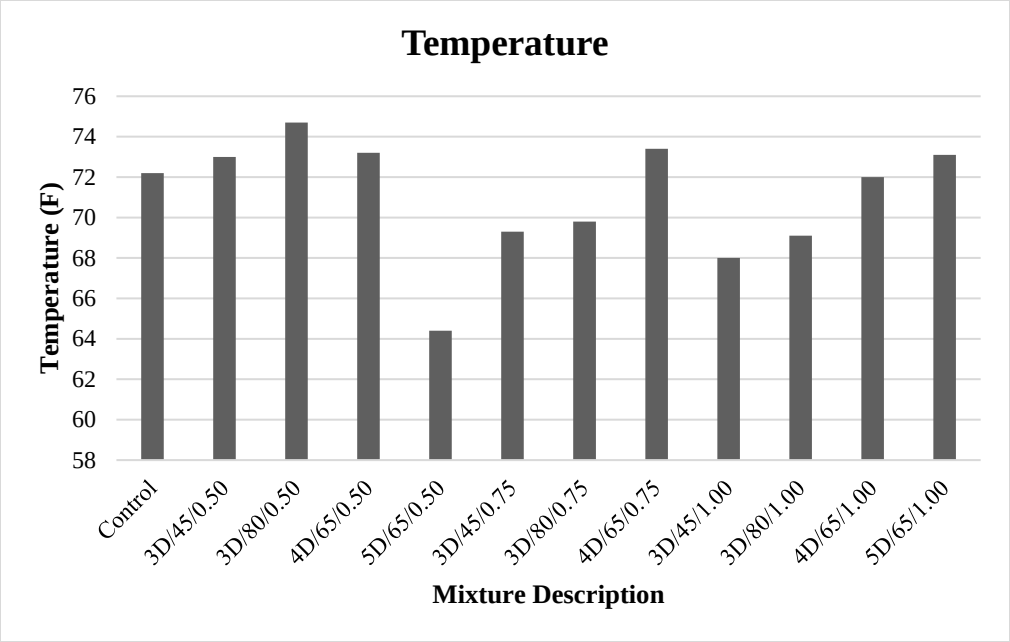

Figure 32: Phase I Temperature Results

7.1.2 Hardened Properties of Investigative Mixtures

Compressive strength and MOR were measured for each of the Phase I mixtures. Given the statistical discrepancies of the drop-hammer impact tests seen within literature review, this test was omitted from the study. Compressive strength tests were performed at 1, 7, and 28 days of age, while MOR was measured at 28 days of age. The compressive strength and MOR values are the most important properties studied within the Phase I investigative mixtures as these properties are used to further optimize the mixtures and help with beam design for Phase II scaled beam tests.

7.1.2.1 Compressive Strength Results of Investigative Mixtures

The compressive strength of the SFRC mixtures increased with increasing fiber content up to 0.75% fiber by volume, with a steep decrease in compressive strength for mixtures containing long fibers at the 1.00% volume ratio. The increase in compressive strength from the inclusion of steel fibers ranged from 9.80% for 3D/80/1.0 to 83.30% for 4D/65/0.75. The steep decrease in compressive strength of mixtures containing long fibers at the 1.0% fiber volume ratio could be

due to fiber clumping between the aggregates, or the end anchorages creating internal cracks as suggested in literature. On average, the SFRC mixtures reached 78.00% of their total compressive strength by seven days of age, with all mixtures surpassing the GDOT Class AA concrete compressive strength requirement of 3,500 psi (24.1 MPa) by seven days of age. The average compressive strength results are summarized within Table 14, while Figure 33 shows the development of the compressive strength of the SFRC mixtures for 1, 7, and 28 days of age. Interestingly, the 3D/45 fibers produced the highest compressive strength of the fibers with fiber volume ratios of 0.50% and 1.00%, but the lowest compressive strength for the 0.75% fiber volume ratio. The trend of these compressive strength results agrees with results reported by Al-Ameeri (2013), with the compressive strength increasing up to 0.75% fiber volume fraction and decreasing thereafter. The compressive strength of SFRC appeared to be mostly influenced by fiber length.

Table 14: Average Compressive Strength Results of Investigative Mixtures

Mix Description	Day 1, psi (MPa)	Day 7, psi (MPa)	Day 28, psi (MPa)
Control	1273 (8.78)	3895 (26.9)	4562 (31.5)
3D/45/0.50	1614 (11.1)	5259 (36.3)	7497 (51.7)
3D/80/0.50	1933 (13.3)	5572 (38.4)	7005 (48.3)
4D/65/0.50	1360 (9.38)	4001 (27.6)	6272 (43.2)
5D/65/0.50	1876 (12.9)	4725 (32.6)	6499 (44.8)
3D/45/0.75	2194 (15.1)	5369 (37.0)	7077 (48.8)
3D/80/0.75	2534 (17.5)	5961 (41.1)	7774 (53.6)
4D/65/0.75	2533 (17.5)	6352 (43.8)	8360 (57.6)
3D/45/1.00	1900 (13.1)	6657 (45.9)	8226 (56.7)
3D/80/1.00	0905 (6.24)	4174 (28.8)	5010 (34.5)
4D/65/1.00	1195 (8.24)	4449 (30.7)	5393 (37.2)
5D/65/1.00	1211 (8.35)	5262 (36.3)	5845 (40.3)

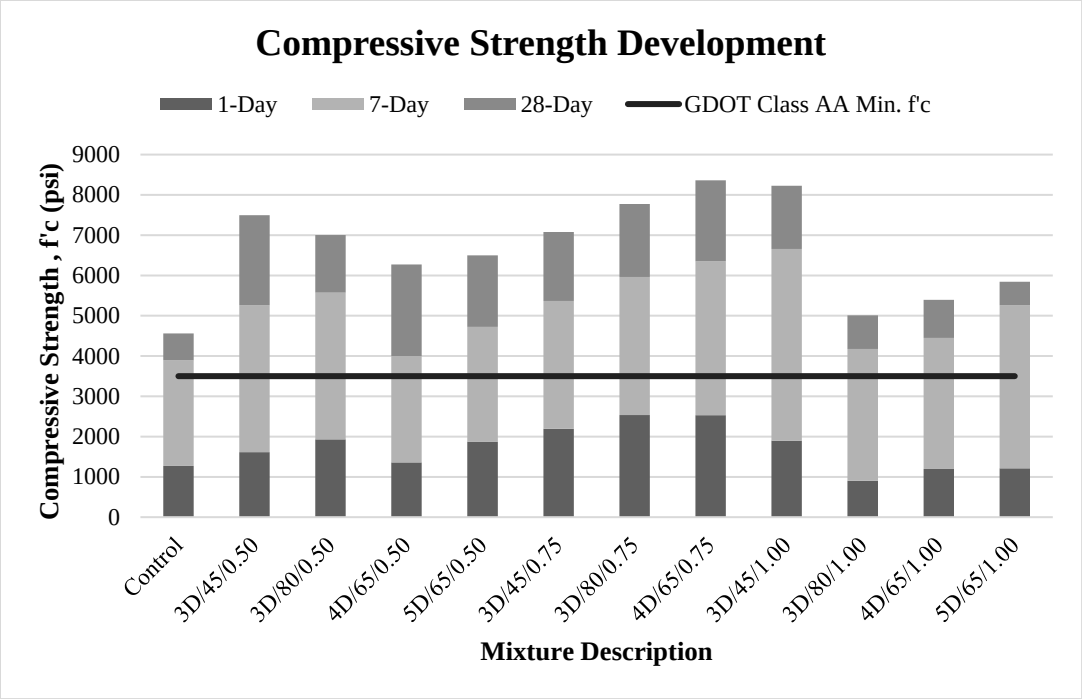

Figure 33: Compressive Strength Development of Investigative Mixtures

To better understand the compressive test results, the failure mechanisms of the compressive cylinder specimens were analyzed. Most cylinders tested exhibited crushing failure, as shown within Figure 34, while localized failures were observed in some cylinders primarily due to fiber clumping, as shown by Figure 35. It was observed that in the case of crushing failure, very little shrapnel was ejected from the concrete cylinder due to fibers holding the concrete together. The orientation of fibers within the concrete is an important factor when considering compressive strength. As the internal stresses within the specimen increase, fibers could buckle causing a localized failure within the concrete specimen as suggested by literature, which is visible in Figure 36. Based on results from this testing, it can be concluded that the addition of steel fibers increases the compressive strength of the concrete up to the 1.00% fiber volume ratio. At the 0.75% fiber volume ratio, 4D/65 fibers out performed other fiber geometries, though at the 1.00% fiber volume

ratio, the 3D/45 fibers were at an advantage due to their shorter length allowing the fibers to further integrate themselves in between the coarse aggregate of the concrete.

Figure 34: Crushing Failure Observed During Compressive Strength Tests

Figure 35: Localized Failure Observed During Compressive Strength Tests

Figure 36: Local Buckling of Fiber Observed During Compressive Strength Tests

7.1.2.2 Modulus of Rupture Test Results of Investigative Mixtures

As previously stated, the MOR tests were performed at twenty-eight days of age. As suggested by literature, the MOR increased with increasing fiber volume ratio. On average, the MOR increased by 39.70%, 50.10%, and 73.30% in comparison to the control for fiber volume ratios of 0.50%, 0.75%, and 1.00%, respectively. In each fiber volume ratio category, the 5D/65 fibers outperformed other fiber geometries, which is due to the five-dimensional end anchorage contributing to the fiber pull-out resistance. At the 1.00% fiber volume ratio the 5D/65 SFRC mixture possessed a MOR strength of 1,360 psi (9.38 MPa), a 105.70% increase in comparison to

the control mixture. Despite the high MOR measurement of the 5D/65/1.00 mixture, this mixture had a lower compressive strength when compared to the other fiber volume mixtures. The results of the MOR testing is summarized in Table 15 and illustrated within Figure 37.

Table 15: Average MOR Strength Results of Investigative Mixtures

	Average MOR, psi (Mpa)			
Fiber Volume (%)	**3D/45**	**3D/80**	**4D/65**	**5D/65**
0.50	929 (6.41)	883 (6.09)	933 (6.43)	948 (6.54)
0.75	825 (5.69)	1023 (7.05)	1128 (7.78)	--
1.00	1114 (7.68)	1018 (7.02)	1092 (7.53)	1360 (9.37)

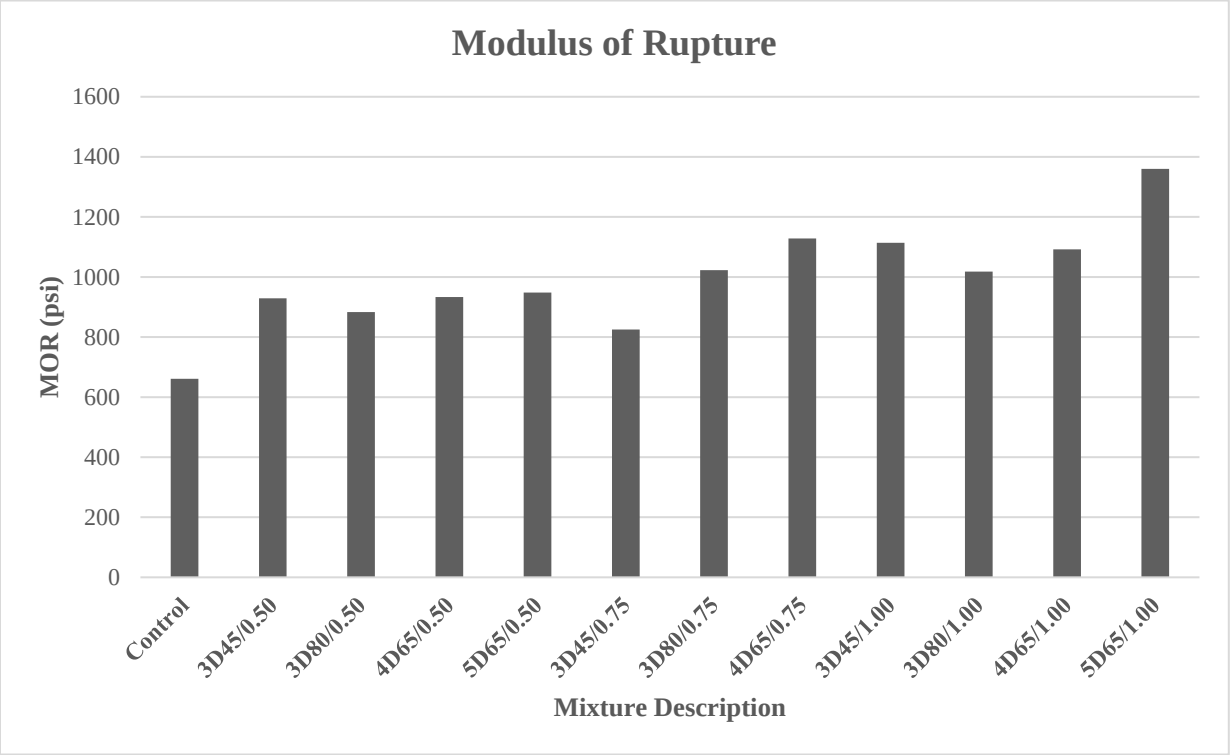

Figure 37: Results of MOR Testing

7.1.3 ANOVA Analysis of Phase I Results

In an effort to better understand the significance of influence the fibers had on fresh and hardened properties, an analysis of variance (ANOVA) was performed. Comparisons of the observed strengths of the SFRC and control mixtures were made to analyze how interactions between fiber

volume percentage (Vf %), end anchorage (EA), and aspect ratio (AR) influence the compressive strength and MOR. The results of the analysis are summarized in Table 16.

Table 16: ANOVA Summary

Comparison	Source of Variation	Sum of Square	df	Mean Square	F-Value	P-Value
3D/45 Comp. Str.	Vf %	1351822	2	675911	4.35	0.129
3D/45 MOR	Vf %	128300	2	64150	14.91	0.005
3D/80 Comp. Str.	Vf %	8140721	2	4070361	13.84	0.031
3D/80 MOR	Vf %	28002	2	14001	2.01	0.215
4D/65 Comp. Str.	Vf %	9292880	2	4646440	38.71	0.007
4D/65 MOR	Vf %	64756	2	32378	5.31	0.047
0.50% Vf Comp. Str.	EA	651196	2	325598	0.62	0.549
1.00% Vf MOR	EA, AR	238028	2	119014	11.98	0.008

Overall, the 4D/65 fibers appear to have the greatest statistical significance with changing volume percentage, resulting in p-values of 0.007 and 0.047 ($\leq$ 0.05) for compressive strength and MOR variations, respectively. While the 3D/45 MOR results showed statistical significance with a p-value of 0.031, compressive strength results showed no significance. As each MOR result was found to be statistically significant, it can be concluded that the addition of fiber reinforcement increases MOR. Lastly, the influence of the end anchorages and aspect ratios on compressive strength and MOR were analyzed. The 0.50% fiber volume compressive strength results were chosen for the ANOVA comparison as there was more data readily available, which provides a stronger statistical model. The 1.00% fiber volume MOR results were chosen based on available data. From the analysis, the end anchorage and aspect ratio had significant influence on MOR values with a p-value of 0.008. However, they were insignificant in increasing compressive strength. The end anchorage primarily aids in increasing fiber pull-out strength, which directly influences MOR.

Based on the results of investigative mixture test data, the 4D/65/0.75 SFRC mixture looked promising to move forward into Phase II static beam testing. The 4D/65/0.75 mixture provided the highest compressive strength, enhanced MOR results, and showed the greatest statistical significance with changing fiber volume percentage in comparison to other mixtures studied. As the majority of currently available research papers focuses on SFRC containing 3D steel fibers, there is potential to expand available data on SFRC containing 4D steel fibers. Based on results of investigative testing, the 4D/65/0.75 mixture was selected for testing in Phase II.

7.2 Phase II – Laboratory-Scale SFRC Beam Static Test Results

7.2.1 SFRC Static Beam Test Results

To begin Phase II testing, a preliminary set of laboratory-scale static beams were batched with fiber volume percentages of 0.50%. For these preliminary beams, the compressive strength of six cylinders were measured at 28 days of age. The static beams were subjected to a three-point bending test by applying a load at mid-span using a 220-kip (978.6 kN) hydraulic actuator. The load versus deflection curve developed from testing is shown in Figure 38, in which beams are denoted by their beam identification followed by their respective average compressive strength value within the legend in the figure. These beam identification numbers follow those discussed in Section 6.4.1. From the load versus deflection curve, the toughness was calculated by determining the area under the curve. Additionally, the linear stiffness of each mixture was analyzed and the estimated value calculated. Table 17 summarizes the static test results for Phase II beams. The maximum moment, M_u, and corresponding shear force, V_u, are calculated using the maximum load, P_u, recorded by the hydraulic actuator.

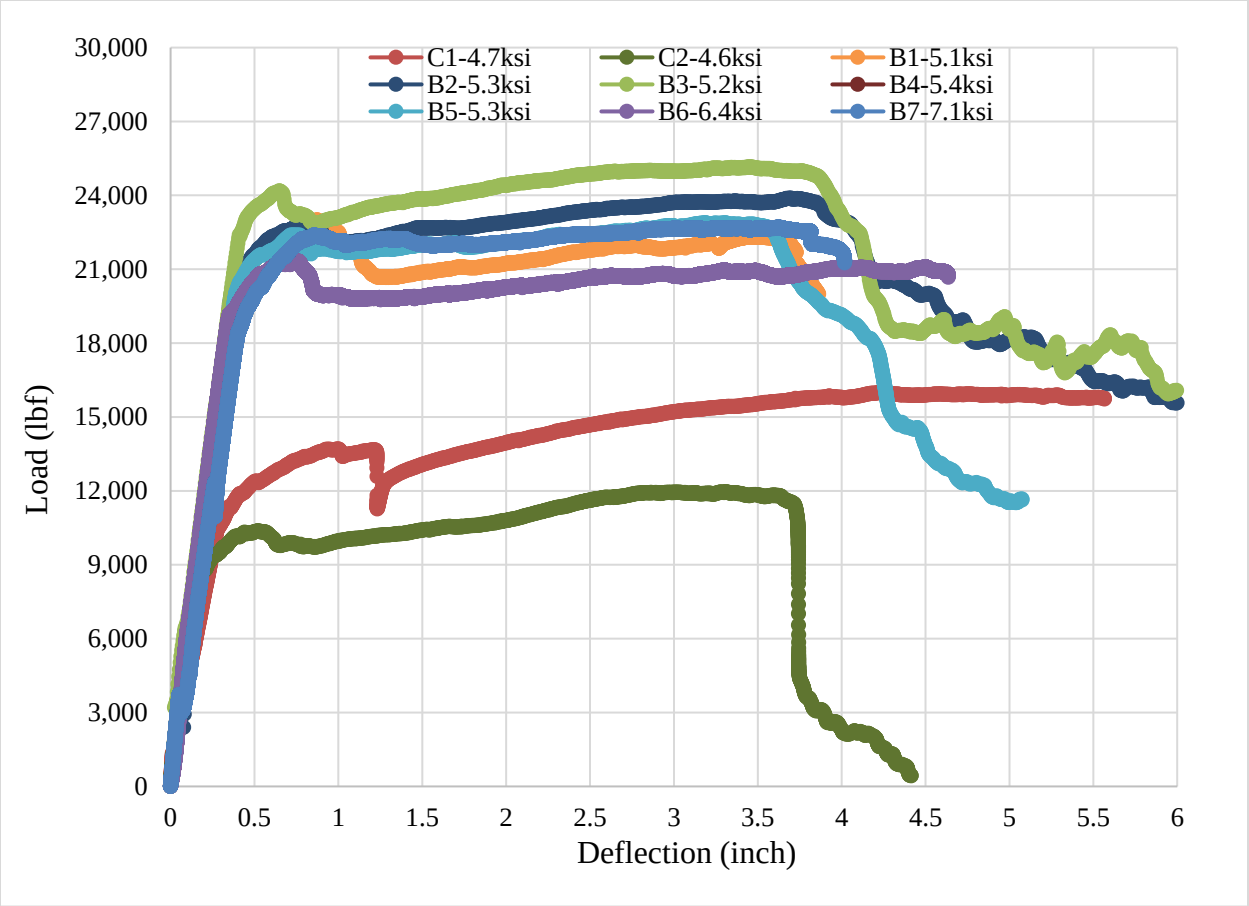

Figure 38: Phase II SFRC Beam Static Testing Load vs. Deflection Results

Table 17: SFRC Beam Static Test Results

Beam ID	P_u, kip (kN)	M_u, kip-ft (kN-m)	V_u, kip (kN)	Toughness, kip-in (kN-mm)
C1	16.8 (74.8)	24.3 (32.9)	8.4 (37.4)	79.0 (8,928)
C2	12.0 (53.4)	18.2 (24.6)	6.0 (26.7)	41.2 (4,655)
B1	23.0 (102.4)	34.9 (47.2)	11.5 (51.2)	86.3 (9,752)
B2	23.8 (98.2)	36.3 (49.1)	11.9 (53.1)	145.9 (16,484)
B3	25.2 (111.8)	38.3 (51.8)	12.6 (55.9)	135.9 (15,352)
B4	24.6 (109.6)	37.6 (50.9)	12.3 (54.8)	139.8 (15,790)
B5	22.8 (101.8)	34.8 (47.1)	11.4 (50.9)	98.8 (11,165)
B6	21.6 (95.8)	32.4 (43.8)	10.8 (47.9)	95.7 (10,813)
B7	20.4 (90.4)	34.5 (46.7)	10.2 (45.2)	85.2 (9,636)

7.2.2 Analysis of Fiber Geometry Effects on Static Loading Performance of SFRC Beams

As previously stated, the first set of beams tested within this study phase included beams C1, and B1 through B4. This set of beams were subjected to static loading using a 220-kip hydraulic actuator to place a point load at midspan of the simply supported beam. This portion of the study phase was conducted to observe the influence fiber has on laboratory-scale reinforced concrete beams. Figure 39 shows the crack development from static testing of the first set of laboratory-scale SFRC beams tested, as well as the results of static testing. Within Figure 39, beams B1 and B2 were pictured at the point of max load, while beams B3 and B4 were pictured at the termination of testing. Regretfully, the research team was unable to procure a picture of beams B1 and B2 at failure.

From static testing, flexural and flexural-shear cracks were observed on all beams within this test set. The type of crack can be determined by inspecting the inclination of the crack from the bottom of the beam. Flexural cracks propagated straight up from the bottom of the beam. Flexural-shear cracks grew perpendicular to the bottom of the beam, after which they inclined towards the point of loadng.

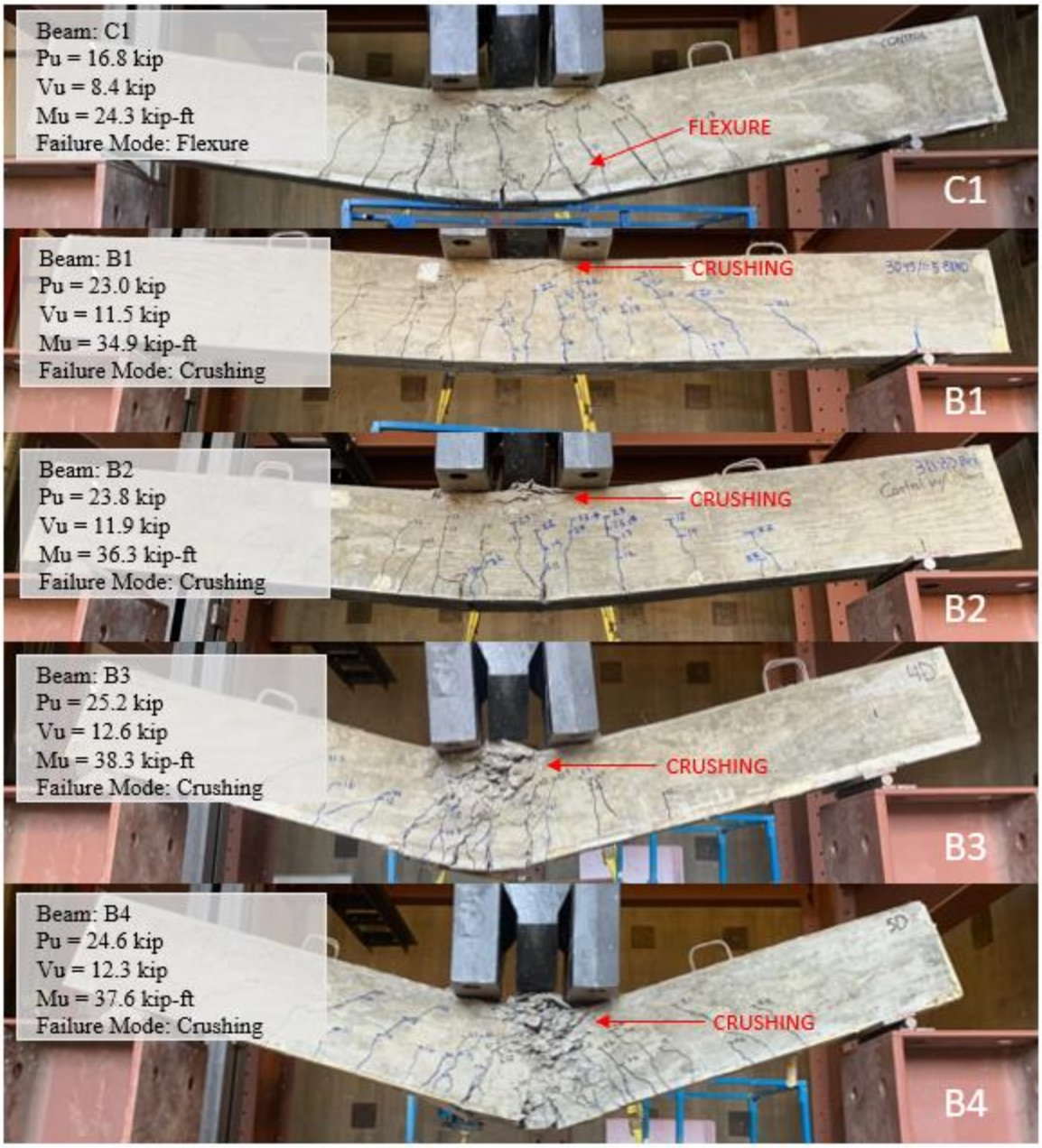

Figure 39 – Crack Propogations of C1 and SFRC Beams B1 Through B4

The distribution of the flexural cracks showed how well the concrete was able to redistribute enternal stresses throughout the material. More flexural cracks showed that the load was more evenly distributed across the tensile face of the beam. From Figure 39 it is shown that all of the SFRC beams experienced similar crack development. In comparison to beam C1, the

SFRC beams were more efficient at distributing the tensile stresses throughout the beam. Beam C1 developed fewer, larger flexural cracks that were very concentrated at the point of loading. All beams experienced crushing of concrete within the compression zone, which resulted in increased deflection before tensile steel could yield. This is undesirable as this allows for a rapid increase in deflection upon failure, as shown from the load-deflection curves presented within Figure 38.

7.2.2.1 Analysis of Fiber Geometry Influence on Flexural and Shear Capacities of SFRC Beams

On average, flexural capacity was increased by 51.30% when comparing the average results of the preliminary SFRC beams to the C1 beam. The SFRC beams B1-B4 possessed an additional tensile reinforcing bar to combat the increase compressive capacity obtained from steel fibers, similar to the study conducted by Lopez et al. (2018) and Tate et al. (2019). By analyzing the cross sections of the concrete beam design, it was determined that the additional reinforcement bar increases the flexural capacity by approximately 20.00%, resulting in a flexural capacity increase of 31.30% from steel fibers. Within the prelimary test set, the highest capacity was obtained by beam B3, withstanding a maximum moment of 38.3 kip-ft (51.8 kN-m) and maximum shear of 12.6 kip (55.9 kN). While beam B4 contains 5D/65 fibers, the observed flexural capacity of 37.6 kip-ft (50.9 kN-m) was only 3.5% higher than that of B2 with the 3D/80 fibers. As expected, the use of 3D/45 within beam B1 resulted in the lowest flexural performance enhancement compared to other fiber types tested, due to the short length of the fibers. Results from static testing closely resembled patterns observed in Phase I MOR observations. None of the beams within this test set experienced shear cracking.

7.2.2.2 Analysis of Fiber Geometry Influence on Toughness of SFRC Beams

On average, there was a 91.98% increase in toughness from the addition of fibers at 0.50% by volume, in comparison to the control beam. Overall, the SFRC mixtures performed similarly to one another, with B2 resulting in the highest toughness value of 145.9 kip-in (16,484 kN-mm), and the highest linear stiffness of 55.6 kip/in (9,737 kN/mm). B2, which utilized the 3D/80/0.5 mixture possessed a higher toughness than B3, due to better redistribution of the post-crack load. The higher observed toughness of B2 can be contributed to possessing the longest fiber of those studied in this research. The additional fiber length allowed for more development length of fibers, and increased the load required for fiber pullout to occur. If only the strain hardening region of the load-deflection curves are considered, beam B3 outperforms all other beams within the test set. The 3D/45/0.5 mixture resulted in the lowest toughness of all the SFRC mixtures, due to the low aspect ratio and short fiber length resulting in a lower post-crack performance.

Based on the findings of the preliminary static beam testing set, mixture 4D/65/0.75 was selected for use in the remainder of phase II static beams. This mixture was selected based on the impressive static beam results of beam B3, and the hardened property results from phase I testing.

7.2.3 Influence of Fiber Content of Shear Strength of SFRC Beams

The remaining beams tested within Phase II were batched to study the flexural and shear capacities of SFRC beams containing varying amounts of shear reinforcement. Figure 43 illustrates the load-deflection curves for beams C1, C2, B3, and B5 along with the 28-day compressive strengths.

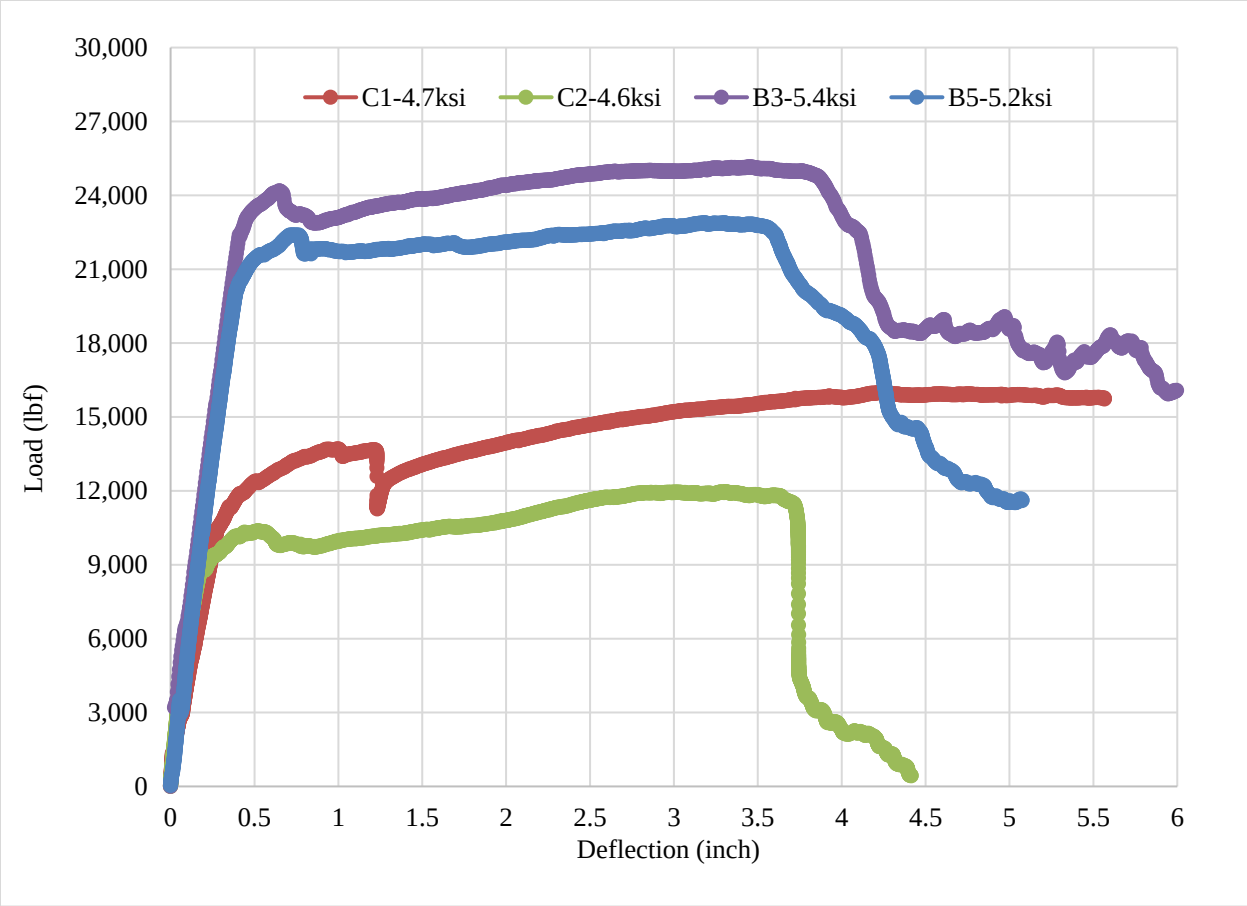

Figure 40 – Load Deflection Curves of B3, B5, and Control Beams

As previously discussed, both beams B3 and B5 were batched using the 4D/65/0.5 SFRC mixture. Beam B3 contains stirrups at four inches on center, like beam C1, while beam B5 features stirrups at eight inches on center, like beam C2. By comparing beam B3 with beam B5, it is shown that the increased spacing of the shear stirrups decreased the flexural capacity of the SFRC beams by 9.1%, which is much less than the decrease of 25.1% between beams C1 and C2. The increased stirrup spacing of beam C2 resulted in a shear failure, however beam B5 only experienced the development of flexural-shear cracks, and ultimately failed from crushing failure. From Figure 40, it is observed that the onset of crushing failure within the compression zone resulted in beam B5 to fail rapidly, while beam B3 was able to continue carrying load through a larger deflection.

Figure 41 shows a comparison of the crack propagation observed in beamsC1, C2, B3, and B5 from static loading. From this comparison, both beams experienced crushing failure and the development of flexural cracks. With the increased shear stirrup spacing, beam B5 experienced the development of flexural shear cracks at the mid-span of the beam. A reduction in shear reinforcement led to the toughness of the SFRC beams to be reduced by 27.3%, dropping from 135.9 kip-in (15,790 kN-mm) to 98.8 kip-in (11,165 kN-mm) for beams B3 and B5, respectively. For comparison, the drop in toughness comparing beams C1 and C2 was 47.8%, a drop from 79.0 kip-in (8,928 kN-mm) to 41.2 kip-in (4,655 kN-mm). The change from a shear failure to a flexure-shear failure shows that fibers may be used as a partial replacement for shear reinforcement, however for this particular beam design a higher volume of fiber is required to procure a flexural failure mode for the SFRC beam.

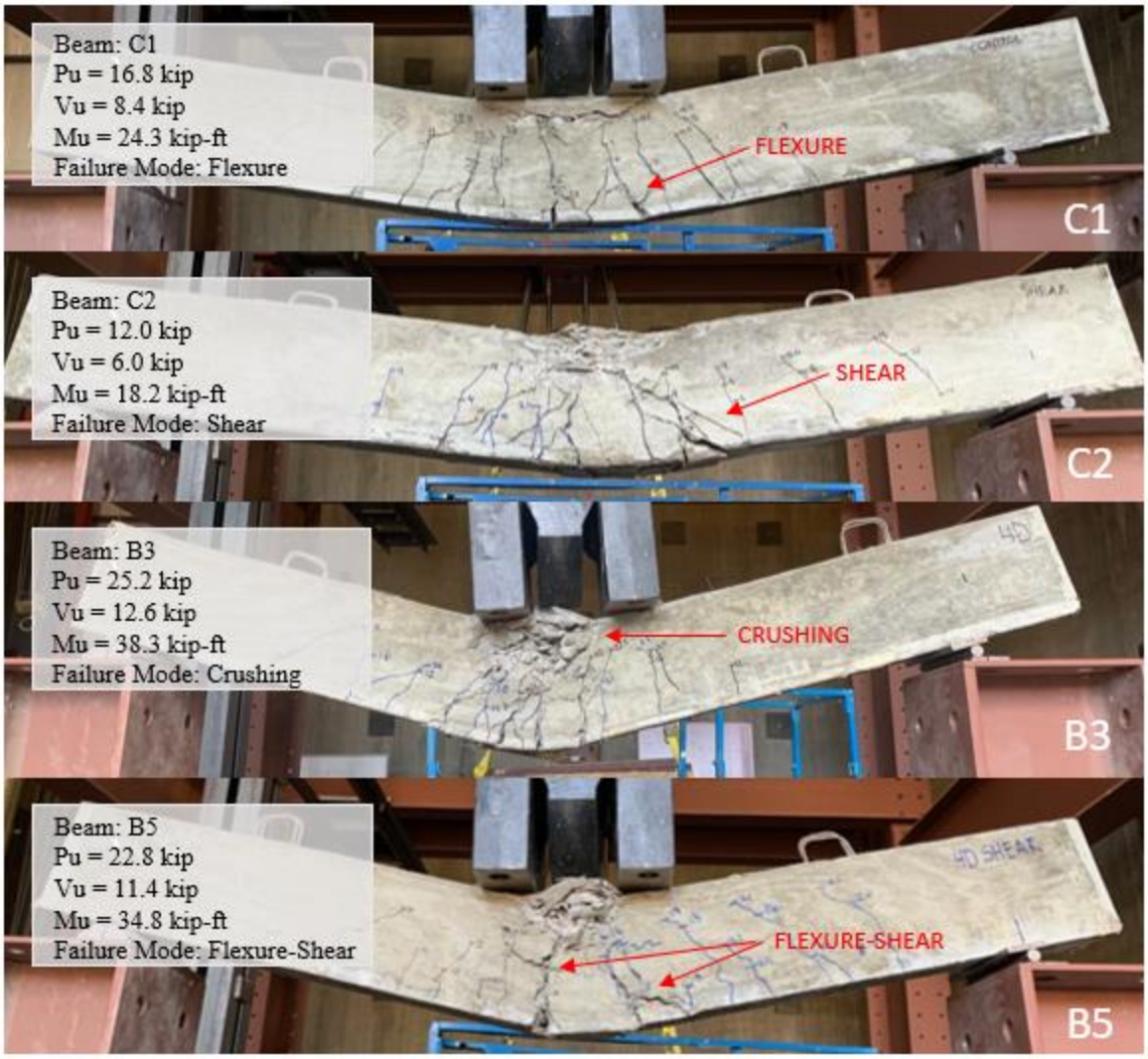

Figure 41 – Failure Modes of Beams C1, C2, B3, and B5

Beams B6 and B7 were batched using the 4D/65/0.75 SFRC mixture, which possessed the highest compressive strength results within phase I testing. Beam B6 contains stirrups at four inches on center, while beam B7 contains stirrups at eight inches on center. This mixture was chosen to combat the early crushing failure observed in beams B3 and B5. In comparison to beams B3 and B5 made with a tensile reinforcement ratio (ρ) of 1.21%, beams B6 and B7 feature optimized tensile reinforcement ratio (ρ) of 1.03%. With the decrease in flexural reinforcement, beam B6 resulted in a flexural toughness of 95.7 kip-in (10,813 kN-mm), which is 29.6% lower

than the flexural toughness of 135.9 kip-in (15,790 kN-mm) observed by beam B3. The increased stirrup spacing within beam B7 led to a decrease in flexural toughness of 10.9% of that observed by B6. This is not as significant as the 27.3% reduction of toughness observed by comparing beam B3 to B5.

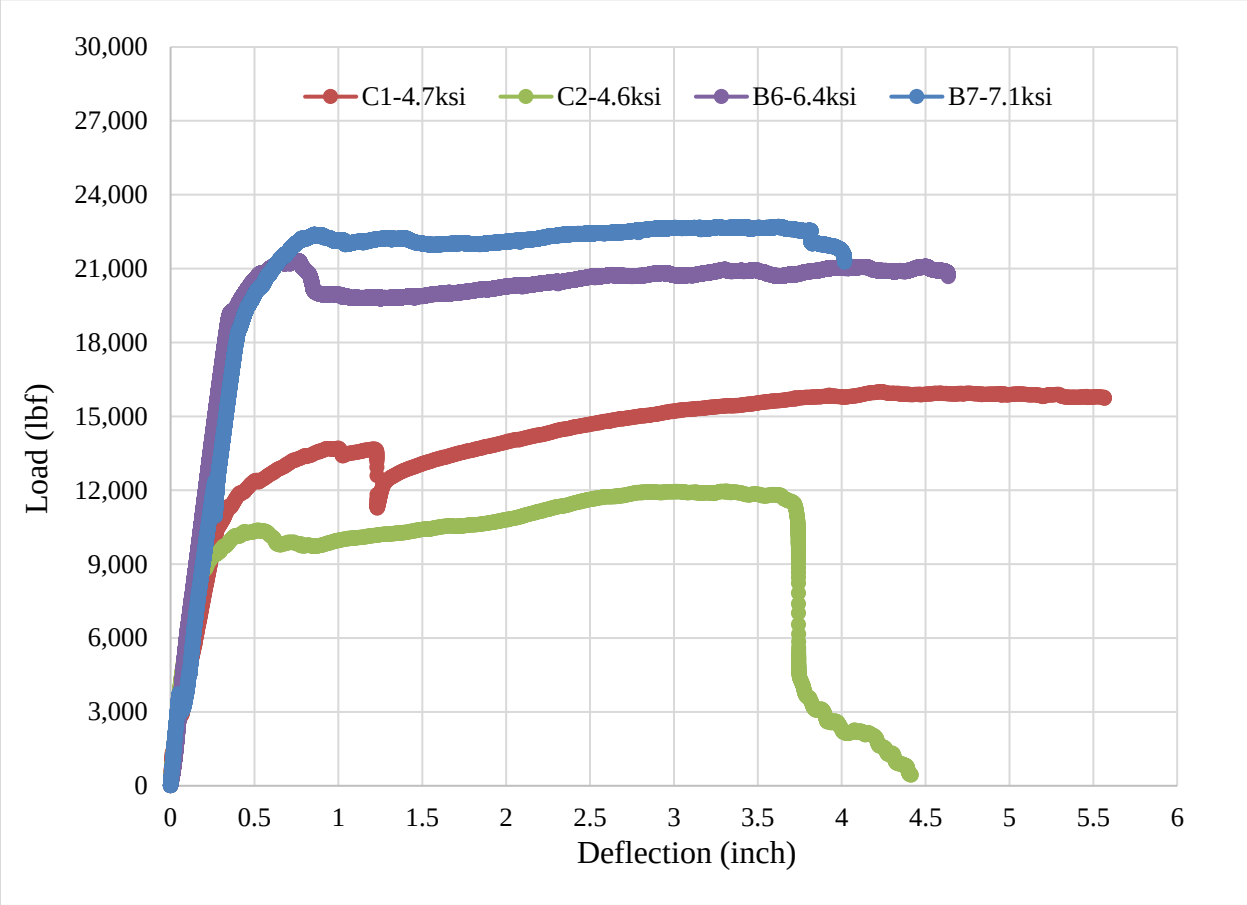

Figure 42 – Load Deflection Curves of B3, B5, and Control Beams

Figure 42 shows the load-deflection curve of beams C1, C2, B6, and B7 along with the respective average 28-day compressive strength. Both beams B6 and B7 experienced flexural failure, with full yielding of flexural steel reinforcement. With the increased compressive strength and decreased flexural steel ratio, in comparison to preliminary beams, a longer strain hardening region was obtained. Both beams B6 and B7 experienced little crushing of concrete within the

compressive zone, allowing for the flexural steel to be fully utilized until yielding occurred. Additionally, the load drop experienced at initial concrete cracking of beam B7 was less than that experienced by beam B6, which can be attributed to the increased compressive strength of the SFRC mixture. The failure modes of beams B6 and B7 are shown in Figure 43. Flexural shear cracks that beam B7 developed during static test are shown in Figure 44. The cross section of beam B6 yielded tensile reinforcing steel testing is shown in Figure 45.

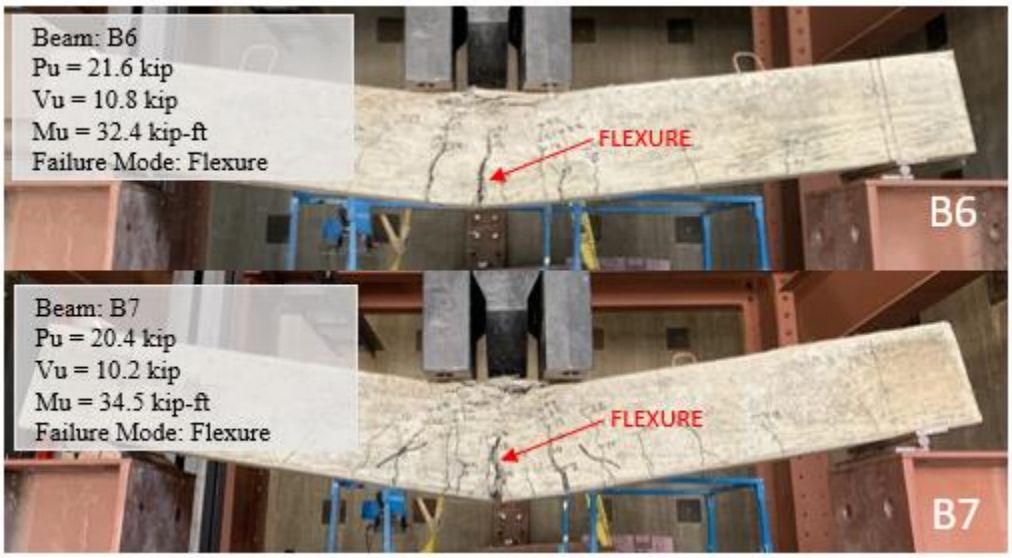

Figure 43 – Comparison of B6 and B7 Failure Modes

This testing phase has shown that fiber reinforcement may be used as a partial replacement for shear reinforcement at fiber volumes of 0.75% or greater. The results of this study agree with the findings of the study conducted by Choi et al. (2007), in which a fiber volume ratio of 0.75% was used to replace the minimum stirrup requirements set by ACI 318-14. By incorporating steel fibers, the flexural and shear capacity of the reinforced concrete beam was increased, and partial amounts of reinforcing steel were able to be removed from the design without loss of strength.

Figure 44 – Flexural Shear Cracks Developed During Beam B7 Testing

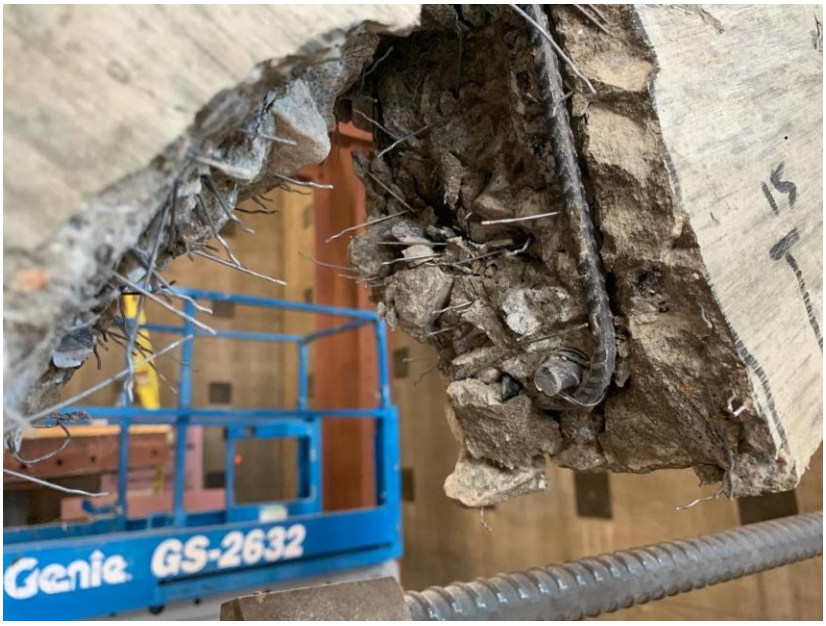

Figure 45 – Cross-Section of Yielded Flexural Steel in Beam B6

7.3 Phase III – Machine Learning Decision Tree Model Results

7.3.1 Development of Decision Trees

To begin the analysis, the random forests method was used to develop decision trees. The decision trees developed with the random forest method for compressive strength and MOR are shown by Figure 46 and Figure 47, respectively. The decision trees help to show the hiarchy of parameter importance in the decision making process of the models. The top three most important parameters for compressive strength were determined to be water/cement ratio, fiber reinforcement index, and fiber length. The top three most important parameters for MOR were fine aggregate proportion, coarse aggregate proportion, and fiber reinforcement index.

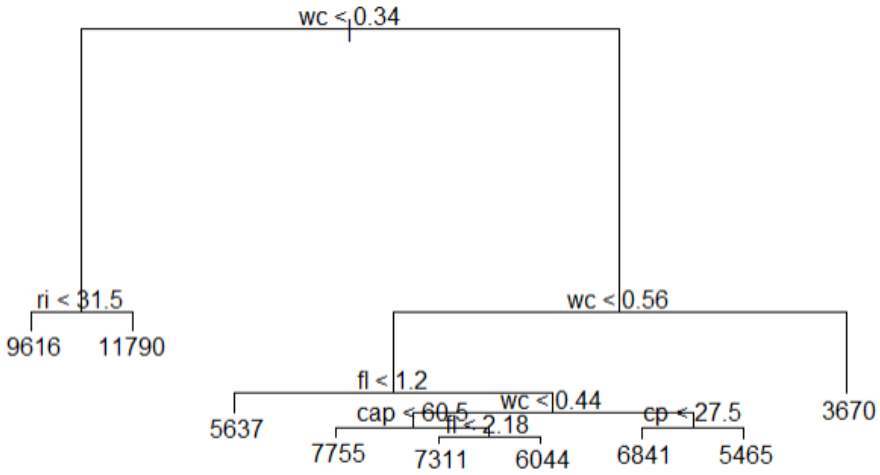

Figure 46 – Decision Tree for SFRC Compressive Strength

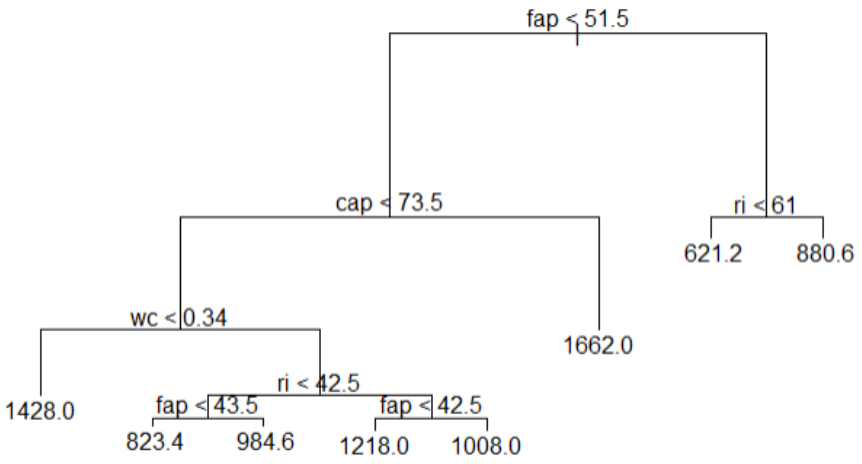

Figure 47 – Random Forest Decision Tree for MOR Predictions

It is widely known that water/cement ratio has the greatest influence on the compressive strength of concrete. When the water/cement ratio of the mixture is lower than 0.34, then fiber reinforcement index is the next referenced parameter by the decision trees, showing that fibers have a greater influence on concrete mixtures with low water/cement ratios than those with high water/cement ratios. The fine aggregate proportion is shown to have the greatest influence on the flexural strength of SFRC according to the developed decision tree model. As the fine aggregate proportion increases, the coarse aggregate proportion will decrease, allowing for the fibers to have a greater impact on the flexural strength.

Pruning of the decision trees was performed to increase the performance of the models. By pruning the tree, unnecessary terminal nodes are determined through cross-validation and removed to achieve the optimal level of tree complexity. Pruning of the trees led to a decrease in the MSE of the predictions and a less cluttered decision tree, as shown by Figure 48 and Figure 49.

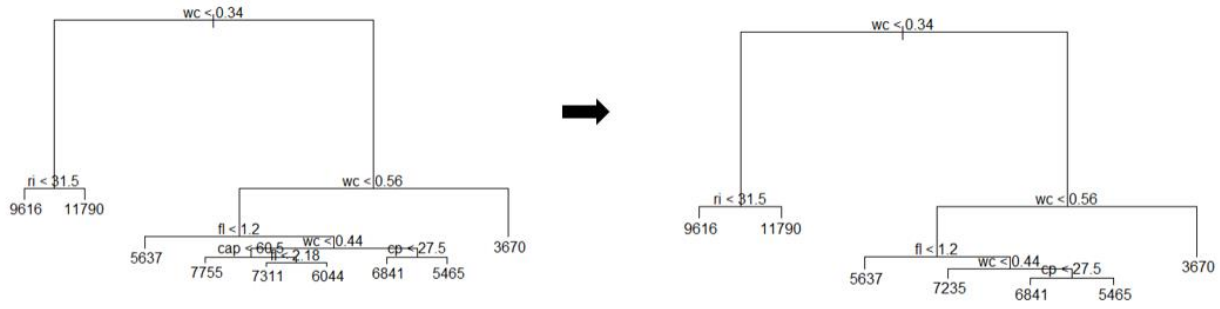

Figure 48 – Random Forest Decision Tree for Compressive Strength Predictions

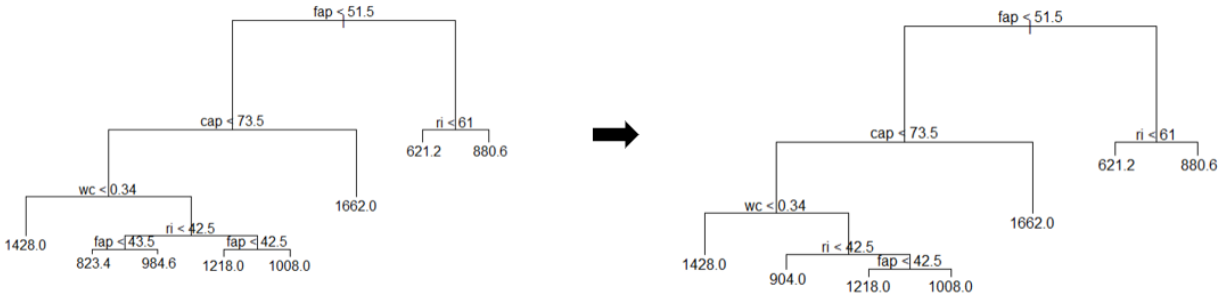

Figure 49 – Random Forest Decision Tree for MOR Predictions

7.3.2 Correlation of SFRC Mixture Parameters

To better understand how the mixture parameters of the models influence one another, correlation matrices were plotted to illustrate the interaction of parameters and their influence on the mechanical properties of SFRC. Within Figure 50, each parameter is plotted against all other parameters, resulting in a blue marker if it is a positive correlation, or red if it is a negative correlation with each other parameter. The size of the correlation circles designates the influence, or change, the parameter has on the other input parameters with larger circles signifying greater influence. This is especially useful for visualizing the considerations made by the decision trees and seeing how each parameter effects the compressive strength and MOR of concrete.

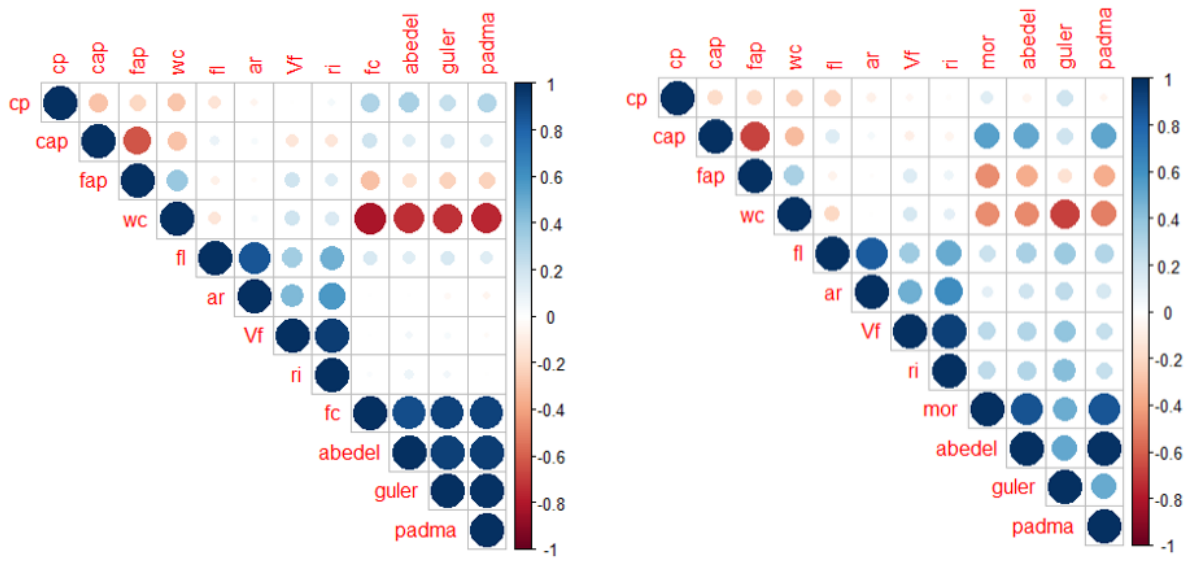

(a) Compressive Strength Correlation (b) MOR Correlation

Figure 50 – Parameter Correlation Plots

From the matrices, an increase in coarse aggregate proportion has a positive effect on compressive strength and MOR, while an increase in fine aggregate proportion has an inverse effect. This was due to higher contents of coarse aggregate allowing for the coarse aggregate to interlock within the concrete matrix and carry a great portion of the load. As is expected, an increase in water/cement ratio leads to a decrease in compressive strength and MOR. The only fiber property that had an influence on compressive strength was the fiber length, which increased the compressive strength slightly as the length of the fibers increased. This was due to an increased fiber length allowing for more bridging of microcracks by the fibers. In respect to MOR, an increase in any fiber property leads to an increase in flexural strength.

Using the two most defining parameters shown by the decision trees, a 2D partition was created in which data points were plotted based on the defining parameters of the corresponding mixture. The two most influential parameters for compressive strength are water/cement ratio and fiber reinforcement index. For MOR, the two most influential parameters were coarse aggregate

proportion and fiber reinforcement index. The training set data points are sorted into boxes showing the average compressive strength or MOR (shown in psi) of the data as shown in Figure 51. These plots help to further illustrate the correlation between the two defining parameters.

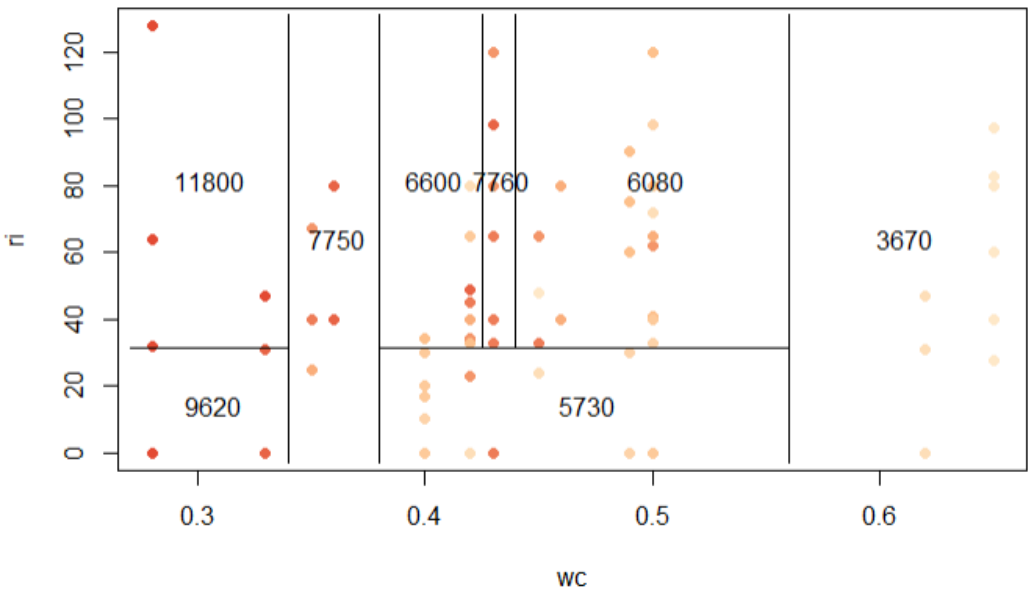

Figure 51 – 2D Partition of Compressive Strength Data

Figure 51 shows that as reinforcement index (ri) of fibers increases, the compressive strength of the SFRC mixtures increases. The 2D partition shows that fiber reinforcement index has a greater influence on compressive strength in mixtures with lower water/cement values, as was shown with the decision tree. SFRC mixtures with a water/cement ratio around 0.3 showed a larger variation in the average compressive strength values with increasing fiber reinforcement index than concrete mixtures with a water/cement ratio of 0.6. As the water/cement ratio decreases, the strength of the cement paste increases and thus the strength of the bonds between the fibers and aggregates increase. This allows for more load to be transferred across internal microcracks as they form, and aids with aggregate interlock.

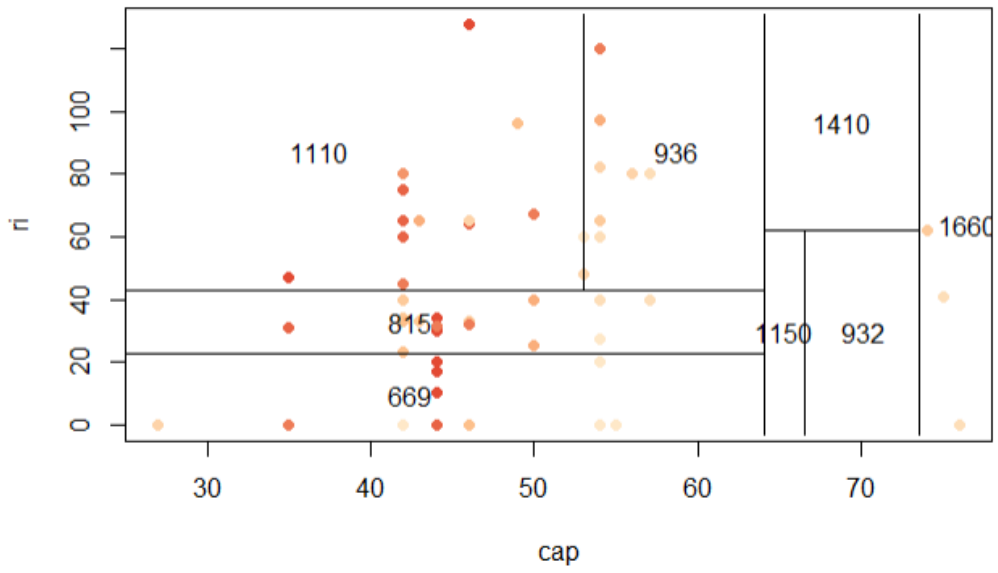

Figure 52 – 2D Partition of MOR Data

The influence of fiber reinforcement index with varying coarse aggregate proportion on MOR of SFRC mixtures is illustrated in Figure 52. As the coarse aggregate proportion decreases, less aggregate interlocking occurs and more load is transferred through the fibers. Essentially, the fibers begin to act as the coarse aggregate within the mixture as they become the largest ingredient within the mixture. The fibers act similar to reinforcing bars in reinforced concrete beams and add additional tensile capacity to MOR test specimens.

Figure 53 shows the relative influence of each parameter on the strength predictions. The influence of each parameter is a measurement of the accumulated reduction in MSE each time a parameter was used as a node split in a decision tree. For compressive strength, the water/cement (wc) is considered the most influential with a relative influence score of 40. Further, Figure 53 shows that the remaining parameters did not influence the compressive strength as much as the water/cement did, with cement proportion being the second most influential parameter with a relative influence of around 15. Overall, the fiber parameters had close to the same relative influence score on MOR as that of the compressive strength.

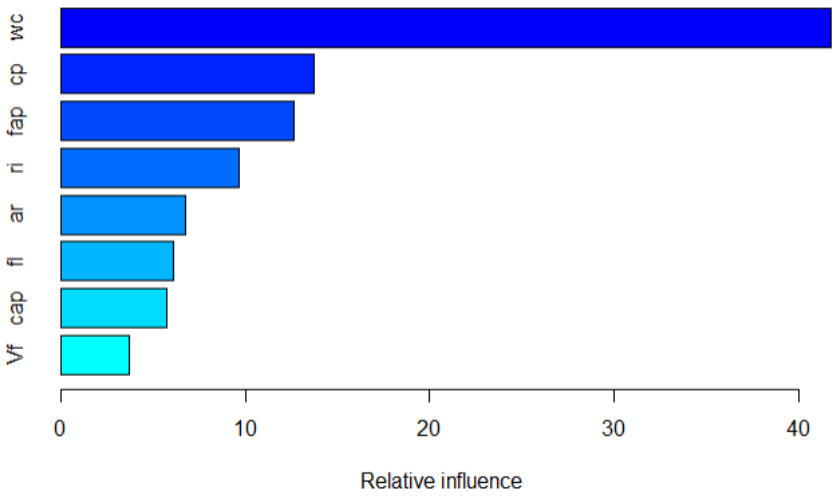

(a) Compressive Strength

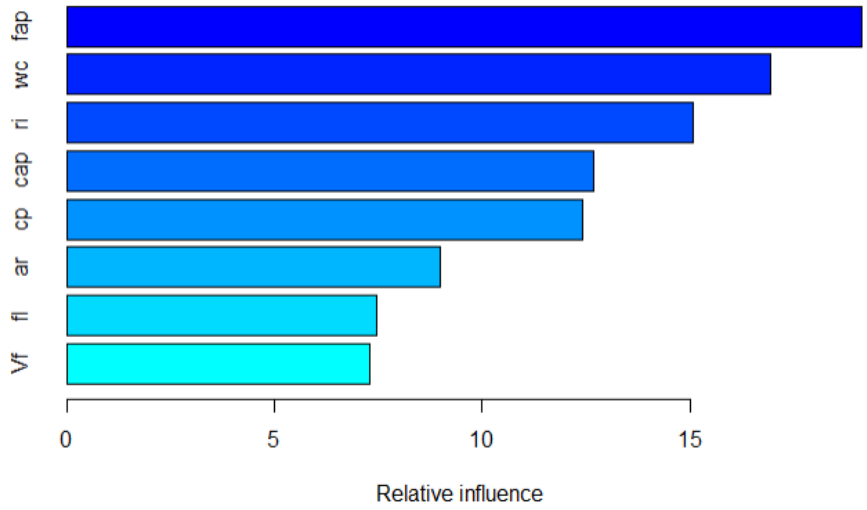

(b) MOR

Figure 53 – Relative Influence of Mixture Parameters on GBM Predictions

7.3.3 Prediction Accuracy and Validation of Machine Learning Models

7.3.3.1 Comparison of Machine Learning Methods and Proposed Expressions

The accuracy of the prediction models were determined by measuring the RMSE and R^2 as shown by Equations 9 and 10 discussed within the literature review. To recap, the RMSE is the standard

deviation of the prediction errors, or residuals. The RMSE value shows how much the predictions vary on average to the observed values. R^2 is the coefficient of determination which provides the proportion of the variance between the predicted and observed values that are explained by the model. Table 18 lists the design expressions used for comparison against the machine learning models.

Table 18: Design Expressions

Researcher	Compressive Strength	Flexural Strength
Abedel et al.	$f'_{cp} = f'_c + 5.222RI_v$	$f'_{fp} = f'_f + 5.222RI_v$
Guler et al.	$f'_{cp} = 0.92f'_c - 1.44V_f + 14.6RI_v$	$f'_{cp} = 0.24f'_c + 1.12V_f + 7.1RI_v$
Padmarajaiah	$f'_{cp} = f'_c + 1.998RI_v$	$f'_{fp} = f'_f + 4.419RI_v$

In which f'_{cp} is the prediction value obtained from the expression, f'_c is the compressive strength of the control mixture for compressive strength and the SFRC mixture for flexural strength, V_f is the volume of fibers, and RI_v is the fiber reinforcement index.

Overall, all machine learning methods implemented within this study phase produced strength predictions of mixtures within the SFRC dataset with great accuracy. Compared to design expressions, the machine learning models developed predictions with less MSE. The gradient boosting machine (GBM) is the most accurate prediction model for SFRC mechanical properties. Table 19 summarizes the RMSE and R^2 results of each prediction method used. The results show that the GBM model was the most accurate of the prediction methods with RMSE and R^2 values of 575 and 0.947, respectively, for compressive strength, and 115 and 0.936, respectively, for MOR. This shows that the larger the variation between the predicted and observed values was explained better by the GBM model than other models considered by this study.

Table 19: Machine Learning Model Accuracy Measurements

		Prediction Method					
Prediction	Measurement	Random Forest	Bagged	GBM	Abedel et al.	Guler et al.	Padmarajaiah
Compressive Strength	RMSE	787	629	575	970	1341	1070
	R^2	0.926	0.945	0.947	0.864	0.833	0.870
MOR	RMSE	208	172	115	229	866	242
	R^2	0.851	0.927	0.936	0.794	0.305	0.804

Figures 54 and 55 show the comparisons of the observed and predicted values of all strength prediction methods considered, as well as the coefficient of determination of the machine learning model graphed. These figures illustrate that the predictions made by the machine learning models are all in close proximity of the line of equality between the predicted and observed test values. There are no outliers amongst the predictions by the machine learning models. The prediction values obtained from the proposed SFRC compressive strength expressions were plotted against the machine learning model predictions for comparison. The coefficient of determination is shown in the bottom right corner of each graph for the proposed machine learning model. These graphs display the measured strength value of the SFRC mixture in the x-plane, and the corresponding predicted value of the SFRC mixture in the y-plane. If a data point falls below the line of equality between the predicted and measured values, then it is considered underestimated. If the data point lies above the line, then it is considered overestimated.

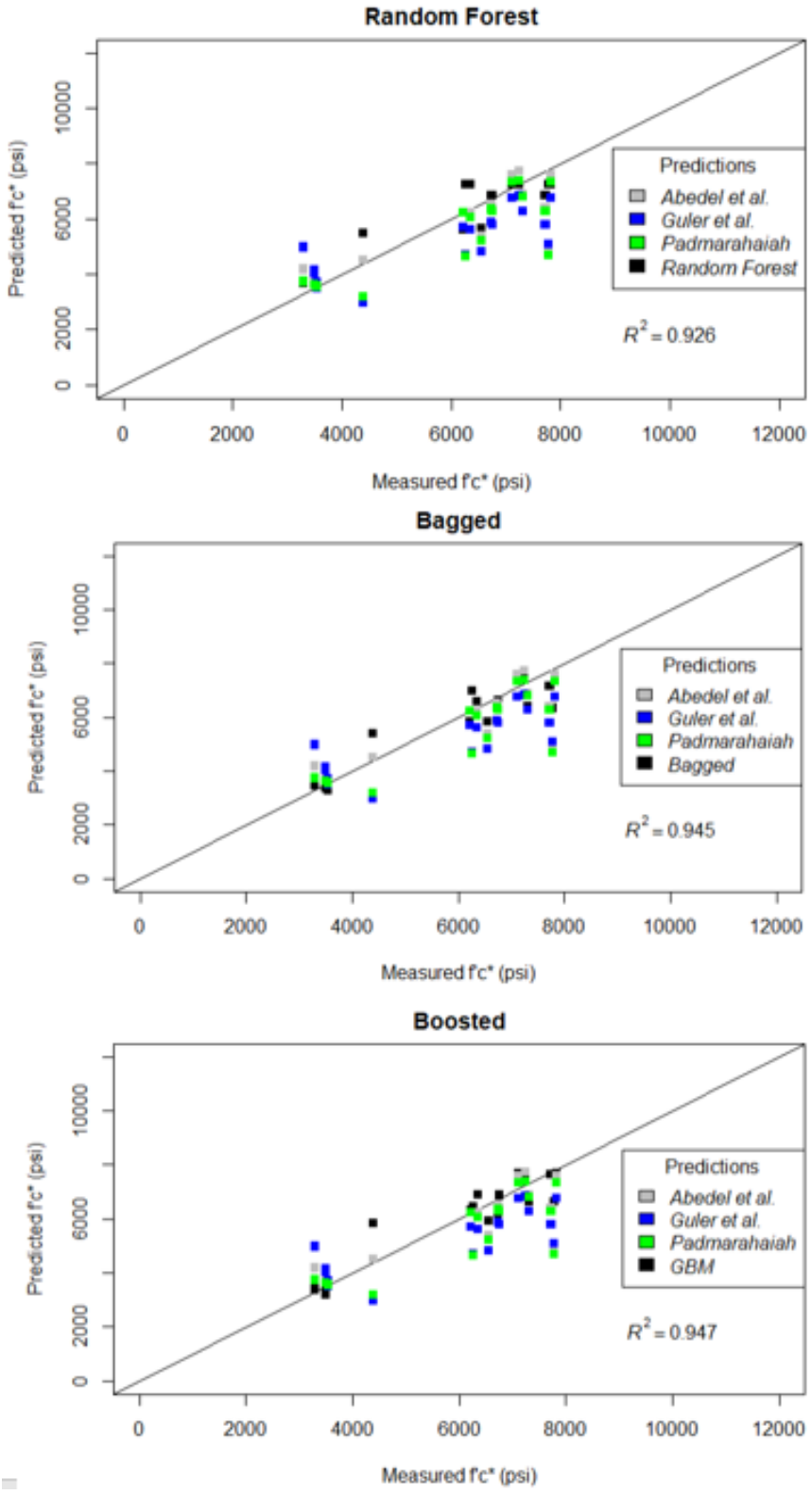

Figure 54 – Accuracy of Compressive Strength Prediction Models

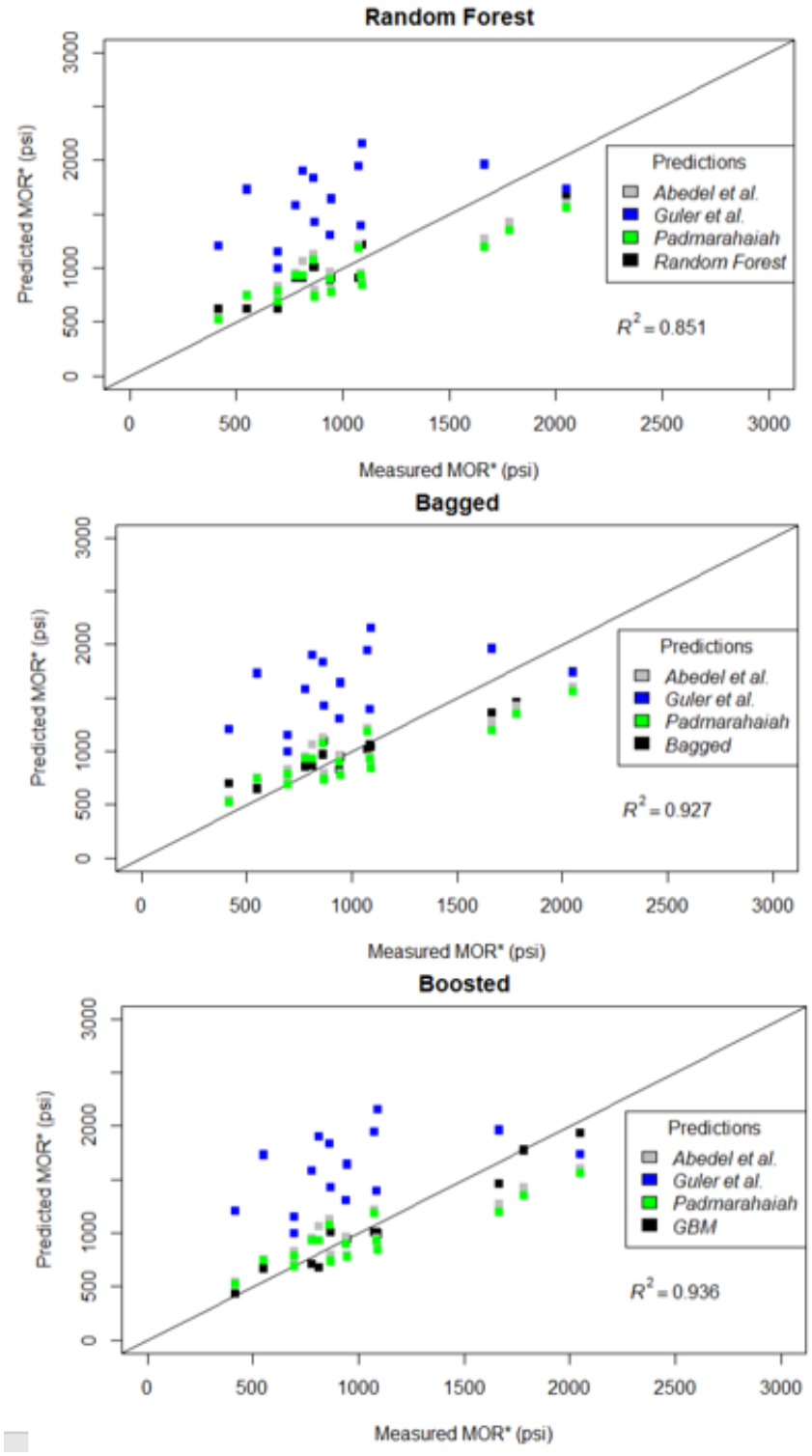

Figure 55 – Accuracy of MOR Strength Prediction Models

Figure 54 indicates that the proposed SFRC compressive strength expressions underestimated the strength of the SFRC mixtures. Mixtures with lower compressive strength values tended to be overestimated by the proposed expressions, while mixtures with higher measured compressive strength tended to be underestimated. This is contributed to the fact that the proposed expressions do not account for other more influential parameters of the concrete mixture, such as the water/cement ratio or aggregate proportioning. Interestingly, from Figure 54 it is evident that the proposed expressions overestimated the flexural strength of the SFRC mixtures, with the expression proposed by Abedel et al. being the least accurate for the testing set. This analysis concludes that the machine learning models more accurately predicted the compressive and flexural strengths of the SFRC mixture testing set. While the researchers who proposed the expressions found them to be accurate for their mixture data as discussed in literature, these expressions do not consider other aspects of the SFRC mixture that influence mechanical properties. The machine learning models are able to take these parameters into consideration when developing strength predictions by learning how the individual mixture components interact with each other through determining trends in the data.

7.3.4 Validation of the Machine Learning Models

Model validation is important for determining whether a model is performing as expected, and provides insight to potential limitations and uses of the model. From Table 18, the GBM model has the lowest number of residual error and the greatest R^2 results in comparison to other models considered. Because of this high accuracy, the GBM model was used moving forward with the study. For model validation, strength predictions of Phase I SFRC mixtures were developed using the GBM model and proposed strength expressions. Comparisons of the GBM model with the proposed strength expressions was performed to examine the prediction method accuracy. It was

important to validate the model with GDOT SFRC mixture data to ensure that the models are reliable predictors for GDOT.

Figures 56 and 57 display the comparison between the predicted and the observed compressive and flexural strength values of Phase I SFRC mixtures, respectively.

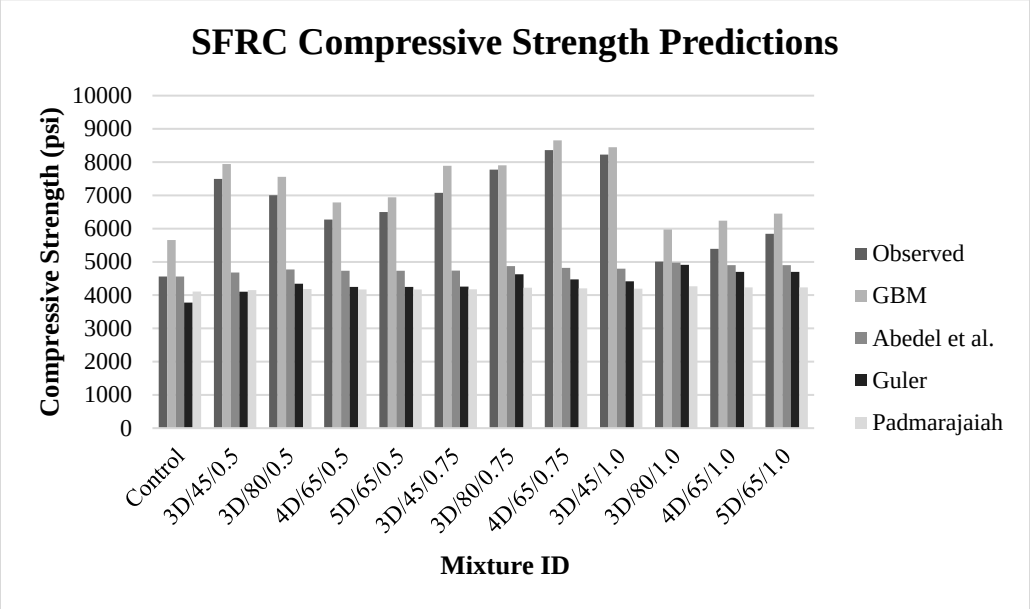

Figure 56 – Comparison of Compressive Strength Prediction Models

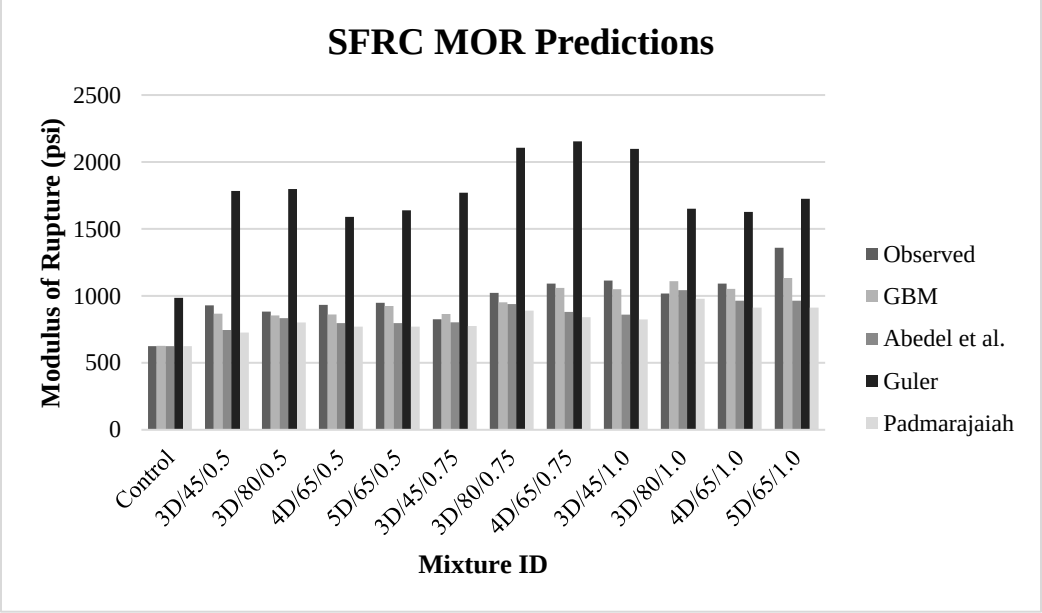

Figure 57 – Comparison of Flexural Strength Prediction Models

As shown in Figure 56 the proposed design expressions underestimated the compressive strength of the phase I mixtures. In general, the GBM model overestimated the compressive strength value while still being more accurate than the proposed expressions. The difference between the observed values and GBM predicted values ranged from 131 to 1095 (psi), with the greatest difference occurring with the mixtures containing 1.00% fibers by volume. The proposed expressions predict a slight increase in the compressive strength of SFRC mixtures with an increase in fiber volume, which is expected as an increase in fiber volume increases the reinforcing index, the only fiber parameter used in the expressions proposed by Abedel et al. and Padamarajaiah.

Figure 57 illustrates that the majority of the prediction methods are close in accuracy, with the expression proposed by Guler et al. sginificantly overestimating the flexural strength of the phase I SFRC mixtures. The majority of the predictions aggreed with the trends found in MOR experimental data, showing that flexural strength increased with increased fiber volume fraction. The equation proposed by Guler et al. uses the compressive strength of the SFRC mixture within the expression, a potential cause of the increased error. A comparison of the prediction methods was performed by determining the ratio between the measured and predictied values. These ratios are summarized in Table 20.

Table 20: SFRC Strength Prediction Method Accuracy Comparison

	GBM		Abedel et al.		Guler et al.		Padmarajaiah	
Mixture ID	f'_c / f'_{cp}	f'_f / f'_{fp}	f'_c / f'_{cp}	f'_f / f'_{fp}	f'_c / f'_{cp}	f'_f / f'_{fp}	f'_c / f'_{cp}	f'_f / f'_{fp}
Control	0.806	0.997	1.000	1.000	1.208	0.634	1.111	1.000
3D/45/0.5	0.944	1.072	1.601	1.247	1.827	0.521	1.806	1.278
3D/80/0.5	0.927	1.034	1.468	1.059	1.612	0.491	1.674	1.101
4D/65/0.5	0.924	1.084	1.325	1.170	1.477	0.587	1.504	1.210
5D/65/0.5	0.936	1.025	1.373	1.189	1.531	0.579	1.558	1.230
3D/45/0.75	0.897	0.954	1.493	1.028	1.662	0.466	1.696	1.064
3D/80/0.75	0.983	1.075	1.595	1.090	1.680	0.486	1.840	1.149
4D/65/0.75	0.966	1.030	1.735	1.240	1.869	0.507	1.989	1.298
3D/45/1.0	0.974	1.061	1.715	1.295	1.863	0.531	1.961	1.352
3D/80/1.0	0.838	0.917	1.006	0.976	1.020	0.616	1.175	1.040
4D/65/1.0	0.865	1.038	1.100	1.132	1.148	0.671	1.273	1.197
5D/65/1.0	0.906	1.199	1.193	1.410	1.244	0.788	1.380	1.491
Avg. Acc.	**0.914**	**1.04**	**1.384**	**1.153**	**1.512**	**0.573**	**1.580**	**1.201**

The results of the comparisons reinforce the accuracy of the GBM model. According to Table 20, the GBM model over predicted Phase I compressive strength by 8.60% on average, and under predicted the flexural strengths by 4.00%. Expressions proposed by Abedel et al. were the second most accurate prediction method having under predicted both the compressive and flexural strengths by 38.40% and 15.30%, respectively. These results indicate that the GBM model predicts the compressive and flexural strength of SFRC with far greater accuracy than other proposed expressions. The GBM model is able to consider all aspects of the SFRC mixture when developing a prediction, rather than only considering the base compressive or flexural strength and the fiber reinforcing indexes as the other prediction expressions offer.

7.3.5 Model Deployment

The GBM model is useful for estimating the compressive and flexural strengths of SFRC mixtures without having to perform time consuming destructive testing. Deployment of the model allows for users to have access to the GBM model without needing to have Rstudio to run the model code.

Any person with the webpage link is able to access the full potential of the GBM model for SFRC strength predictions. The GBM model developed within this study phase is deployed using the shinyapps R package, which allows for the program to run in the cloud on shared servers operated by RStudio. This deployment method allows for the GBM model to be ran from a webpage where users, such as the GDOT, may develop SFRC strength predictions and mixture costs based on mixture parameter inputs. Figure 58 shows the shinyapp webpage developed for the GBM model.

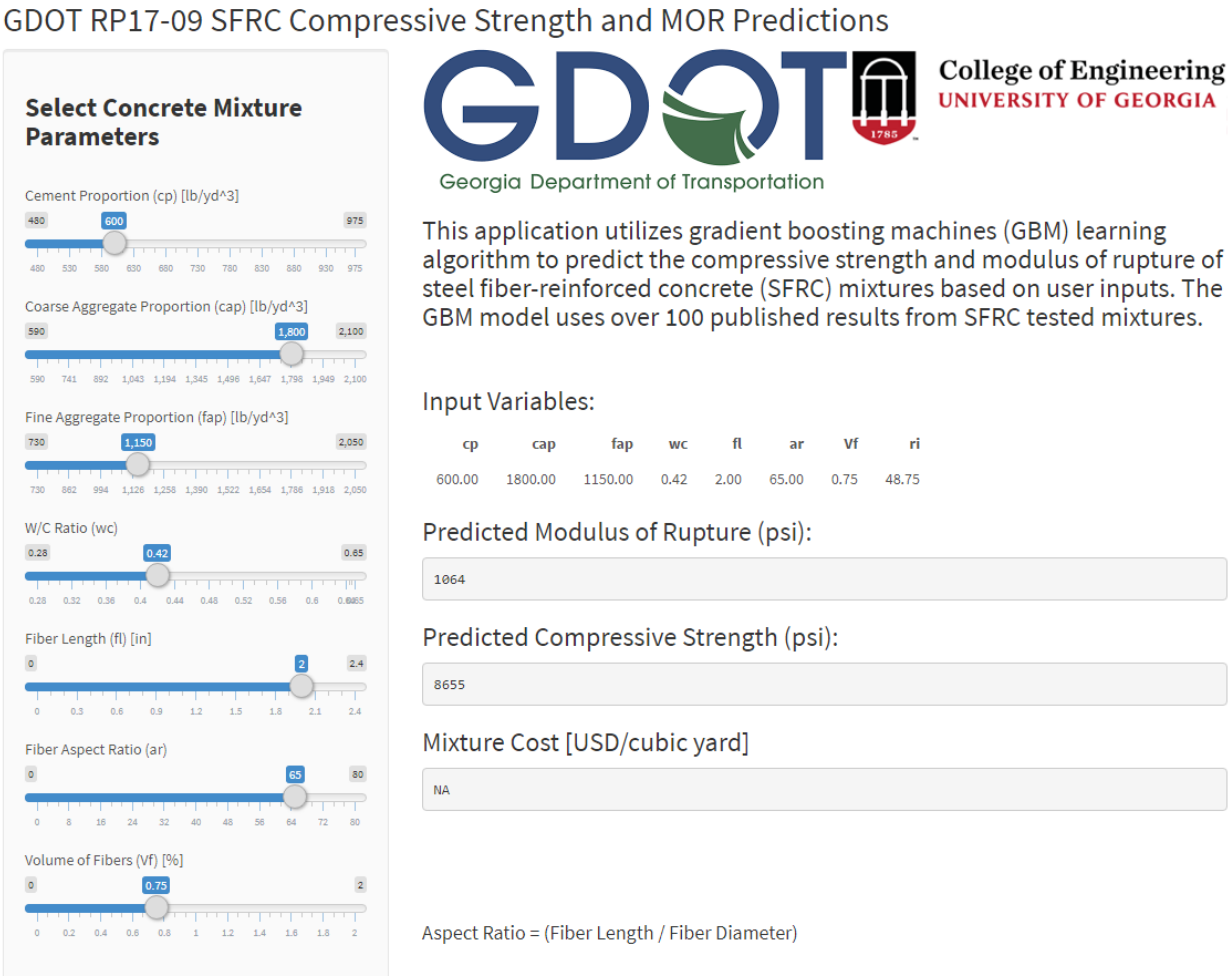

Figure 58 – Deployed Model Webpage (Cost Inputs Excluded)

7.3.5.1 Development of User Interface

Shinyapps deploys the machine learning model in the form of a webpage. This user interface was developed taking into account the limits of the dataset and the prediction model. On the left side of the webpage, users may input SFRC mixture parameters using the input sliders. These inputs are used by the GBM model to develop strengths predictions, displayed on the right side of the webpage. When the user updates one of the input sliders, the strength predictions automatically update to reflect this change. A user may change the value of the input slider by either dragging the slider to the desired value, or by hovering the mouse cursor over the slider and using the arrow keys to adjust the value by one tick.

The input ranges of the mixture parameters were selected based on the range of each respective mixture parameter within the training dataset. The range of mixture parameters within the dataset are summarized in Table 21. Limiting the range of user inputs is important for ensuring the development of an accurate strength predictions for SFRC mixtures. This is to say that if a mixture had a cement proportion greater than 1,000 lb/yd^3, the GBM model would be unable to develop an accurate prediction for said mixture as there is no data within the training data set for a SFRC mixture containing a cement proportion greater than 1,000 lb/yd^3.

Table 21: SFRC Mixture Parameter Ranges in Data Base

	Mixture Parameters							
	cp (lb/yd^3)	**cap (lb/yd^3)**	**fap (lb/yd^3)**	**wc**	**fl (in)**	**ar**	**Vf (%)**	**ri**
Min	486	594	729	0.28	1.22	40	0.00	0
Median	729	1458	1242	0.43	2.18	65	0.75	40
Mean	718	1535	1282	0.45	1.81	59	0.73	47
Max	972	2106	2052	0.65	2.40	80	2.00	128

7.3.5.2 Uses of Deployed Model

Deployment of the machine learning model allows for users to develop predictions of their own SFRC mixutres with reliable accuracy. With this powerful prediction method, one can analyze a variety of concrete mixtures for their suitability for fiber reinforcement. As fiber reinforcement adds upfront costs to the concrete mixture, it's important to ensure that the addition of fibers will enhance the mechanical properties of the mixture enough to justify the increased cost. By first developing strength predictions for potential SFRC mixtures, one is able to conclude if the addition of fibers are beneficial before needing to produce test samples or even ordering the fibers. As this model accounts for all aspects of mixture proportions, it is far more reliable than other proposed SFRC strength expressions, and may be referenced during the mixture design process.

It should be stated that while the deployed model is able to develop accurate mechanical property estimations, it does not consider the state of the fresh properties of the mixture, such as air content, unit weight, or slump. It is recommended that if a user designs a mixture using the deployed model, a test mixture should still be performed to both validate the strength prediction and to determine admixture proportioning to conteract the unfavorable fresh properties of the SFRC mixture.

8.0 ECONOMIC CONSIDERATIONS

The use of SFRC has many benefits aside from the enhanced mechanical properties. With the use of fiber reinforcement, traditional steel reinforcement may be replaced, which saves both material and labor costs. Additionally, the durability of the concrete element is increased, which may lead to lowered maintenance costs and longer life spans. These savings should be considered when performing an economic analysis on the use of SFRC in comparison to convential reinforced concrete. As fiber reinforcement is an additive to concrete mixtures, as they do not replace any of the mixture proportioning, the upfront material cost with using SFRC is higher than conventional concrete mixtures.

8.1 Economic Analysis of Phase I SFRC Mixtures

An economic analysis was performed to determine the cost effectiveness of using steel fibers in GDOT standard concrete mixtures. Material costs were collected from suppliers for the purpose of this analysis. The costs of materials are shown as USD ($) / ton (0.91 metric ton). Table 22 summarizes the cost analysis, with the total unit cost for one cubic yard of the concrete mixture shown. Costs of materials used in this analysis reflect the cost of materials from suppliers within Georgia.

Table 22: Phase I SFRC Mixture Costs per Cubic Yard

	Material/Cost								
Mixture	Cement $140/ton	Coarse Agg. $24/ton	Fine Agg. $18/ton	Water $0.60/ton	Steel Fibers Varies*	AEA $3.50/gal	HRWRA $8/gal	VMA $15/gal	**TOTAL**
Control	$44.45	$21.60	$10.22	$0.08	--	$0.08	$2.28	$3.35	**$82.06/cy**
3D/45/0.50	$44.45	$21.60	$10.22	$0.08	$62.42	$0.08	$2.28	$3.35	**$144.47/cy**
3D/80/0.50	$44.45	$21.60	$10.22	$0.08	$57.82	$0.08	$2.28	$3.35	**$139.87/cy**
4D/65/0.50	$44.45	$21.60	$10.22	$0.08	$60.44	$0.08	$2.28	$3.35	**$142.50/cy**
5D/65/0.50	$44.45	$21.60	$10.22	$0.08	$77.53	$0.08	$2.28	$3.35	**$159.58/cy**
3D/45/0.75	$44.45	$21.60	$10.22	$0.08	$93.67	$0.08	$2.28	$3.35	**$175.73/cy**
3D/80/0.75	$44.45	$21.60	$10.22	$0.08	$86.77	$0.08	$2.28	$3.35	**$168.82/cy**
4D/65/0.75	$44.45	$21.60	$10.22	$0.08	$90.71	$0.08	$2.28	$3.35	**$172.77/cy**
3D/45/1.00	$44.45	$21.60	$10.22	$0.08	$124.83	$0.08	$2.28	$3.35	**$206.89/cy**
3D/80/1.00	$44.45	$21.60	$10.22	$0.08	$115.63	$0.08	$2.28	$3.35	**$197.69/cy**
4D/65/1.00	$44.45	$21.60	$10.22	$0.08	$120.89	$0.08	$2.28	$3.35	**$202.94/cy**
5D/65/1.00	$44.45	$21.60	$10.22	$0.08	$155.05	$0.08	$2.28	$3.35	**$237.11/cy**

*Fiber costs: 3D/45 = $0.95/lb; 3D/80 = $0.88/lb; 4D/65 = $0.92/lb; 5D/65 = $1.18/lb

As expected, the addition of steel fibers into the concrete mixture greatly increased the unit cost of the concrete mixture. The costs of fibers differ based on the geometry of the fiber, and fiber coating. The cost of the 3D/45, 3D/80, 4D/65, and 5D/65 are $0.95/lb, $0.88/lb, $0.92/lb, and $1.18/lb, respectively. The 5D/65 is the most expensive fiber per pound, due to the advanced end anchorage and a special galvanized coating that reduces exposed fiber corrosion. On average, there was an increase in unit cost of 78.66%, 120.63%, and 157.30% for fiber volume fractions of 0.50%, 0.75%, and 1.00%, respectively. While the use of steel fibers may increase the unit cost of the concrete mixtures dramatically, the benefits obtained through the use of fibers can outweigh the additional cost if used correctly in the proper application. Figure 59 provides a cost comparison of the SFRC mixtures in this study to the control mixture.

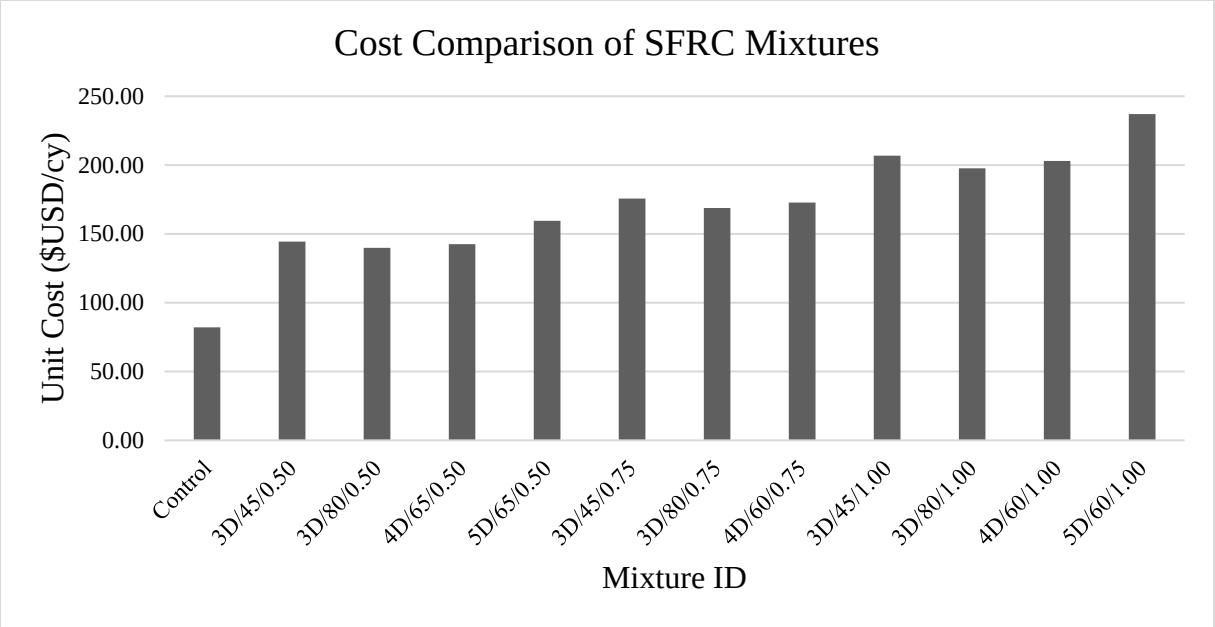

Figure 59 – Cost Comparison of SFRC Mixtures

One method of considering the costs and benefits of fiber reinforcement is by determining the cost per unit increase in concrete strength. To do this, the correlation between the increase in compressive strength and the increase in unit cost of the concrete mixture were determined. Table 23 summarizes the cost per unit (1 psi) increase in compressive strength and MOR of Phase I mixtures. Figures 60 through 62 illustrate the correlation between cost and increase in compressive strength. On these graphs, the results of phase I testing is used to plot the increase in either compressive or flexural strength against the increase in cost determined within Table 22. The steeper the line, the less cost effective the SFRC mixture.

Table 23: Cost ($USD) Per Unit Increase in Strength of Fibers Studied

	Cost per Unit Increase in f'c			**Cost per Unit Increase in MOR**		
Fiber	**Vf = 0.5%**	**Vf = 0.75%**	**Vf = 1.0%**	**Vf = 0.5%**	**Vf = 0.75%**	**Vf = 1.0%**
3D/45	0.021	0.037	0.034	0.233	0.570	0.276
3D/80	0.024	0.027	0.258	0.260	0.240	0.324
4D/65	0.035	0.024	0.146	0.222	0.194	0.280
5D/65	0.040	---	0.121	0.270	---	0.222

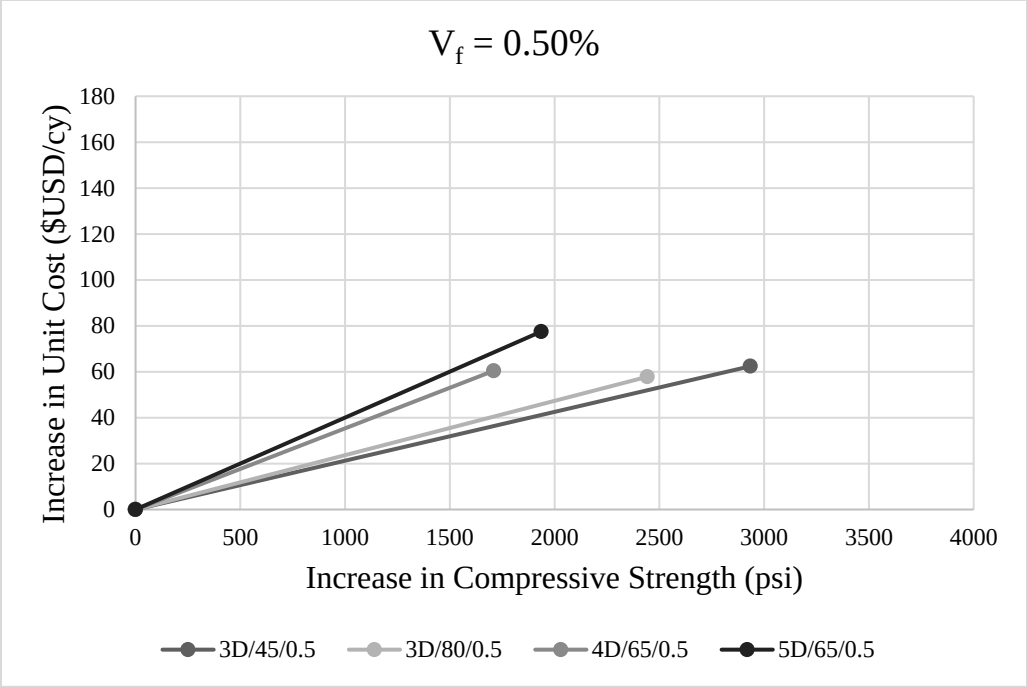

Figure 60 – Cost per Unit Increase in Compressive Strength of V_f = 0.5% Mixtures

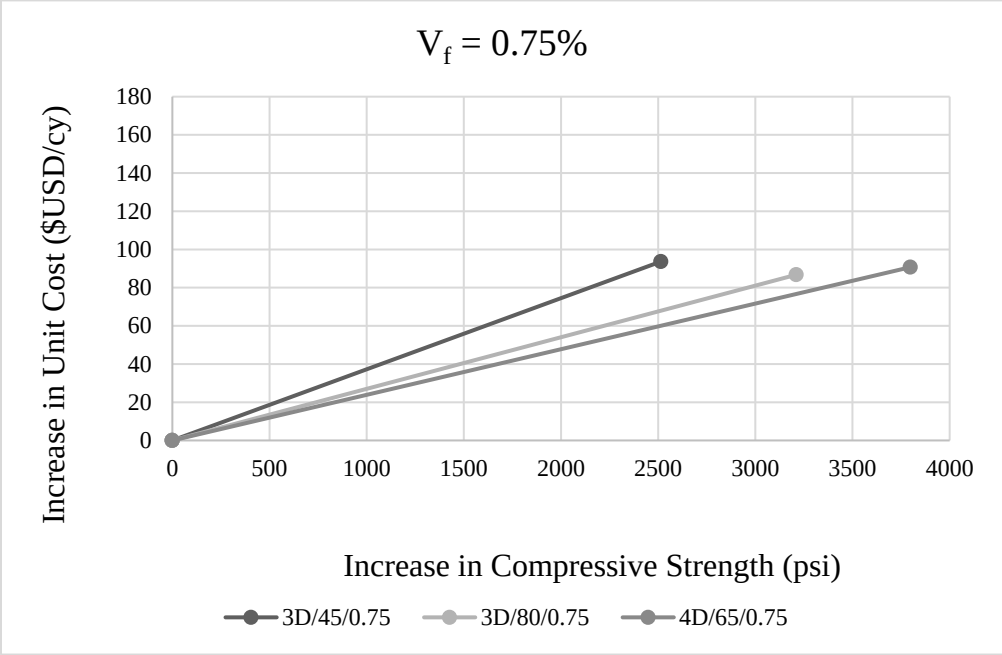

Figure 61 – Cost per Unit Increase in Compressive Strength of V_f = 0.75% Mixtures

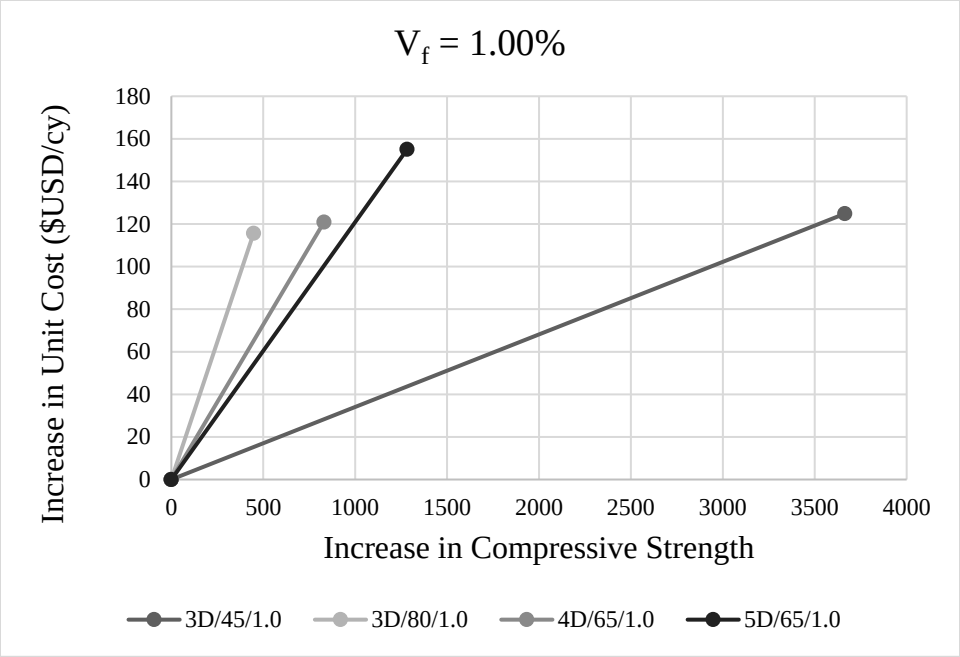

Figure 62 – Cost per Unit Increase in Compressive Strength of V_f = 1.0% Mixtures

The cost effectiveness of fibers differed with fiber content. For example, the 3D/45 fiber was the most cost effective for increasing the compressive strength for fiber volumes of 0.50% and 1.00%, however was the least effective at a fiber volume of 0.75%. Overall, the 3D/45 fiber was determined to be the most cost effective for increasing compressive strength, showing a 1 psi (0.0068 MPa) increase in compressive strength for approximately $0.03 on average. In contrast, the 3D/80 fiber was the least cost effective of the fibers studied, showing a 1psi (0.0068 MPa) increase in compressive strength for an average of $0.10. Inspecting the change in flexural strength, 4D/65 fibers were the most cost effective for improving the flexural capacity of concrete mixtures, costing an average of $0.23 per unit increase in flexural strength. In contrast, the 3D/45 fibers were the least cost effective for improving flexural capacity, costing $0.36 per unit strength increase on average.

8.2 Cost Savings Potentials with Fiber Reinforced Concrete

The use of SFRC provides cost benefits in other forms than just increased strength. As discussed within the literature review, fibers can be used as a replacement of traditional steel reinforcement in various applications. Most notably, as a replacement for shear stirrups in reinforced concrete beams, or as primary or secondary reinforcing steel in concrete slabs and bridge decks. By replacing traditional reinforcing steel, both material and labor cost savings are obtained. Steel fibers may be added to the concrete mixture at the batch plant, and transported onto the job site for placement. The amount of labor and time required for laying reinforcing bars is reduced as workers need only to place the SFRC into the forms and finish as normal.

SFRC possesses enhanced shrinkage crack resistance, reduced permeability, and overall greater strength than conventional concrete. The increased strength reduces maintenance costs significantly. Areas that are often prone to deteriorating first, such as control joints and slab corners, are reinforced to withstand more loading. Additionally, joint spacing can be increased, which reduces the amount of critical loads and edges and corners that typically control the design of slabs. Slab thickness may be reduced with the use of SFRC, as flexural strength is increased. As observed from Phase II SFRC beam testing, SFRC beams possessed far greater flexural strength.

9.0 CONCLUSIONS AND RECOMMENDATIONS

This study investigated the influence of steel fiber reinforcement on GDOT Class AA concrete mixtures. The objectives for this research project were to investigate the strength enhancement capabilities from incorporating steel fiber reinforcement into conventional concrete mixtures. Through an experimental investigation, SFRC mixtures were produced and tested. Additionally, machine learning methods were utilizied for the development of an accurate SFRC strength prediction model. Through this three phase research project, the following conclusions were drawn.

9.1 Phase I Conclusions

Phase I included the testing of fresh and hardened concrete properties of twelve investigative mixtures. The conclusions from this testing are as follows.

- The addition of steel fiber reinforcement into concrete mixtures improved the compressive strength. Compressive strength increased as the volume of fibers increased, up to a fiber volume of 0.75%, at which the increase in strength began to diminish.
- SFRC possessed 54.36% more flexural strength than conventional concrete mixtures on average. Flexural strength increased with increasing fiber volume.
- Fresh concrete properties were affected negatively by the addition of steel fiber reinforcement. Workability of fresh concrete mixtures was reduced, unit weight increased by a small amount, and air content decreased.

- Shorter fibers were more effective at increasing compressive strength at higher fiber volumes. Long fibers were not as effective at increasing compressive strength at fiber volumes ratios greater than 0.75%.
- Overall, the end anchorage did not appear to have a significant impact on the increase in compressive strength. However, the end anchorage had a substantial influence on the flexural strength of the SFRC mixtures. The 5D/65 outperformed all other fibers in the flexural strength test. The enhanced end anchorage aids in increasing the fiber pull-out strength.
- Long fibers were more effective at increasing flexural strength than short fibers, as they have more development length across internal cracks.
- Ultimately, the 4D/65/0.75 mixture resulted in the most desirable hardened property strengths of the Phase I mixtures, and was selected for use within Phase II static beam testing.

9.2 Phase II Conclusions

Phase II focused on static testing of laboratory-scale SFRC beams containing conventional flexural and shear reinforcing steel. The conclusions drawn from the testing includes:

- Similar to what was observed from Phase I MOR results, the inclusion of fibers increased the flexural and shear capacity of reinforced concrete beams by 51.30%.
- The 4D/65 fiber was the most effective at reducing flexural cracks. Additionally, the 4D/65/0.5 mixture utilized in beam B3 resulted in the greatest maximum moment and shear capacity of the fibers studied in this research.

- Steel fibers proved to be a potential partial replacement for shear stirrups within SFRC beams. With an addition of fibers at 0.75% by volume, the spacing in shear stirrups were able to be doubled without a noticeable affect on the load capacity.
- Average crack width decreased as fiber volume percentage increased.
- Addition of fibers at 0.50% fiber volume resulted in a shift from shear failure to a flexural-shear failure. Addition of fibers at 0.75% fiber volume resulted in a shift from flexural-shear failure to flexural failure.

9.3 Phase III Conclusions

The objective of phase III was to develop a machine learning model with the power to predict SFRC compressive and flexural strengths at great accuracy. The following observations are concluded from this study phase.

- Of the machine learning methods used, the GBM was more accurate at predicting SFRC compressive and flexural strength than the Random Forest or Bagged decision tree models.
- The GBM is a more accurate predictor of SFRC compressive and flexural strength than proposed design equations. This is primarily due to the GBM's ability to consider all aspect of the SFRC mixture design when predicting strength, while proposed design equations are more limited.
- MOR was influenced by all aspects of the fiber. Fibers have a greater impact on flexural strength of concrete in mixtures with higher fine aggregate proportions and lower coarse aggregate proportions.

9.4 Recommendations

Based on the findings of this study, the following recommendations are made for the use of steel fibers in GDOT applications:

- When using SFRC, fibers should be proportioned using the absolute volume method. Steel fibers are to be measured as a volume fraction of the total batch volume.
- As steel fibers reduce the workability of fresh concrete, it is recommended that additional dosages of HRWRA be included in the mixture. Trial batches should be tested to determine the workability of the designed mixture, and make any necessary adjustments to admixture dosages.
- Steel fibers could be integrated into concrete structures that are subjected to intense loading or impact loading. The increased toughness of SFRC provides better dissipation of energy.
- Fiber reinforcement can be used as a partial replacement of tensile or shear reinforcement, however designs should be reviewed and approved by a licensed structural engineer.

9.5 Future Work

9.5.1 Impact Testing of SFRC Beams

Laboratory-scale impact beam testing is recommended to be performed in order to observe the ability of SFRC to redistribute impact loads and to measure the influence of fiber aspect ratio and volume concentration on impact ductility. This testing would provide useful information on the impact resistance capabilities of SFRC in applications such as beams, bridge decks, and barrier walls and would build off of the work conducted by Lopez (2018) and Tate (2019). Impact testing allows for the response to impact force of SFRC beams to be observed and measured. In addition to monitoring reaction forces and displacements as a result of the impact, the failure mode and level of damage experienced by the SFRC beams, or the amount of spalling caused by impact, is

also important to consider. By investiating how these concrete elements react to impact loading, the degree of safety for projectile impacts either an automobile or other heavy objects may be considered.

Laboratory-scale impact testing would provide the opportunity to study the impact resistance enhancements provided by the inclusion of steel fibers. Considering the large statistical variation in the standard drop-weight tests denoted in literature, the large-scale impact tests would provide a more precise reading of the concrete impact performance. Additionally, the impact loading response of SFRC beams with minimal shear reinforcement may be studied.

This study program would allow for the effects of shear mechanisms of SFRC beams subjected to impact loads to be observed and provides data useful for design and optimization of impact resistant reinforced concrete structures. Based on the information gathered from Phase II testing, there is potential to use steel fibers as a partial replacement of traditional steel reinforcement. Prior to recommending that shear reinforcement be replaced by steel fibers in applications such as CMB walls, testing should be conducted to quantify the impact resistance of SFRC members with reduced shear reinforcement.

9.5.2 Development of GDOT Approved SFRC Mixture Database

As discussed in previous sections, the database built for training of the machine learning models was comprised of data from a variety of researchers in various parts of the world. The materials used by researchers varied with respect to chemical properties of cement types, aggregate sizes, and placement environments. Because of this variation, the models have not yet reached their full potential for predicting GDOT standard SFRC strength. It is recommended that various SFRC mixtures be batched and tested using GDOT standard materials for the development of a new database. By constructing a database comprised of SFRC mixtures with Georgia materials, the

prediction accuracy will be increased and will be more reliable for use by GDOT. Additionally, the model may be expanded to include input parameters such as fiber anchorage type, fiber coating, admixture dosage, and other influential mixture parameters.

REFERENCES

Abadel, A., Abbas, H., Almusallam, T., Al-Salloum, Y., & Siddiqui, N. (2016). Mechanical properties of hybrid fibre-reinforced concrete – analytical modelling and experimental behaviour. *Magazine of Concrete Research, 68*(16), 823-843. doi:10.1680/jmacr.15.00276

Abdallah, S. (2017). Effect of Hooked-End Steel Fibres Geometry. *International Journal of Civil, Environmental, Structural, Construction and Architecture Engineering, 10*.

ACI. (2018). ACI 544.4R-18 Guide for Design with FRC.

Acikgenc, M., Alyamac, K. E., & Ulucan, Z. C. (2013). Fresh and Hardened Properties of Steel Fiber Reinforced Concrete Produced With Fibers of Different Lengths and Diameters. *2nd International Balkans Conference on Challenges of Civil Engineering*.

Acikgenc, M., Alyamac, Kursat E., Ulucan, Zulfu C. (2013). Fresh and Hardened Properties of Steel Fiber Reinforced Concrete Produced With Fibers of Different Lengths and Diameters. *2nd International Balkans Conference on Challenges of Civil Engineering*.

Al-Ameeri, A. (2013). The Effect of Steel Fiber on Some Mechanical Properties of Self Compacting Concrete. *American Journal of Civil Engineering, 1*(3). doi:10.11648/j.ajce.20130103.14

Alavi Nia, A., Hedayatian, M., Nili, M., & Sabet, V. A. (2012). An experimental and numerical study on how steel and polypropylene fibers affect the impact resistance in fiber-reinforced concrete. *International Journal of Impact Engineering, 46*, 62-73. doi:10.1016/j.ijimpeng.2012.01.009

Amirkhanian, A., & Roesler, J. (2019). Overview of Fiber-Reinforced Concrete Bridge Decks.

Amirkhanian, A. R., Jeffery. (2019). Overview of Fiber-Reinforced Concrete Bridge Decks.

Balaguru, R. (1988). Properties of Fiber Reinforced Concrete: Workability, Behavior Under Long-Term Loading, and Air-Void Characteristics. *ACI*.

Banthia, N., & Sappakittipakorn, M. (2007). Toughness enhancement in steel fiber reinforced concrete through fiber hybridization. *Cement and Concrete Research, 37*(9), 1366-1372.

Baun, M. (1992). Steel Fiber Reinforced Concrete Bridge Deck Overlays: Experimental Use by Ohio Department of Transportation. *Transportation Research Board*.

Behnood, A., Behnood, V., Modiri Gharehveran, M., & Alyamac, K. E. (2017). Prediction of the compressive strength of normal and high-performance concretes using M5P model tree algorithm. *Construction and Building Materials, 142*, 199-207. doi:10.1016/j.conbuildmat.2017.03.061

Campione, G., & Letizia Mangiavillano, M. (2008). Fibrous reinforced concrete beams in flexure: Experimental investigation, analytical modelling and design considerations. *Engineering Structures, 30*(11), 2970-2980. doi:10.1016/j.engstruct.2008.04.019

Choi, K.-K., Park, H.-G., & Wight, J. K. (2007). Shear Strength of Steel Fiber-Reinfroced Concrete Beams without Web Reinforcement. *ACI Structural Journal*.

Chou, J.-S., Tsai, C.-F., Pham, A.-D., & Lu, Y.-H. (2014). Machine learning in concrete strength simulations: Multi-nation data analytics. *Construction and Building Materials, 73*, 771-780. doi:10.1016/j.conbuildmat.2014.09.054

Darling, G. (2017). Structural Behavior of TL-4 Recycled Tire Chip and Fiber Reinforced Concrete Single Slope Barriers.

Deepa, C., SathiyaKumari, K., & Pream Sudha, V. (2010). Prediction of the Compressive Strength of High Performance Concrete Mix Using Tree Based Modeling. *International Journal of Computer Applications, 6*.

Deluce, J. R. (2001). Cracking Behavior of Steel Fibre Reinforced Concrete Containing Conventional Steel Reinforcement.

Dopko, M. (2018). Fiber Reinforced Concrete: Tailoring Composite Properties with Discrete Fibers.

Feng, D.-C., Liu, Z.-T., Wang, X.-D., Chen, Y., Chang, J.-Q., Wei, D.-F., & Jiang, Z.-M. (2020). Machine learning-based compressive strength prediction for concrete: An adaptive boosting approach. *Construction and Building Materials, 230*. doi:10.1016/j.conbuildmat.2019.117000

Guerini, V., Conforti, A., Plizzari, G., & Kawashima, S. (2018). Influence of Steel and Macro-Synthetic Fibers on Concrete Properties. *Fibers, 6*(3). doi:10.3390/fib6030047

Guler, S., Yavuz, D., Korkut, F., & Ashour, A. (2019). Strength prediction models for steel, synthetic, and hybrid fiber reinforced concretes. *Structural Concrete, 20*(1), 428-445. doi:10.1002/suco.201800088

Kopczynski, C., & Whiteley, M. (2016). High-Rises, High Seismicity: New Materials and Design Approaches. *CTBUH Journal*(III).

Kwak, Y.-K., Eberhard, M. O., Kim, W.-S., & Kim, J. (2002). Shear Strength of Steel Fiber-Reinforced Concrete Beams without Stirrups. *ACI Structural Journal*.

Kwak, Y.-K., Eberhard, Marc O., Kim, Woo-Suk, Kim, Jubum. (2002). Shear Strength of Steel Fiber-Reinforced Concrete Beams without Stirrups. *ACI Structural Journal*.

Lee, D. H., Han, S.-J., Kim, K. S., & LaFave, J. M. (2017). Shear capacity of steel fiber-reinforced concrete beams. *Structural Concrete, 18*(2), 278-291. doi:10.1002/suco.201600104

Lee, S.-J., Yoo, D.-Y., & Moon, D.-Y. (2019). Effects of Hooked-End Steel Fiber Geometry and Volume Fraction on the Flexural Behavior of Concrete Pedestrian Decks. *Applied Sciences, 9*(6). doi:10.3390/app9061241

Lopez, V. (2018). Impact Performance Of Recycled Tire Chip And Fiber Reinforced Cementitious Composites.

Marar, K., Eren, Ö., & Roughani, H. (2016). The influence of amount and aspect ratio of fibers on shear behaviour of steel fiber reinforced concrete. *KSCE Journal of Civil Engineering, 21*(4), 1393-1399. doi:10.1007/s12205-016-0787-2

Naaman, A. E. (2003). Engineered Steel Fibers with Optimal Properties for Reinforcement of Cement Composites. *Journal of Advanced Concrete Technology, 1*, 241-252.

Naaman, A. E. (2018). *Fiber reinforced concrete: five decades of progress*. Paper presented at the Proceedings of the 4th Brazilian Conference on Composite Materials.

Nataraja, M. C. D., N.

Gupta, A.P. (1999). Statistical Variations in Impact Resistance of Steel Fiber-Reinforced Concrete Subjected to Drop Weight Tests. *Cement and Concrete Research*.

Roesler, J., Bordelon, A., Brand, A. S., & Amirkhanian, A. (2019). *Fiber-Reinforced Concrete for Pavement Overlays: Technical Overview*. Retrieved from

Song, P. S., & Hwang, S. (2004). Mechanical properties of high-strength steel fiber-reinforced concrete. *Construction and Building Materials, 18*(9), 669-673. doi:10.1016/j.conbuildmat.2004.04.027

Soulioti, D. V., Barkoula, N. M., Paipetis, A., & Matikas, T. E. (2011). Effects of Fibre Geometry and Volume Fraction on the Flexural Behaviour of Steel-Fibre Reinforced Concrete. *Strain, 47,* e535-e541. doi:10.1111/j.1475-1305.2009.00652.x

Tate, S. (2019). Investigation Into The Use of Tire Derived Rubber Aggregates and Recycled Steel Wire Fiber For Use In Concrete Subjected To Impact Loading.

Torres, J. A., & Lantsoght, E. O. L. (2019). Influence of Fiber Content on Shear Capacity of Steel Fiber-Reinforced Concrete Beams. *Fibers, 7*(12). doi:10.3390/fib7120102

Yakoub, H. (2011). Shear Stress Prediction - Steel Fiber-Reinforced Concrete Beams without Stirrups. *ACI Structural Journal, 108*(3), 304-314.

Yazdani, N. S., Lisa

Haroon, Saif. (2002). Application of Fiber Reinforced Concrete in the End Zones of Precast Prestressed Bridge Girders.

Yazıcı, Ş., İnan, G., & Tabak, V. (2007). Effect of aspect ratio and volume fraction of steel fiber on the mechanical properties of SFRC. *Construction and Building Materials, 21*(6), 1250-1253. doi:10.1016/j.conbuildmat.2006.05.025

Yoo, D.-Y., Kim, S., Park, G.-J., Park, J.-J., & Kim, S.-W. (2017). Effects of fiber shape, aspect ratio, and volume fraction on flexural behavior of ultra-high-performance fiber-reinforced cement composites. *Composite Structures, 174,* 375-388.

Young, B. A., Hall, A., Pilon, L., Gupta, P., & Sant, G. (2019). Can the compressive strength of concrete be estimated from knowledge of the mixture proportions?: New insights from statistical analysis and machine learning methods. *Cement and Concrete Research, 115,* 379-388. doi:10.1016/j.cemconres.2018.09.006

Ziolkowski, P., & Niedostatkiewicz, M. (2019). Machine Learning Techniques in Concrete Mix Design. *Materials (Basel), 12*(8). doi:10.3390/ma12081256

Zollo, R. F. (1997). Fiber-reinforced concrete: an overview after 30 years of development. *Cement and Concrete Composites, 19*(2), 107-122.

APPENDICES

Concrete Mixture Design Spreadsheet

Mix Proportion (SSD)

Material	Weight (lbs)	% by Weight	Volume (cf)	Volume Check	Unit Cost ($/ton)	Amount ($)
Cement	635.0	31.63%	3.23	0.120	140	44.45
Fly Ash	0.0	0.00%	0.00	0.000	100	0.00
BFS	0.0	0.00%	0.00	0.000	85	0.00
Micron 3	0.0	0.00%	0.00	0.000	500	0.00
Silica Fume	0.0	0.00%	0.00	0.000	500	0.00
Rock	1800.00	89.67%	10.89	0.403	24	21.60
Sand	1115.62	55.58%	6.75	0.250	18	10.04
Water	256.62	12.78%	4.11	0.152	0.6	0.08
Recycled Steel Fiber	0.00	0.00%	0.00	0.000	125	0.00
*Industrial Steel Fiber	131.41	1.00%	0.27	0.010	2000	131.41
Air	0.075		2.03	0.075	-	-
	2007.3		27.00	#REF!	-	5.70
					Total Cost =	191.68

*Amount calculated by volume fraction, not weight.

ONLY CHANGE YELLOW BOXES

Moisture Content			
sand mc (%)	0.9356725	mc-ssd	-0.01
rock mc (%)	0.049	mc-ssd	-0.00441255

Moisture Content Calculation			
	Wet	Dry	MC (%)
Sand	0.5178	0.513	0.936
Rock	0.821	0.8206	0.049

Rock	683.11	682.78
	445.65	445.65
	237.46	**237.13**
Sand	589.39	584.74
	444.47	444.47
	144.92	**140.27**

Mix Characteristics

w/c	0.42
Unit Weight (pcf)	79.2
Cementitious material (lbs)	611

Suppl. Cementitious Mat.	Percent (%)	Weight (lb)
Fly Ash replacement (%)	0.0%	0.0
BFS replacement (%)	0.0%	0.0
Micron 3 (%)	0.0%	0.0
Silica Fume (%)	0.0%	0.0

Class F only

Material Properties		A.C
Material	S.G.	-
Cement	3.15	
Fly Ash	2.67	-
BFS	2.90	0.49
Micron 3	2.53	1.53
Silica Fume	2.20	
Rock	2.65	
Sand	2.65	
Powdered Rubber	0.87	
Crumb Rubber	1.12	
Tire Chip	1.12	
Steel Fiber	7.80	
PP Fiber	0.91	
PVA Fiber	1.30	

*Includes permeability and CTE (6 cylinders each)

Batch Weights (yd³)

Cement	635	lb
Fly Ash	0	lb
Micron 3	0	lb
Silica Fume	0	lb
Rock	1792	lb
Sand	1109	lb
Water	271	lb
AEA	0.45	fl oz./cwt
AEA	84	ml
HRWRA	5.75	fl oz./cwt
HRWRA	1080	ml
VMA	4.50	fl oz./cwt
VMA	845	ml

Testing Specimens Required		
Compressive cylinders	4	0.23
RCIP cylinders	0	0.00
MOR	0	0.00
Unit weight	1	0.25
Permeameter slabs	0	0.00
Salt Ponding	0	0.00
MOE	0	0.00
Beam Molds (Static Load Displacement)	0	0.00
Split Cylinder	0	0.00
Drop Weight	0	0.00
Impact Beams	0	0
	Total	0.48
	x 1.25	0.60

***use freeze thaw beams instead

Batch Weights (ft³)

Batch size	0.60	cf
Cement	14.2	lb
Fly Ash	0.0	lb
Micron 3	0.0	lb
Silica Fume	0.0	lb
Rock	40.0	lb
Sand	24.8	lb
Steel Fiber	2.9	lb
Water	6.1	lb
AEA	1.9	mL
HRWRA	24.1	mL
VMA	18.9	mL

Admixture Used: 125 mL HRWRA, 150 mL Viscosity

A1 – Complete Mixture Design Spreadsheet

A2 – Shiny App Code for Model Deployment

```
library(shiny)
library(shinythemes)


#User Interface Setup
ui <- fluidPage(theme = shinytheme("lumen"),
titlePanel("GDOT RP17-09 SFRC Compressive Strength and MOR Predictions"),
sidebarLayout(
  sidebarPanel(
    h3(strong("Select Concrete Mixture Parameters")),
    br(),
    sliderInput( "cp", label= "Cement Proportion (cp) [lb/yd^3]", value = 600
, min = 480, max = 975, step = 1),
    sliderInput( "cap", label= "Coarse Aggregate Proportion (cap) [lb/yd^3]",
value = 1800, min = 590, max = 2100, step = 1),
    sliderInput( "fap", label= "Fine Aggregate Proportion (fap) [lb/yd^3]", v
alue = 1000, min = 730, max = 2050, step = 1),
    sliderInput( "wc", label= "W/C Ratio (wc)", value = .5, min = .28, max =
.65),
    sliderInput( "fl", label= "Fiber Length (fl) [in]", value = 2, min = 0, m
ax = 2.4, step = 0.1),
    sliderInput( "ar", label= "Fiber Aspect Ratio (ar)", value = 50, min = 0,
max = 80),
    sliderInput( "Vf", label= "Volume of Fibers (Vf) [%]", value = 1, min = 0
, max = 2, step = 0.05),
    br(),
    br(),
    h3(strong("Input Concrete Material Costs")),
    br(),
    numericInput("cpc", label = "Cement [USD($)/ton]", value = NULL),
    numericInput("capc", label = "Coarse Aggregate [USD($)/ton]", value = NUL
L),
    numericInput("fapc", label = "Fine Aggregate [USD($)/ton]", value = NULL)
,
    numericInput("waterc", label = "Water [USD($)/ton]", value = NULL),
    numericInput("fiberc", label = "Industrial Fibers [USD($)/lb]", value = N
ULL),
```

```
 ),


  mainPanel(
    img(src = "GDOT.png"),
    img(src = "UGAENGR.png", align = "right"),
    h3("This application utilizes gradient boosting machines (GBM) learning a
lgorithm to predict the compressive strength and modulus of rupture of
       steel fiber-reinforced concrete (SFRC) mixtures based on user inputs.
The GBM model uses over 100 published results from SFRC tested mixtures."),
    br(),
    h3("Input Variables:"),
    tableOutput("Var"),
    h3("Predicted Modulus of Rupture (psi):"),
    verbatimTextOutput("MOR"),
    h3("Predicted Compressive Strength (psi):"),
    verbatimTextOutput("comp"),
    h3("Mixture Cost [USD/cubic yard]"),
    verbatimTextOutput("cost"),
    br(),
    br(),
    br(),
    br(),

    h4("Aspect Ratio = (Fiber Length / Fiber Diameter)")
  ),
 ),
)


# load the model previously saved
MOR_model <- readRDS("MOR_model.rds")
comp_model <- readRDS("comp_model.rds")

server <- function(input, output) {
  library(gbm)
  output$Var <- renderTable({
```

```
    Xm <- c(input$cp, input$cap, input$fap, input$wc, input$fl, input$ar, inp
ut$Vf, input$ri)

    Xmf <- data.frame("cp" = Xm[1], "cap" = Xm[2], "fap" = Xm[3], "wc"=Xm[4],
"fl"=Xm[5],"ar"=Xm[6],"Vf" =Xm[7], "ri"= (Xm[6] * Xm[7]))

    Xmf

  })

  output$comp <- renderText({

    Xm <- c(input$cp, input$cap, input$fap, input$wc, input$fl, input$ar, inp
ut$Vf, input$ri)

    Xmf <- data.frame("cp" = (Xm[1]/27), "cap" = (Xm[2]/27), "fap" = (Xm[3]/2
7), "wc"=Xm[4], "fl"=Xm[5],"ar"=Xm[6],"Vf" =Xm[7], "ri"= (Xm[6] * Xm[7]))

    pred_comp <- predict(comp_model, Xmf, n.trees=1000)

    floor(pred_comp)

  })

  output$MOR <- renderText({

    Xm <- c(input$cp, input$cap, input$fap, input$wc, input$fl, input$ar, inp
ut$Vf, input$ri)

    Xmf <- data.frame("cp" = (Xm[1]/27), "cap" = (Xm[2]/27), "fap" = (Xm[3]/2
7), "wc"=Xm[4], "fl"=Xm[5],"ar"=Xm[6],"Vf" =Xm[7], "ri"= (Xm[6] * Xm[7]))

    pred_MOR <- predict(MOR_model, Xmf, n.trees=1000)

    floor(pred_MOR)

  })

  output$cost <- renderText({

    cost <- ((input$cpc/2000) * input$cp) + ((input$capc/2000) * input$cap) +
((input$waterc/2000) * (input$cp/input$wc)) + ((input$fapc/2000) * input$fap)
+ (input$fiberc/27*7.8*62.4*input$Vf)

    format(round(cost, 2), nsmall = 2)

  })


}


shinyApp(ui, server)
```

A3 – R Code for GBM Model for rshiny App

```
library(tree)
library(gbm)
################################################
##COMPRESSIVE STRENGTH PREDICTION MODEL
#import the compressive strength data set
sfrccompprop = read.csv("sfrccomp.csv", nrow=103)
sfrccomp = subset(sfrccompprop, select = c(cp:fc))
#split the data set
warning=FALSE
set.seed(1)
sfrc_comp_train = sfrccomp
sample(sfrccomp, .80)
sfrc_comp_test = sfrccomp
setdiff(sfrc_comp_train,NULL)

#comp_model = tree(fc~., sfrc_comp_train)

#Boosting Model
comp_model = gbm(fc~., data = sfrc_comp_train,
                      distribution = "gaussian",
                      n.trees = 1000,
                      interaction.depth = 4,
                      shrinkage = 0.1,
                      verbose = F)


#save the model to disk
saveRDS(comp_model, "comp_model.rds")


################################################
```

```
##MOR MODEL
#Import the MOR data set
sfrcmorprop = read.csv("sfrcmor.csv", nrow=81)
sfrcmor = subset(sfrcmorprop, select = c(cp:mor))

#split the data set
warning=FALSE

set.seed(1)
sfrc_mor_train = sfrcmor
sample(sfrccomp, .80)

sfrc_mor_test = sfrcmor
setdiff(sfrc_comp_train,NULL)

#tree_sfrc_mor = tree(mor~., sfrc_mor_train)

#Boosting Model
MOR_model = gbm(mor~., data = sfrc_mor_train,
                      distribution = "gaussian",
                      n.trees = 1000,
                      interaction.depth = 4,
                      shrinkage = 0.1,
                      verbose = F)

# save the model to disk
saveRDS(MOR_model, "MOR_model.rds")
```

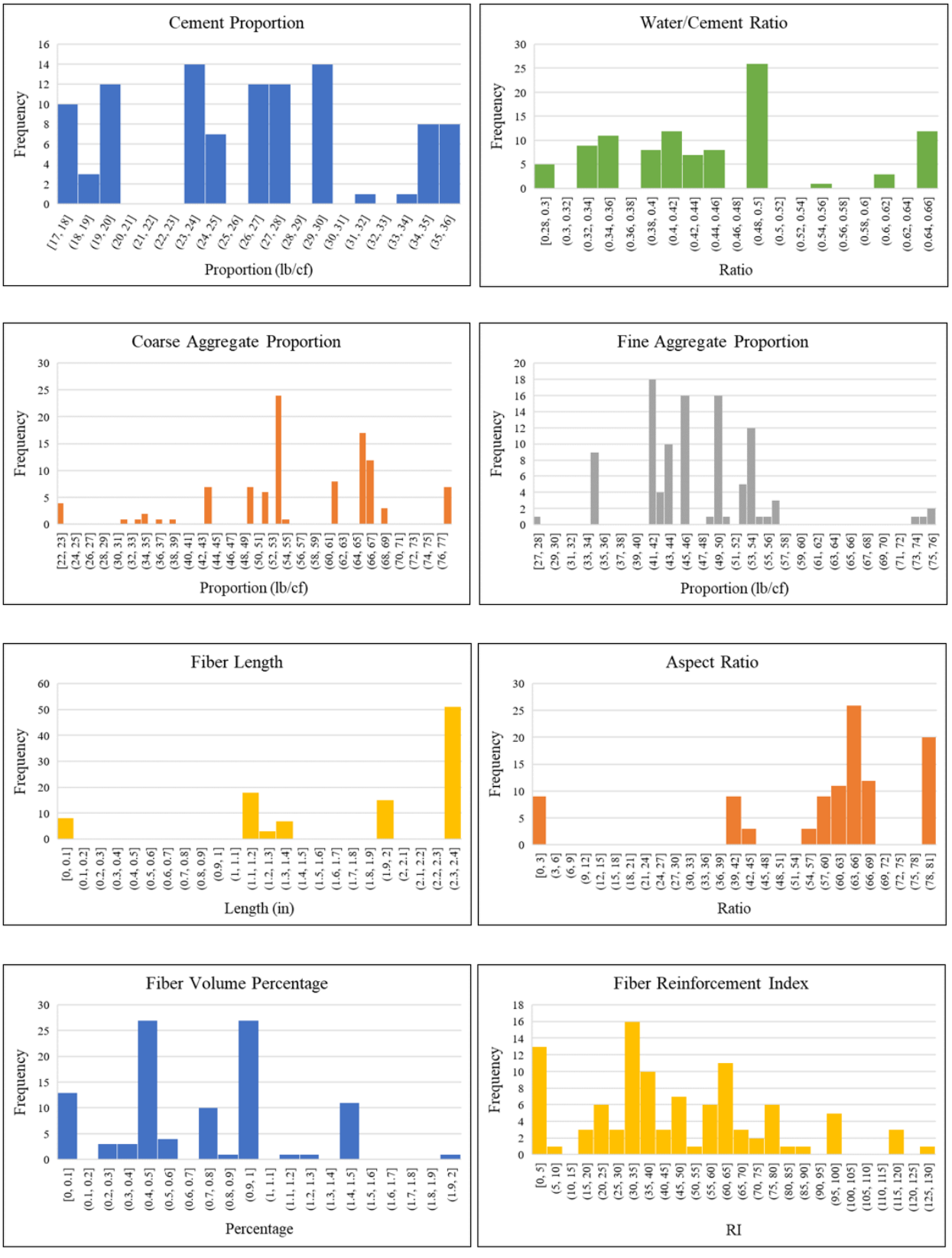

A4 – Histograms of Mixture Parameter Database Variables